PHY862 Accelerator Systems
Beam Measurement Techniques & Beam Instrumentation

Steve Lidia
Facility for Rare Isotope Beams Laboratory
Michigan State University

Two Lecture Outline

- Introduction
- Beam Measurement Techniques
  - Beam Generated Signals
  - Beam Properties
  - Lattice Parameters
  - Beam Processes
- Beam Instrumentation
  - Beam-Sensor Interactions
  - Diagnostic Architecture
- Exercises and References

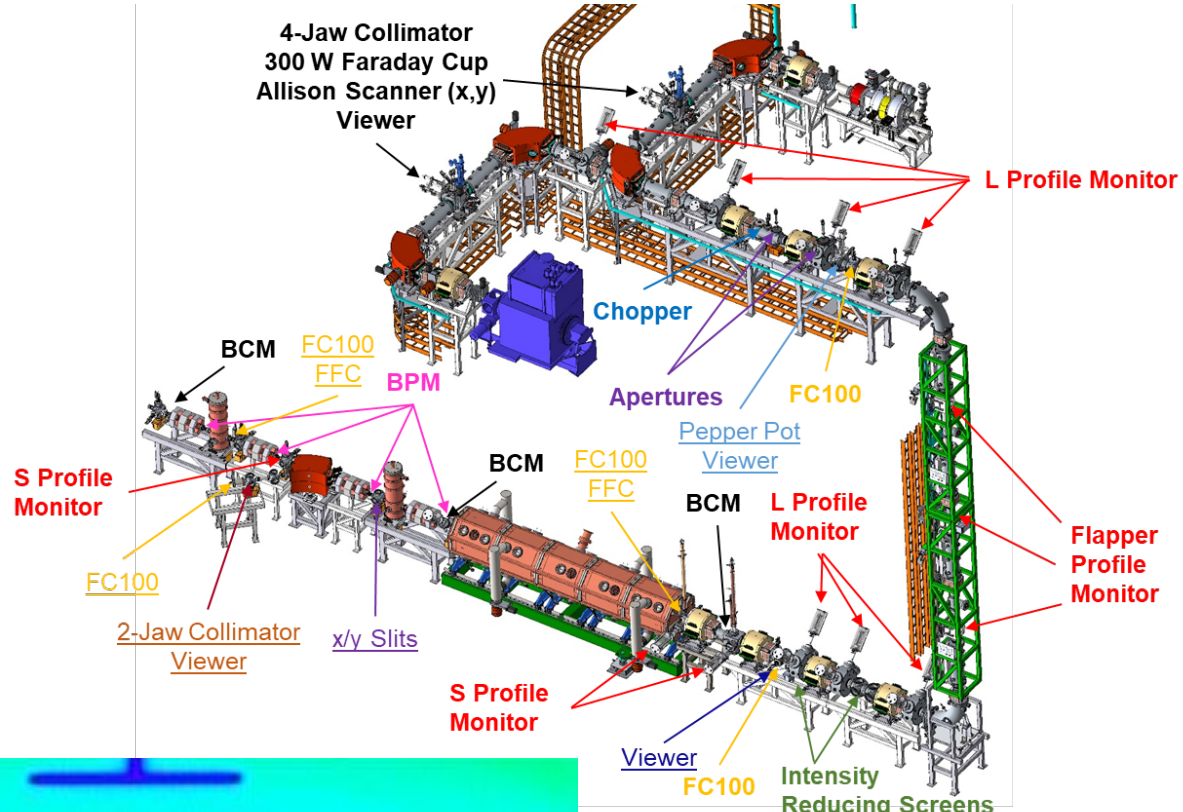

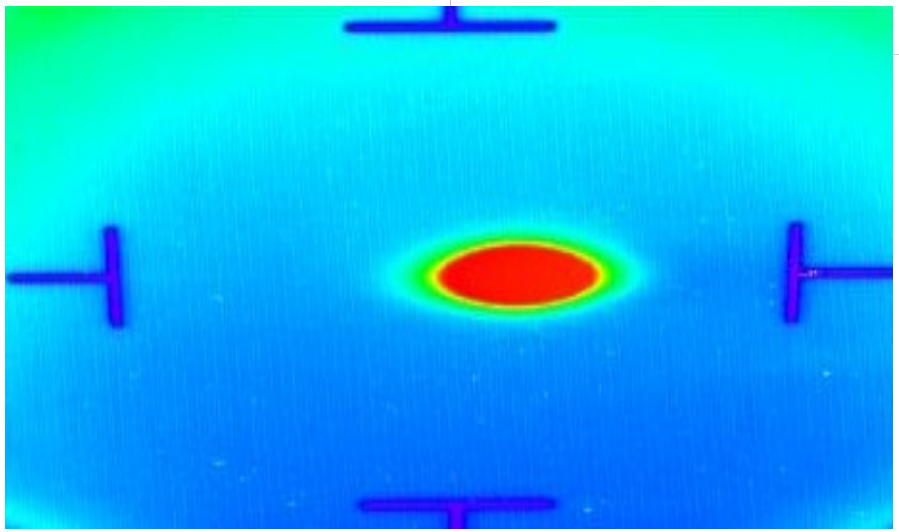

Role of diagnostics and instrumentation

Beams are composed of 100's to 10**8's of individual particles.

Getting them all from point A to point B can be a challenge

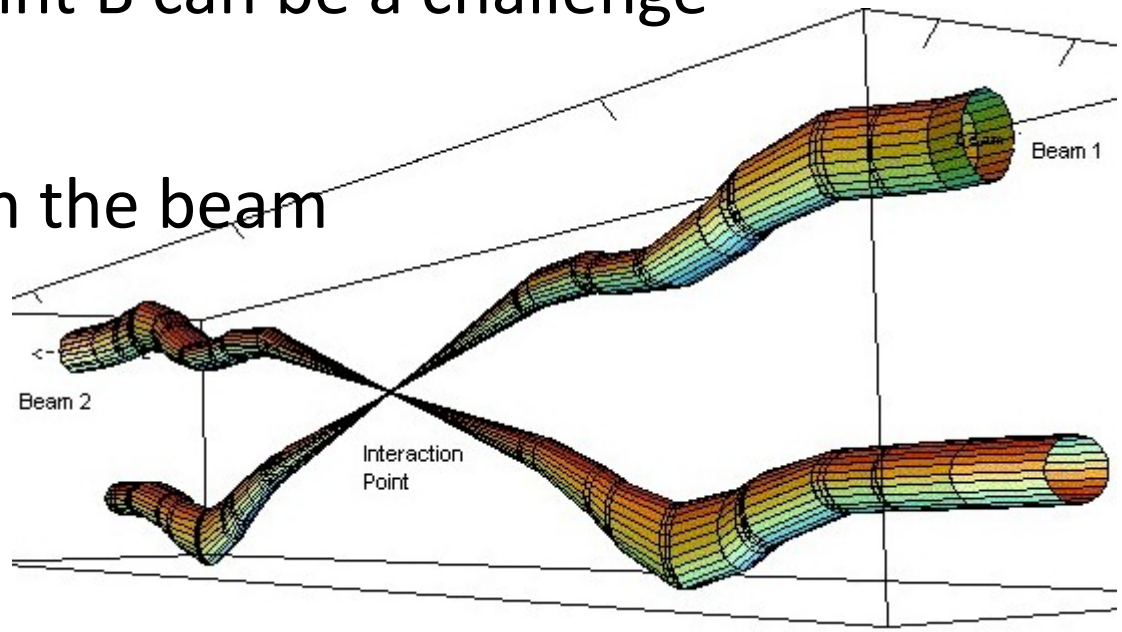

We need to perform certain operations on the beam

- Tuning, optimization of beam quality
- Targetry, beam collisions
- Monitoring, stability, minimizing losses, machine protection

Measurements, diagnostics, and instrumentation

- **Measurements**
  - Incorporate (incomplete) knowledge of lattice, beam dynamics
  - Point vs. Distributed (lattice-dependent) measurements
- **Diagnostics** are techniques involved in performing a measurement
  - Direct vs indirect measurements
  - Correlations – use known dependencies
- **Instrumentation** is the set of particular devices used in the execution of the measurement
  - Set of beam sensors, signal transmission lines, data acquisition and reporting systems, controls and feedback

Diagnostics vs. Instrumentation examples

Measurement	Diagnostic	Instrumentation
Beam current	Beam wall return current	AC Current Transformer + electronics
Beam position	Beam E-field distribution @ walls	Capacitive pickups + electronics
Beam emittance (1DoF)	Quad scan	Quadrupole magnet + view screen + camera

Particular diagnostic/instrumentation methodologies rely on particular types of beams and beam parameters/lattice functions, available beamline space and shielding, required measurement accuracy and precision, cost, . . .

Direct vs Indirect Measurements

- Only *some* beam and lattice parameters are directly measurable
  - Typically involves an interceptive or destructive measurement
- Many quantities of interest are determined by known correlations
  - Lattice parameters and beam parameters are determined iteratively, or through complementary means
  - Space/time and frequency domain measurements are used extensively
    - Single pass vs. multi-pass beamlines employ differing measurement modalities for the same quantity of interest
  - Dedicated diagnostic stations are established with well known positions and alignment characteristics

Typical beam measurements

Measurements and associated diagnostics and instrumentation are specific to

- Geometry of beamline
  - linac, synchrotron booster, storage ring, analyzing beamline, injector, final focus, etc.)
- Particle type
  - Hadron, lepton, neutron, neutral atom, rare isotope
- Beam energy
- Beam intensity
- Beam time structure
- . . .

Beam quantity		LINAC, transfer line	Synchrotron
current I	*general*	transformer (dc, pulsed) Faraday cup	transformer (dc)
	special	particle detector (Scint. IC, SEM)	normalized pick-up signal
position $\overline{x}$	*general*	pick-up	pick-up
	special	using profile measurement	cavity excitation (e^-)
profile x_{width}	*general*	SEM-grid, wire scanner viewing screen, OTR-screen	residual gas monitor synch. radiation (e^-) wire scanner
	special	grid with ampl. (MWPC)	
trans. emittance ϵ_{trans}	*general*	slit grid quadrupole scan	residual gas monitor wire scanner
	special	pepper-pot	transverse Schottky pick-up wire scanner
momentum p and $\Delta p/p$	*general*	pick-up (TOF) magn. spectrometer	pick-up
	special		Schottky noise pick-up
bunch width $\Delta\varphi$	*general*	pick-up	pick-up wall current monitor
	special	particle detector secondary electrons	streak camera (e^-)
long. emittance ϵ_{long}	*general*	magn. spectrometer buncher scan	
	special	TOF application	pick-up + tomography
tune, chromaticity Q, ξ	*general*	—	exciter + pick-up (BTF)
	special	—	transverse Schottky pick-up
beam loss r_{loss}	*general*	particle detector	
polarization P	*general*	particle detector	
	special	Compton scattering with laser	
luminosity $\mathcal{L}$	*general*	particle detector	

SIS-18 Synchrotron at GSI: diagnostic suite

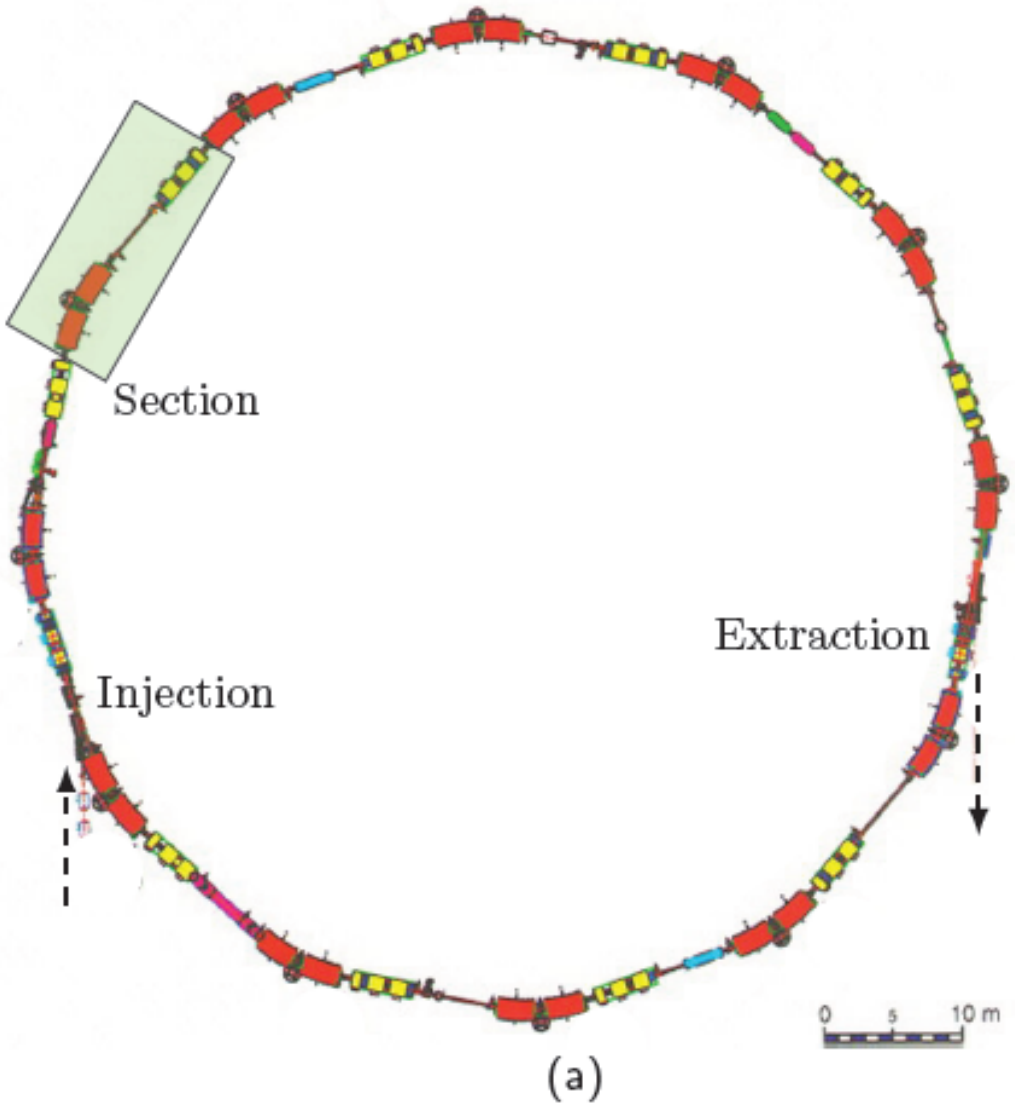

(a)

Device	Purpose
12 BPMs	Position, tune
3 Phase pick-up	Longitudinal structure
Quad pick-up	Tune, Quadrupole oscillations
Schottky pick-up	Schottky diagnostics
2 DC-CTs	Current
1 FCT	Bunch structure
1 ACT	Injected current
1 IPM	Transverse profile
1 Wire grid	Transverse profile
1 Scint. screen	Transverse profile
2 Beam exciters	Excitation
15 BLMs	Beam losses

(b)

Lienard-Wiechert Fields

$$\boldsymbol{E}(\boldsymbol{x},t)=\frac{q}{4\pi\epsilon_0}\left[\frac{\boldsymbol{n}-\boldsymbol{\beta}}{\gamma^2(1-\boldsymbol{\beta}\cdot\boldsymbol{n})^3R^2}+\frac{1}{c}\frac{\boldsymbol{n}\times\left((\boldsymbol{n}-\boldsymbol{\beta})\times\dot{\boldsymbol{\beta}}\right)}{(1-\boldsymbol{\beta}\cdot\boldsymbol{n})^3R}\right]_{ret}$$

$$\boldsymbol{B}(\boldsymbol{x},t)=\frac{1}{c}[\boldsymbol{n}\times\boldsymbol{E}]_{ret}$$

Velocity fields

Acceleration fields

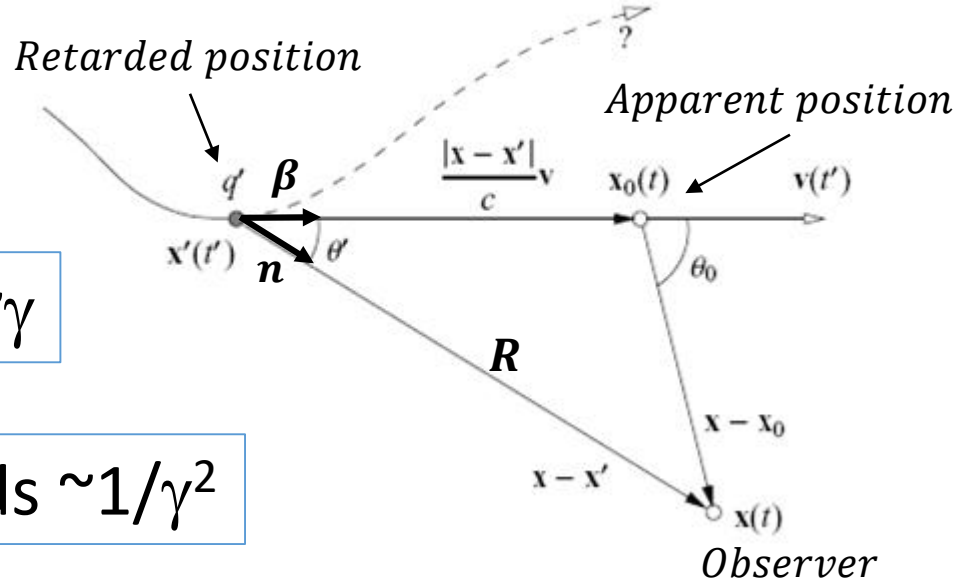

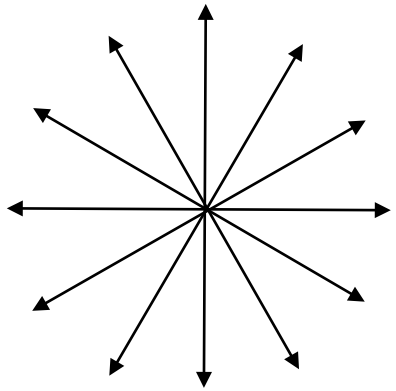

Uniform motion, β<<1

Transverse fields ~γ

Longitudinal fields ~1/γ²

Fields of beam bunches (constant velocity)

- Lorentz Transformation of coordinates (here $\boldsymbol{n}=\boldsymbol{\beta}/\beta$)

$$ct' = \gamma(ct - \beta \boldsymbol{n}\cdot\boldsymbol{r})$$
$$\boldsymbol{r}' = \boldsymbol{r} + (\gamma - 1)(\boldsymbol{r}\cdot\boldsymbol{n})\boldsymbol{n} - \gamma\beta c\boldsymbol{t}\boldsymbol{n}$$

- Lorentz Transformation of fields

$$\boldsymbol{E}_{\parallel}{}' = \boldsymbol{E}_{\parallel} \qquad \boldsymbol{B}_{\parallel}{}' = \boldsymbol{B}_{\parallel}$$
$$\boldsymbol{E}_{\perp}{}' = \gamma(\boldsymbol{E}_{\perp} + \boldsymbol{v}\times\boldsymbol{B}) \qquad \boldsymbol{B}_{\perp}{}' = \gamma\left(\boldsymbol{B}_{\perp} - \frac{\boldsymbol{1}}{\boldsymbol{c^2}}\boldsymbol{v}\times\boldsymbol{E}\right)$$

- Lorentz Transformation of charge and current densities

$$c\rho' = \gamma(c\rho - \beta\boldsymbol{n}\cdot\boldsymbol{J})$$
$$\boldsymbol{J}' = \boldsymbol{J} + (\gamma - 1)(\boldsymbol{J}\cdot\boldsymbol{n})\boldsymbol{n} - \gamma\beta c\rho\boldsymbol{n}$$

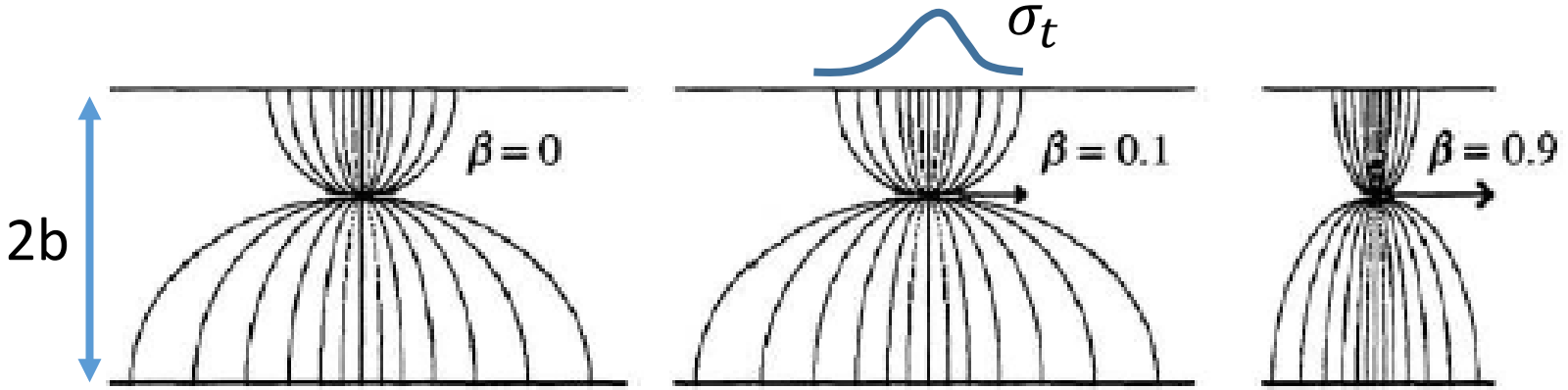

Effect of metallic boundaries

For a point charge <u>on axis</u>, the extent of the pulse is approximated by (cf. Shafer)

$$\sigma_t \cong \frac{b}{\sqrt{2}\gamma\beta c}$$

Field from 2D Laplace Equation

- In the limit of neglecting longitudinal end effects (bunch length >> pipe diameter), we can solve the 2D Laplace equation in the beam rest frame with Doppler shifted spectrum
- Include modulation effects (wavelength >> pipe diameter)
- For long pulses that are nonrelativistic or only mildly relativistic, the fields are well approximated by electrostatics
- Intense beams may require self-magnetic field corrections

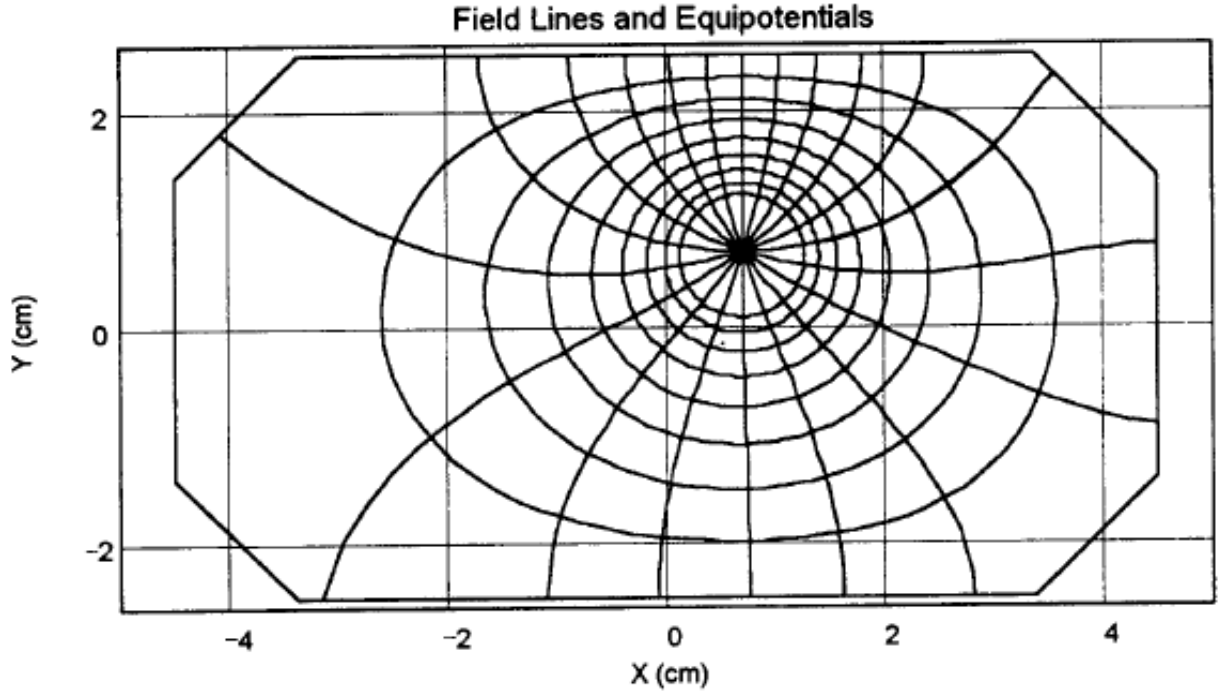

Figure 8. Field lines and equipotential contours found by conformal mapping.

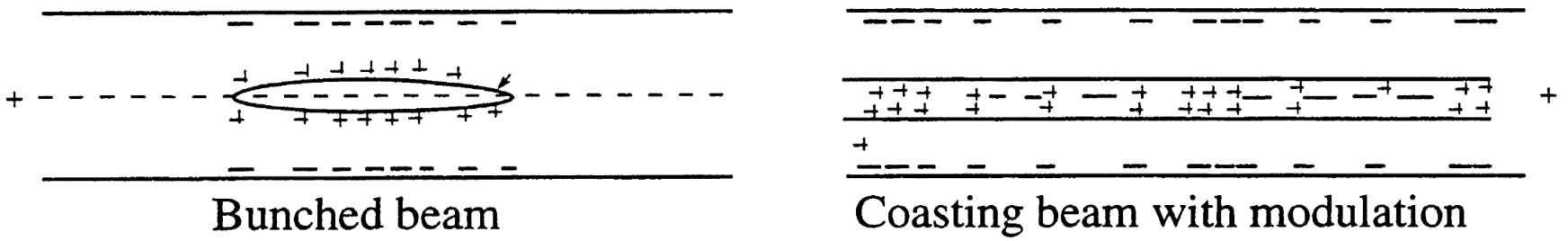

Simple beam model

- Assume a beam, carrying current *I*, of radius *a* centered in a pipe of radius *b*.

$$\rho = \frac{1}{\pi a^2}\frac{I}{v} = \frac{\lambda}{\pi a^2}$$

- The radial electric field at the pipe surface is

$$E_r = \frac{\rho a^2}{2\varepsilon_0 b} = \frac{\lambda}{2\pi\varepsilon_0 b}$$

- The surface charge density induced at *r=b* is

$$\sigma_s = \varepsilon_0 E_r = \frac{\lambda}{2\pi b}$$

- The azimuthal magnetic field at the pipe surface

$$B_\varphi = \frac{\mu_0 I}{2\pi b}$$

- With surface current density (longitudinally)

$$K_s = \frac{-I}{2\pi b} = -v\sigma_s$$

Coulomb field temporal profile

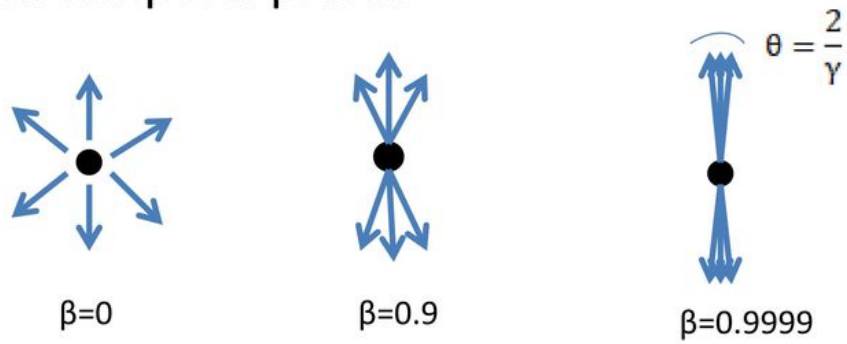

$$E_{e0}(r_0, t) = \frac{e_0\gamma}{4\pi\varepsilon_0}\cdot\frac{r_0}{(r_0^2 + \gamma^2 v_e^2 (t - t_0)^2)^{3/2}}$$

Coulomb field of one electron

- High energy , Coulomb field temporal profile is approximately the bunch temporal profile
- Broadening of profile: $\Delta t \sim \frac{2r}{\gamma}$

Wall currents and charges

- Off center beam in pipe creates azimuthal surface charge density distribution

$$\sigma(\theta) = \frac{-\lambda_b}{2\pi b}\left[\frac{b^2-\rho^2}{b^2+\rho^2-2b\rho\cos(\theta-\phi)}\right]$$

$$E_{\perp,lab}(t) = \gamma \cdot E_{\perp,rest}(t')$$

$$\sigma(\theta) = \frac{-\lambda_b}{2\pi b}\left[1+2\sum_{n=1}^{\infty}\left(\frac{\rho}{b}\right)^n \cos\left(n\{\theta-\phi\}\right)\right]$$

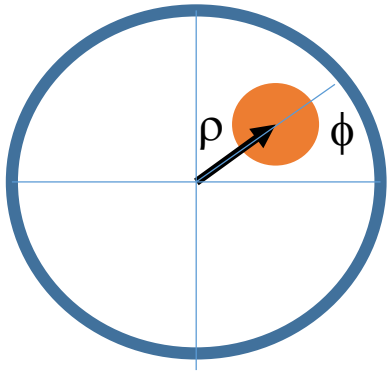

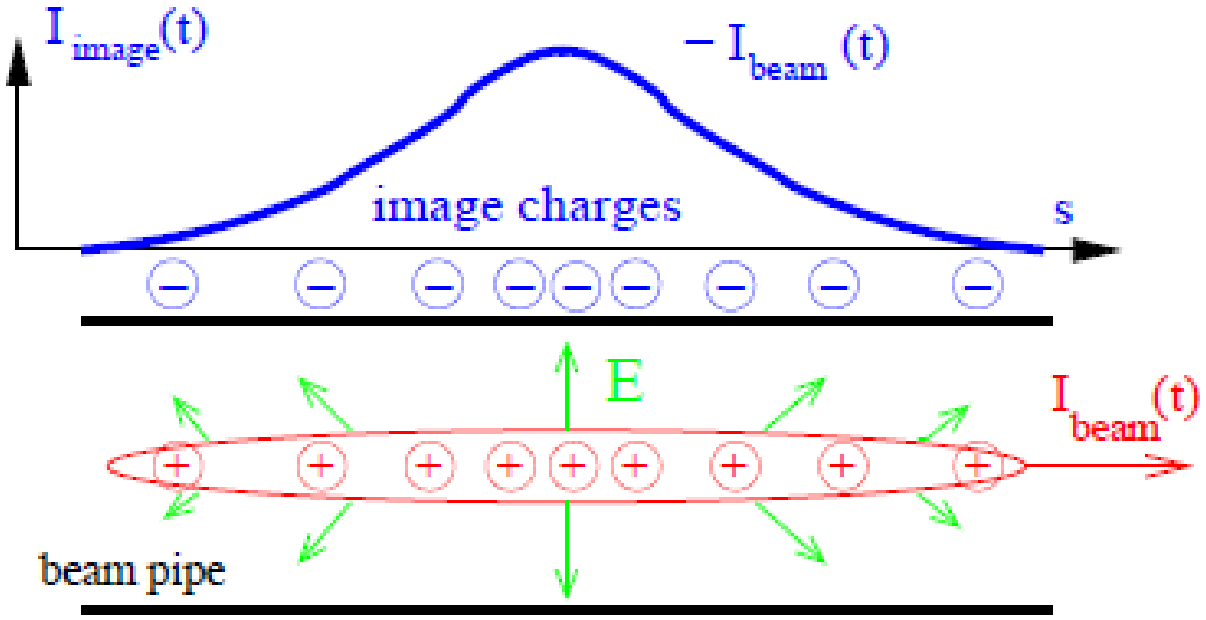

Time/Frequency description of beam signals

- RF and beam pulse structure
- Compromise between
  - Cavity rf frequency (aperture, transit factor)
  - Power generation and handling (CW/pulsed)
  - Experimental requirements

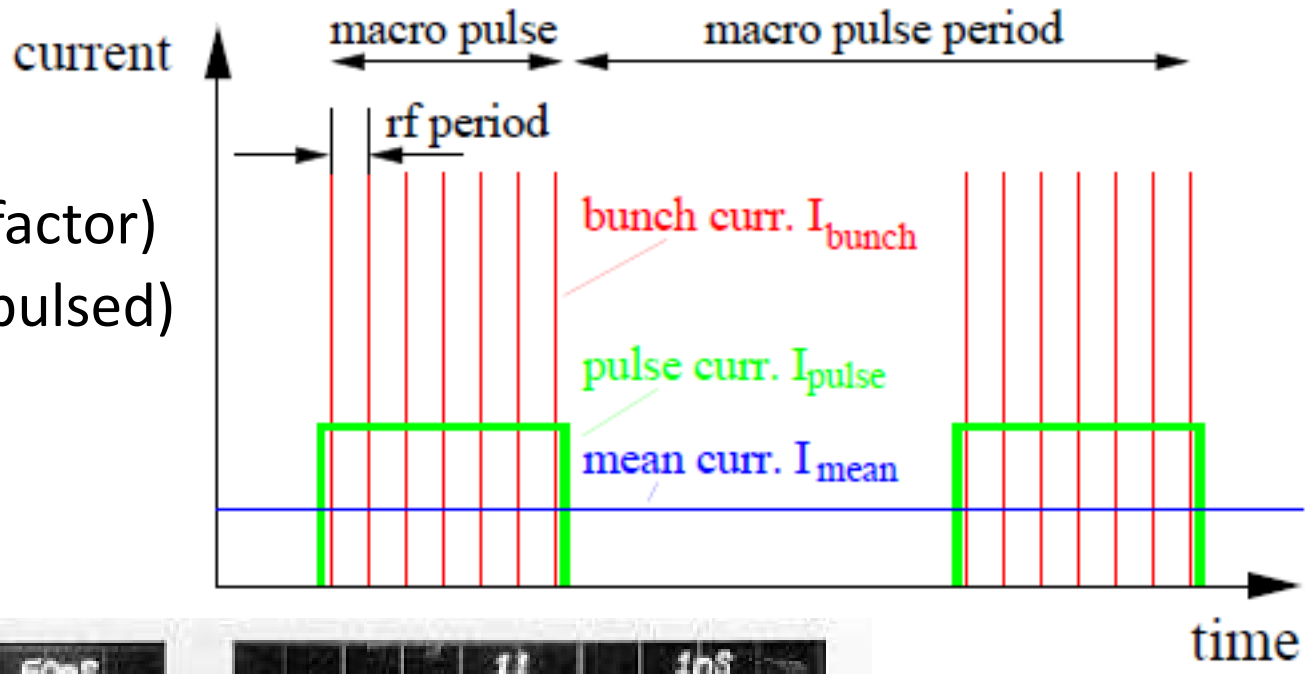

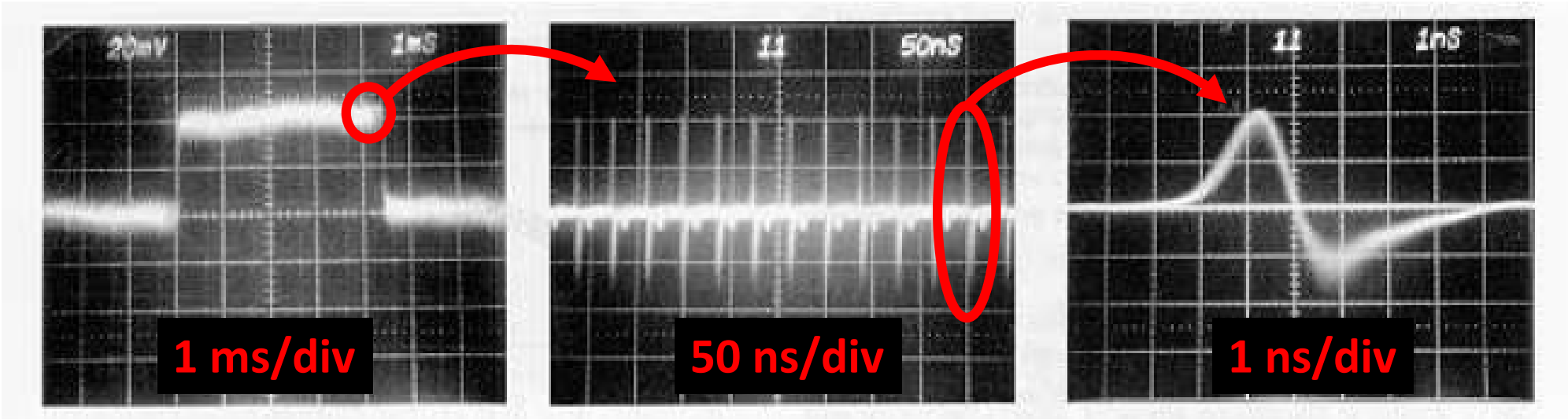

Capacitive probe
Why is the signal bipolar?

Beam spectra examples

- Beam signals reveal the bunch structure and loading or fill pattern
- Multibunch dynamics are revealed in sidebands and harmonics of underlying carrier frequencies

Below is some raw spectra of a BPM sum signal from the ALS showing coupled bunch oscillations. The measurement was made with 328 bunches (all RF buckets) filled as equally as possible. The number of rotation harmonics from the RF frequency is given in each graph. The upper graph was measured at 20 mA and the lower at 95 mA.

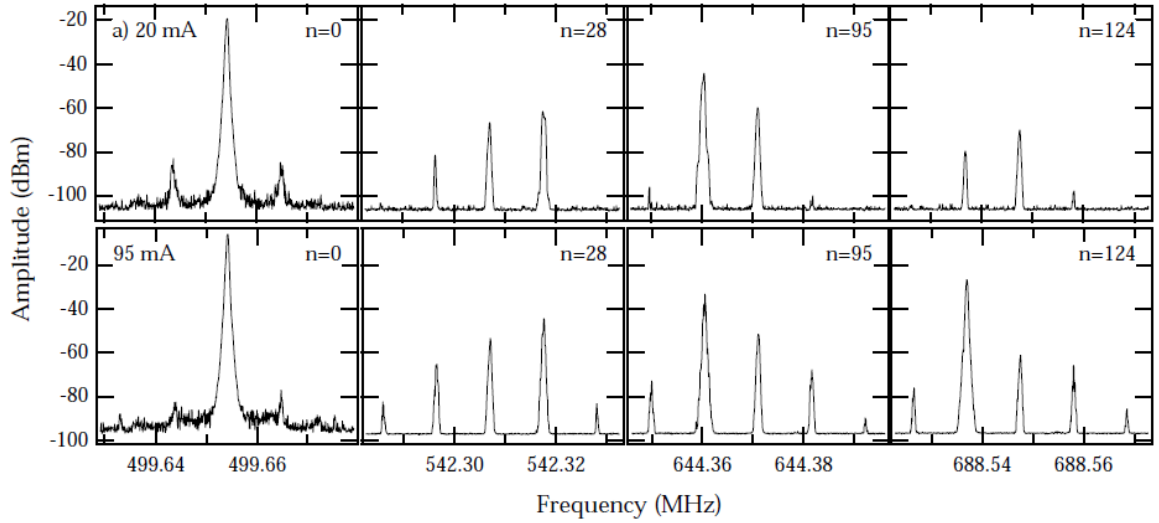

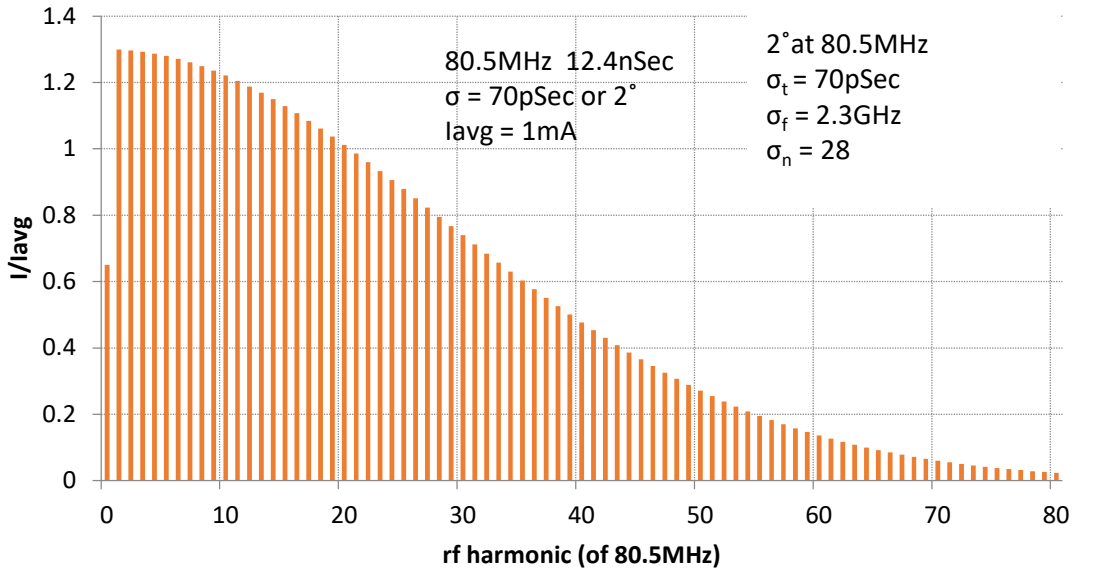

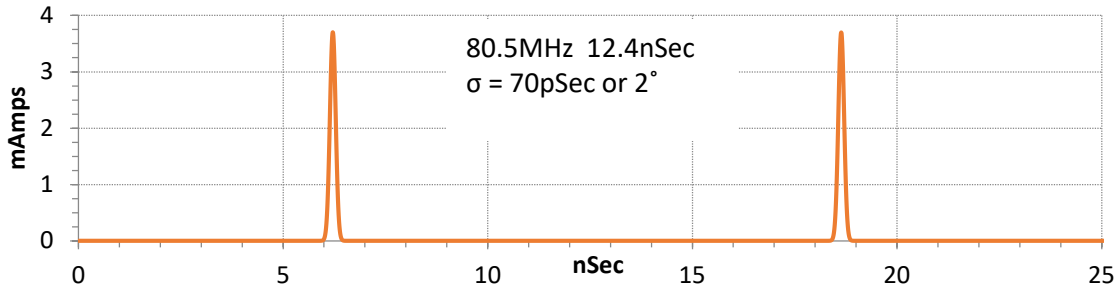

Beam Coupling to its Environment

- Beams carry signals, encoded in their time/frequency structure, transverse position, energy, etc.
  - Time-dependent description (wakefields)
  - Frequency-dependent description (impedances)
- Charged particle beams couple electromagnetically to their environment
  - Noninterceptive means – resistive, capacitive, inductive, resonant, radiative
- Accelerator beams represent 'nearly perfect current sources'
  - Very high source impedance
- Sometimes the environment drives back on the beam
  - Lorenz reciprocity
  - Beam loading, instabilities!

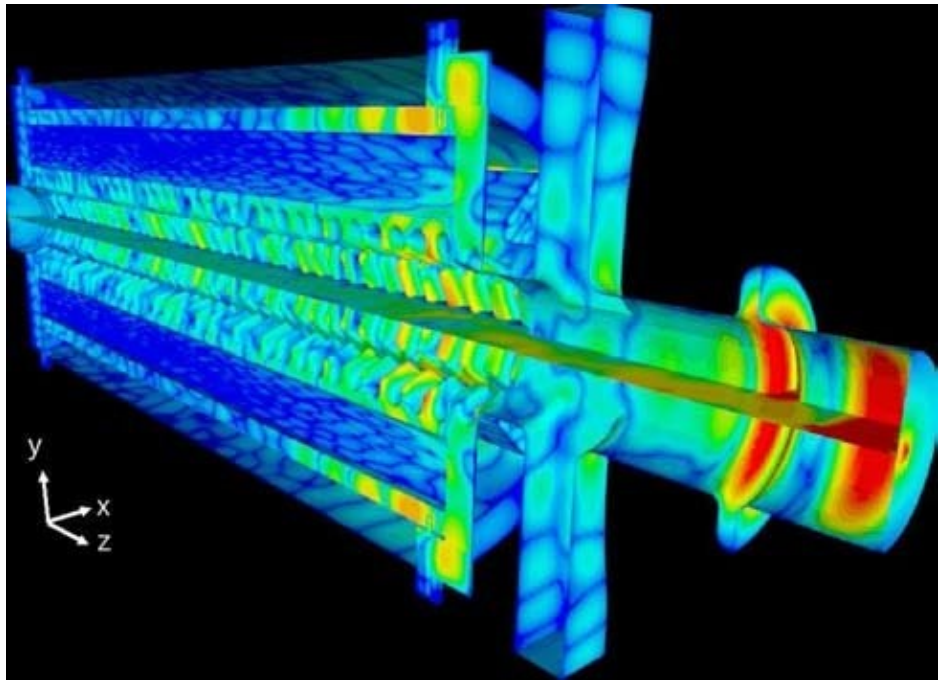

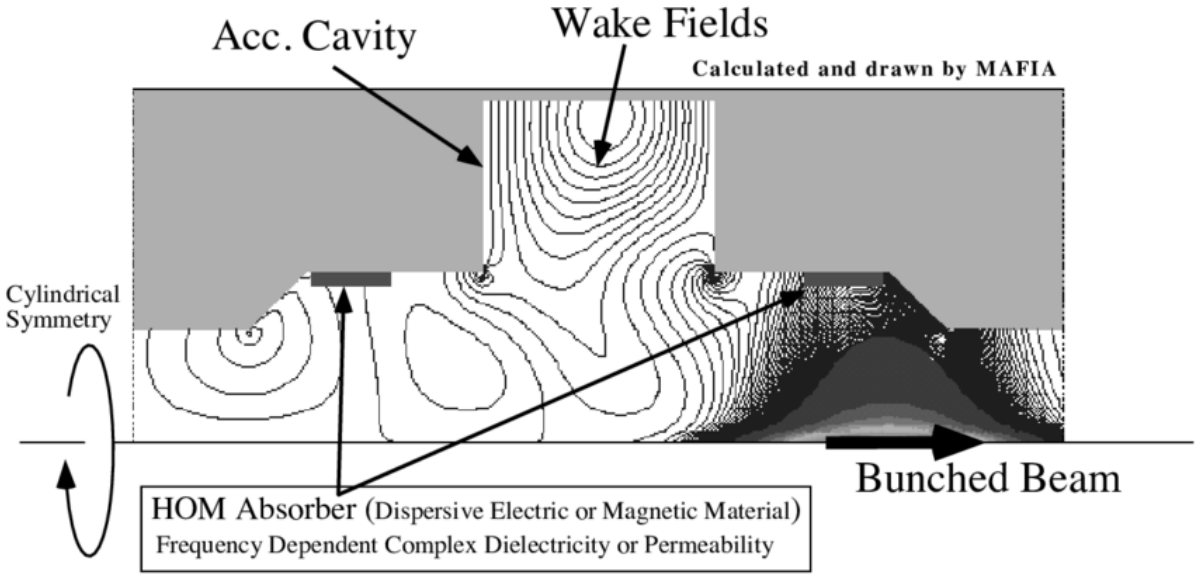

Beam parameters [1] – 1st Order Moments

- Current; charge, mass, polarization states
- Beam energy
- Beam position, orbit, tune

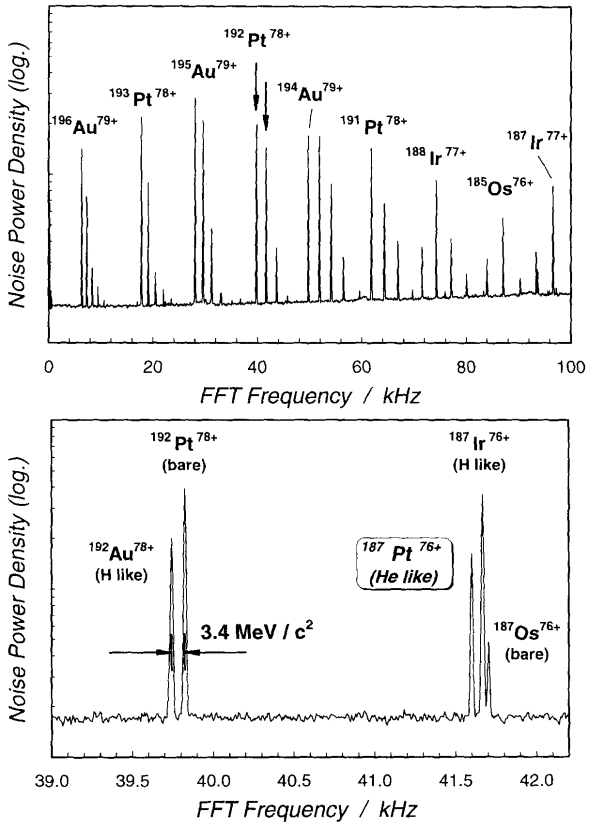

Schottky spectra of stored and cooled rare isotopes from $^{197}Au^{79+}$. Spectra of 16th revolution harmonic.

(Schlitt, et al., Nucl. Phys A626 (1997), 315.)

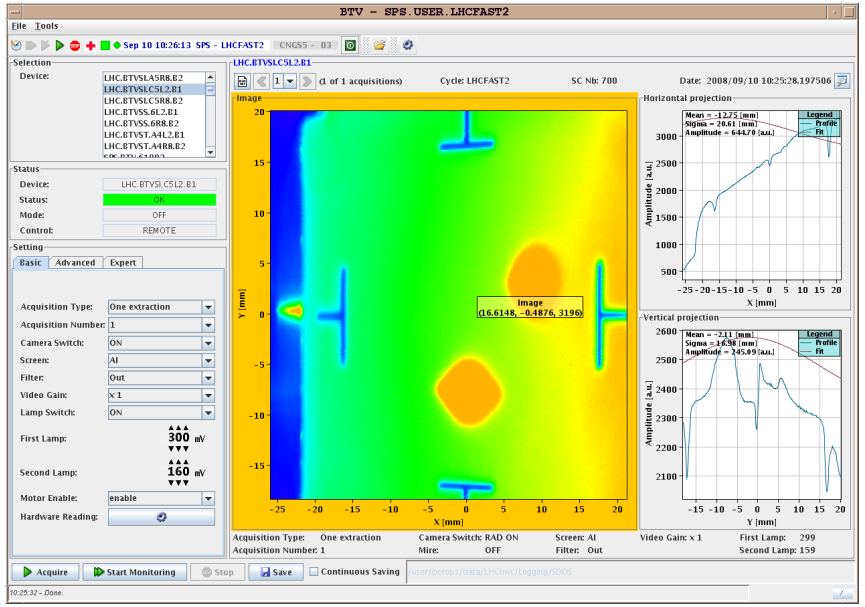

LHC Day 1 Beam Position

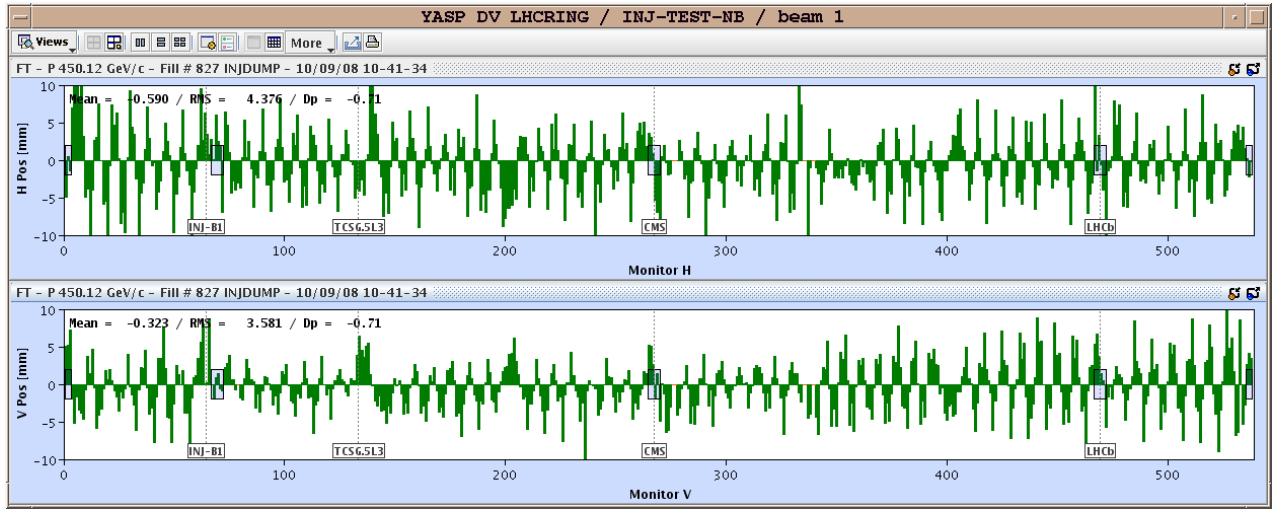

Beam parameters [2] – 2nd Order (+ higher) Moments

- Profile (transverse, longitudinal), envelope, energy spread
- Phase space density, emittance measures
- Beam halo - transverse, longitudinal

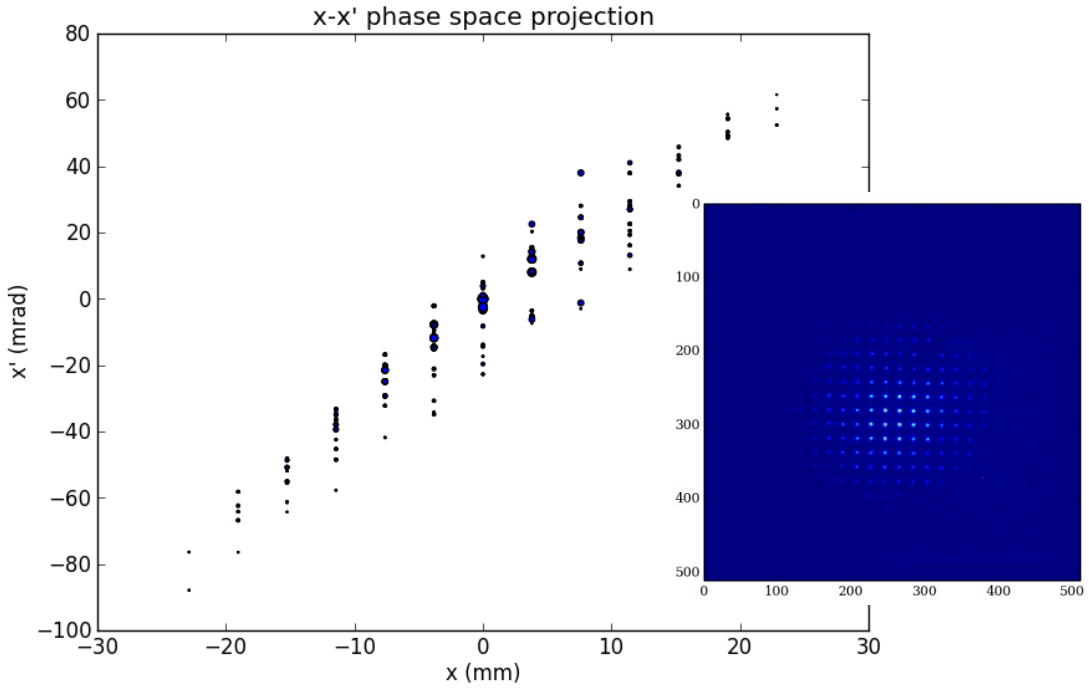

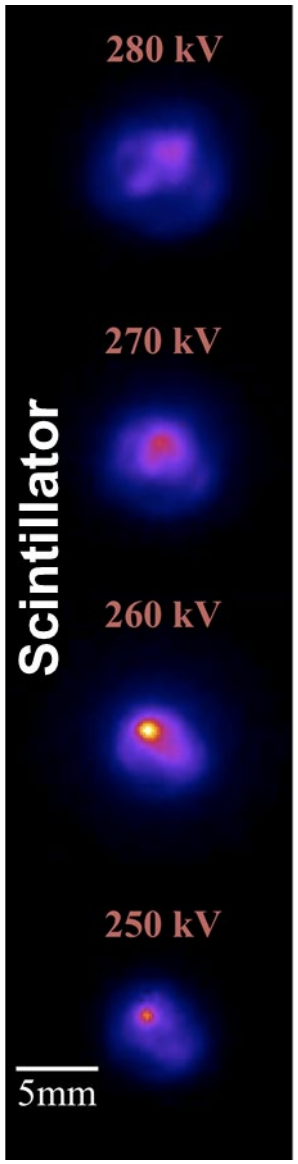

Beam halo with wire scanner measurements

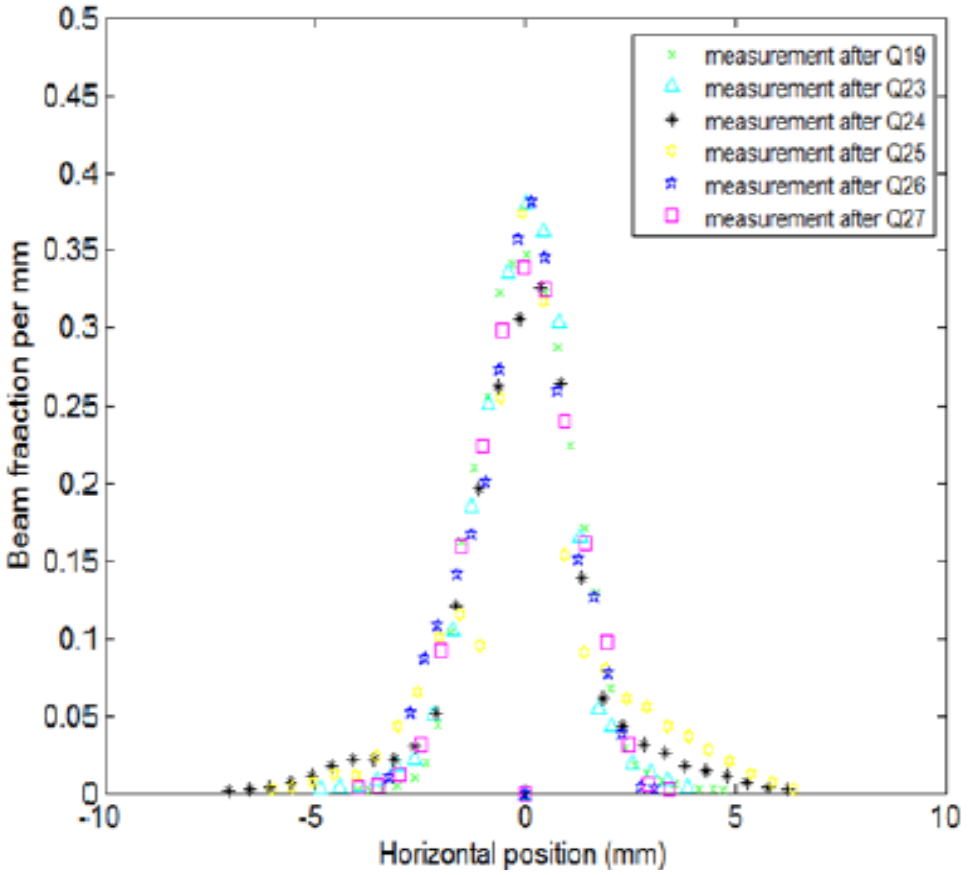

Beam parameters [3] – Bunch Trains

- Single bunch vs. many bunch measurements
- Time domain vs. frequency domain

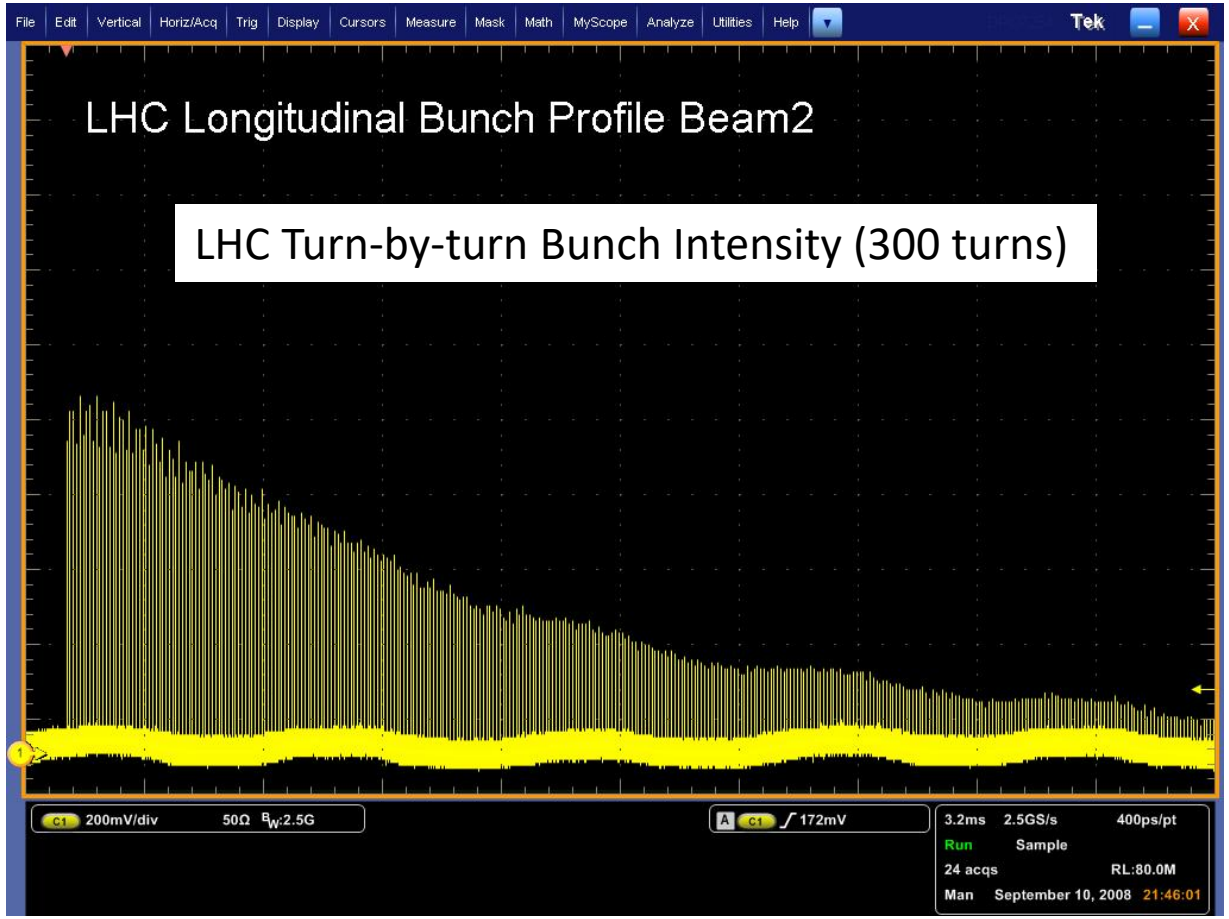

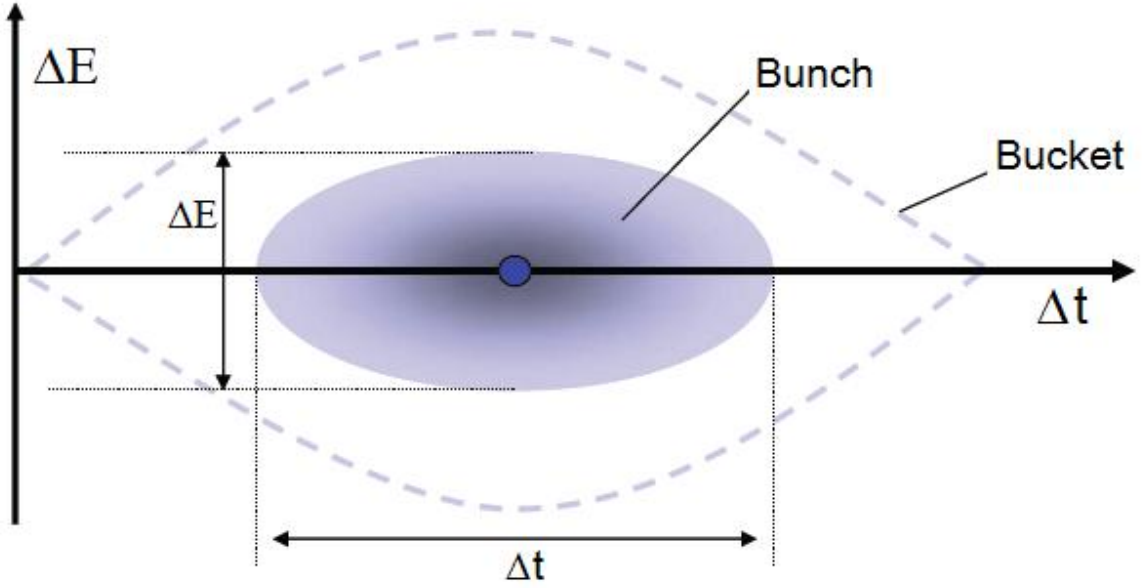

Particle Identification

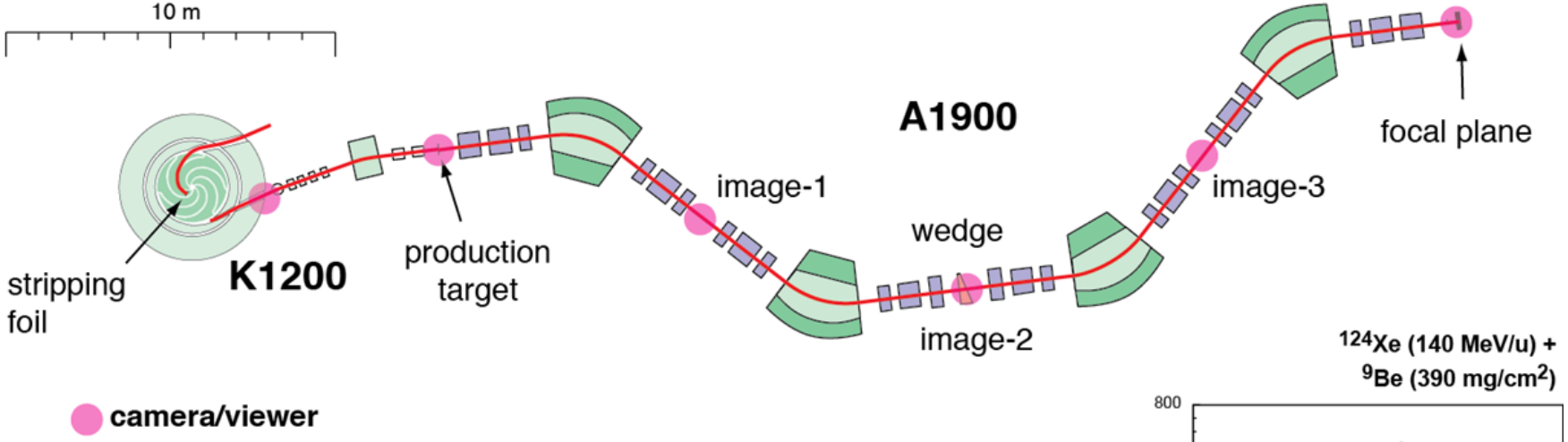

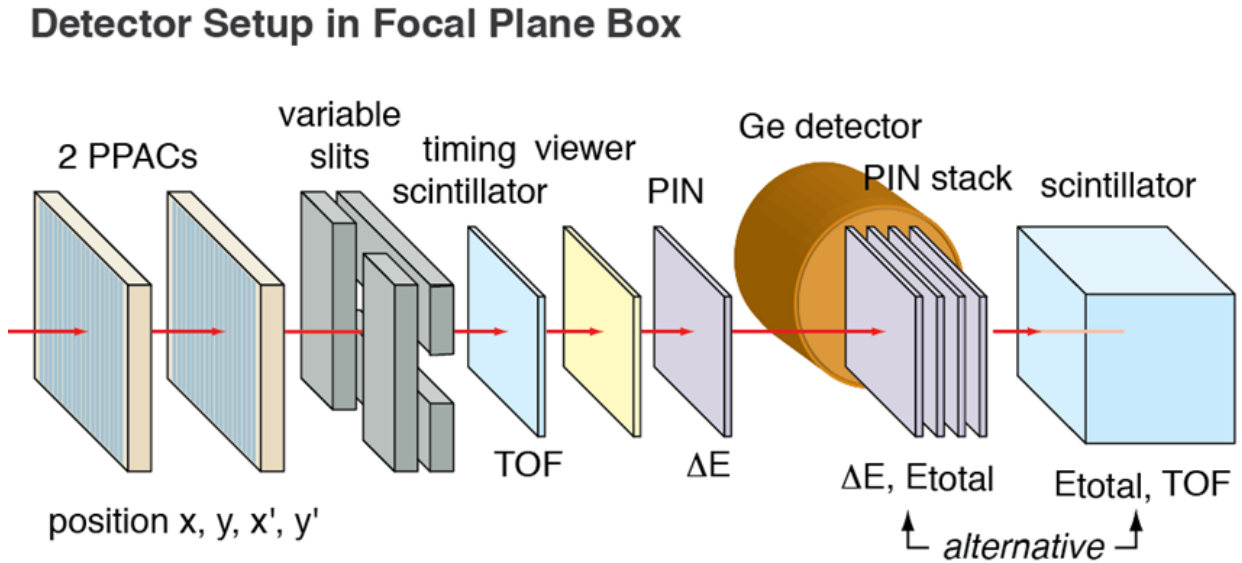

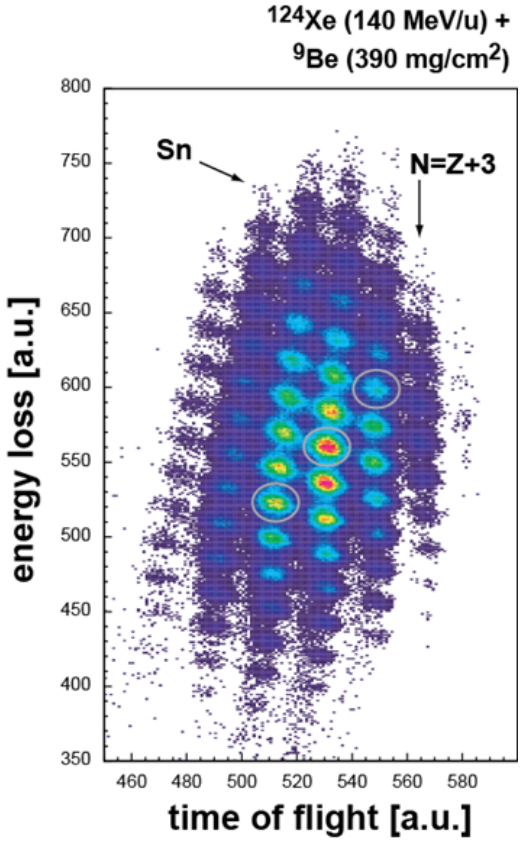

(Courtesy, A. Stolz)

Lattice parameters

- Betatron tune Qx, Qy

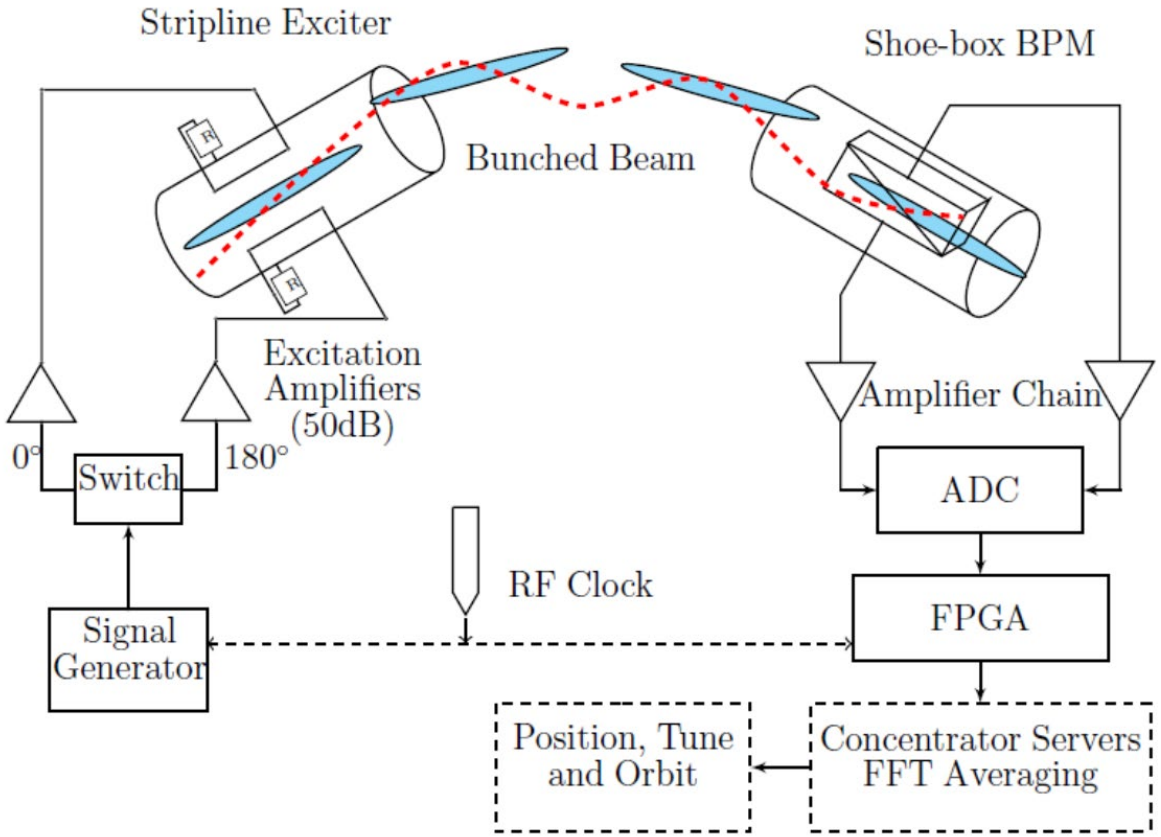

$$x = x_0 + x_\beta + x_D = x_0 + \hat{x}\sqrt{\frac{\beta_x}{\beta_0}}\cos(\psi_x) + D_x\,\delta$$

$$y = y_0 + y_\beta + y_D = y_0 + \hat{y}\sqrt{\frac{\beta_y}{\beta_0}}\cos(\psi_y) + D_y\delta$$

- Dispersion function

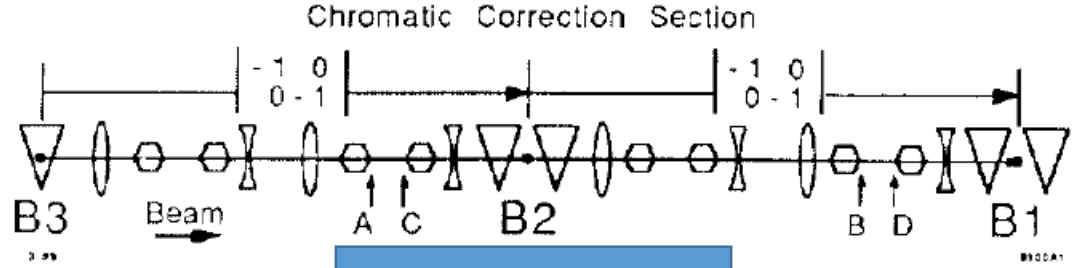

BPMs @ A, B, C, D

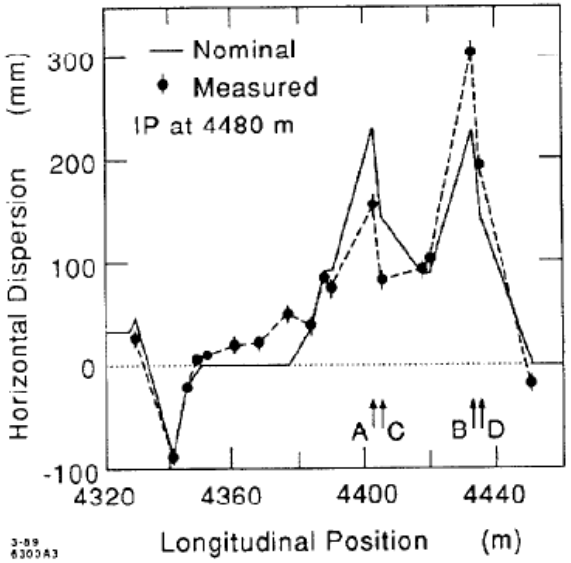

Large energy spread

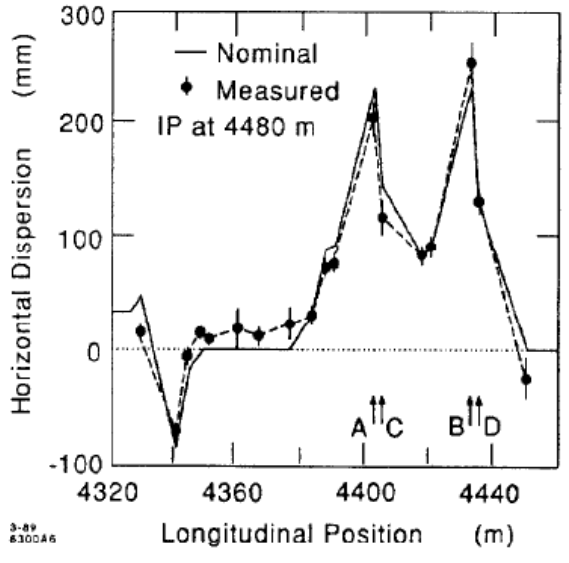

Nominal energy spread

$$\begin{pmatrix} x_0 \\ p_0 \end{pmatrix} \Rightarrow \begin{pmatrix} x \\ p \end{pmatrix} = \begin{pmatrix} D_x(p,s)\dfrac{\Delta p}{p_0} \\ p_0 + \Delta p \end{pmatrix} = \begin{pmatrix} D_x(p,s)\delta \\ p_0(1+\delta) \end{pmatrix}$$

Multi-turn Orbit Measurement on PEP-II

(Courtesy U. Wienands, J. Seeman, et al., 1998)

- At high current, the beam oscillations are self-excited.
- Slow oscillations corresponds to synchrotron motion.
- Fast oscillations are betatron motion.
- FFTs yield betatron and synchrotron tunes.

Turn-by-turn BPM readings of 500th bunch in 1760 bunch train

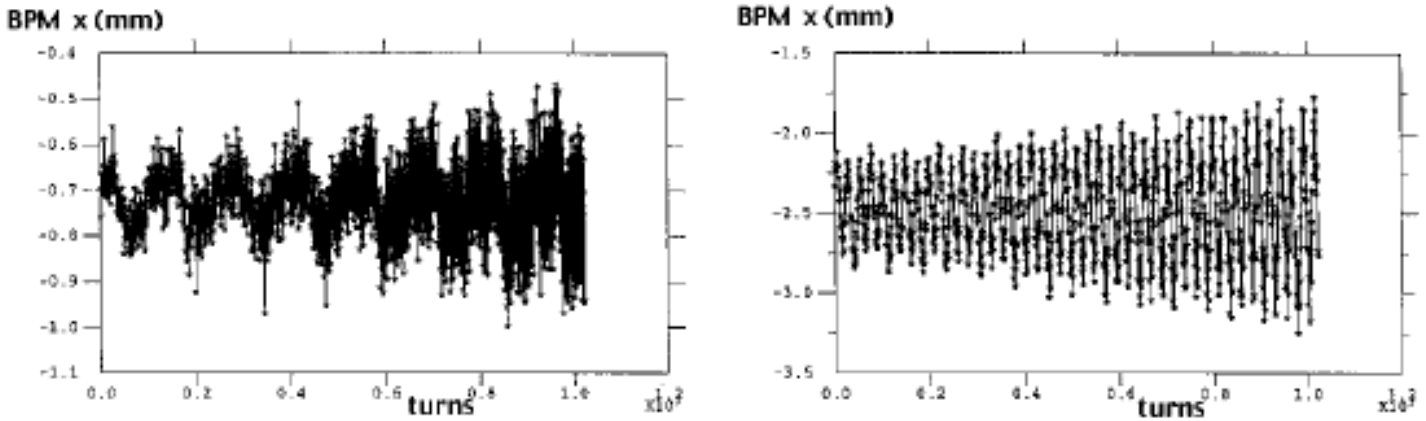

FFT of BPM readings

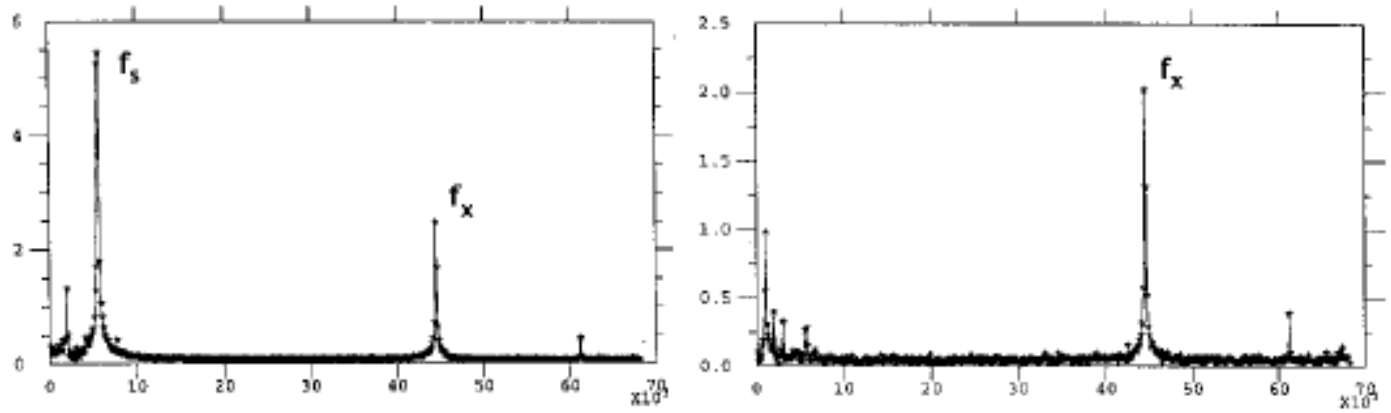

Dispersive region

Non-dispersive region

Lattice parameters

- Loss distributions in SC RF modules
- Beam envelope matching to lattice

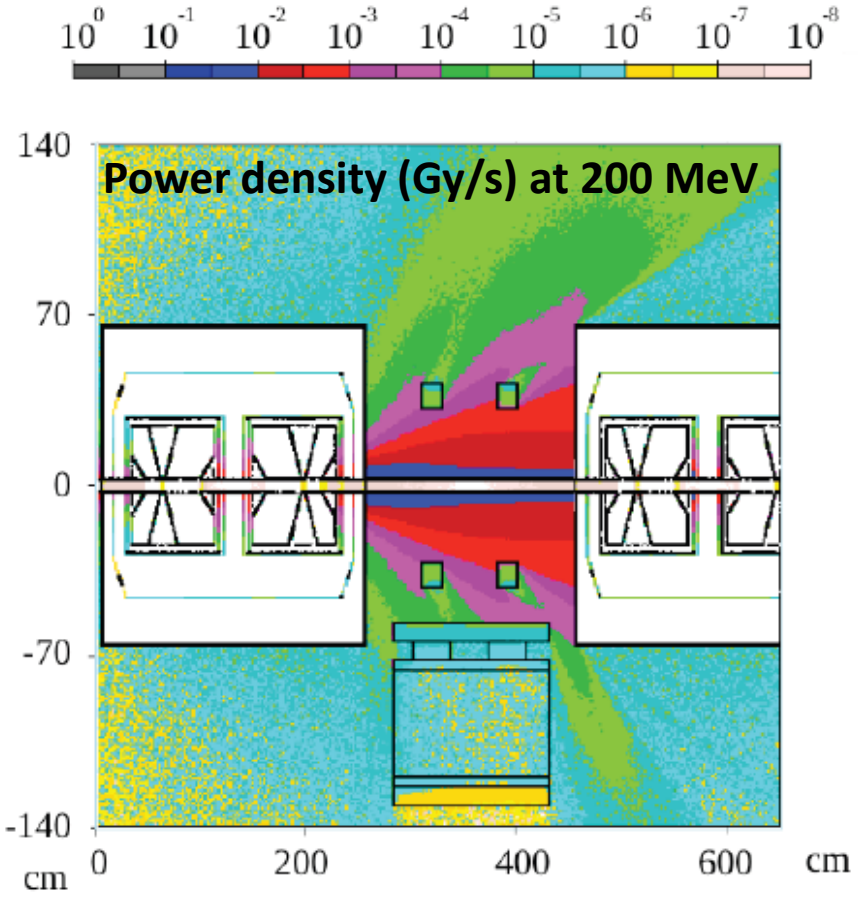

Matched distributions

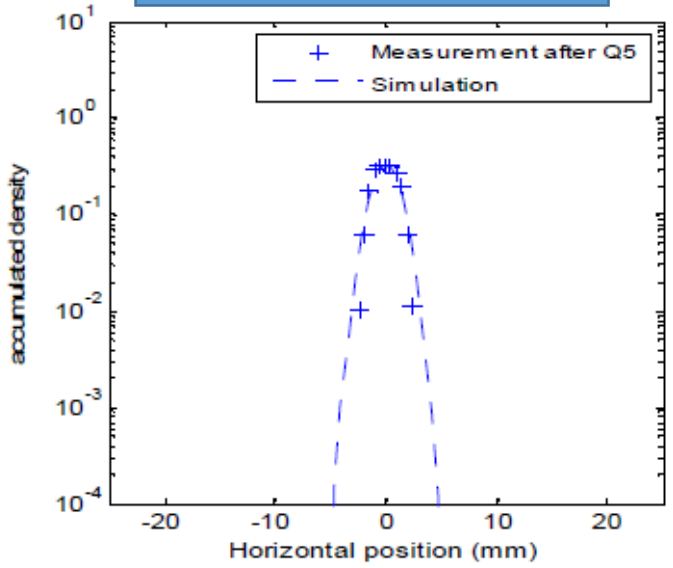

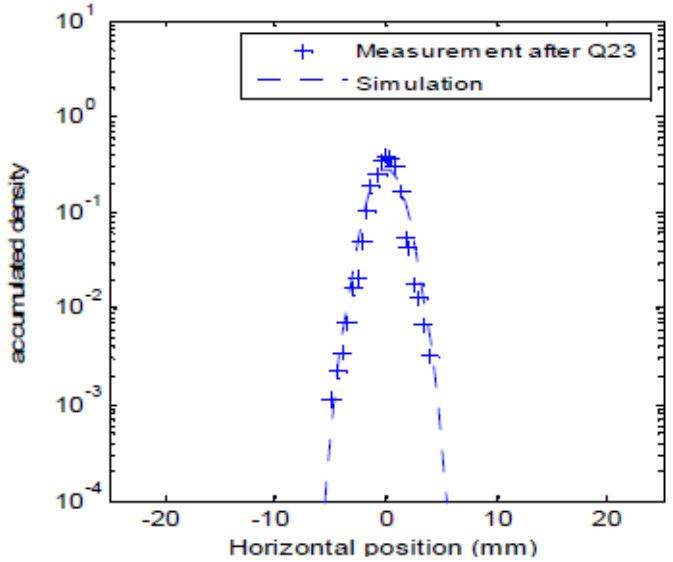

Mismatched distributions

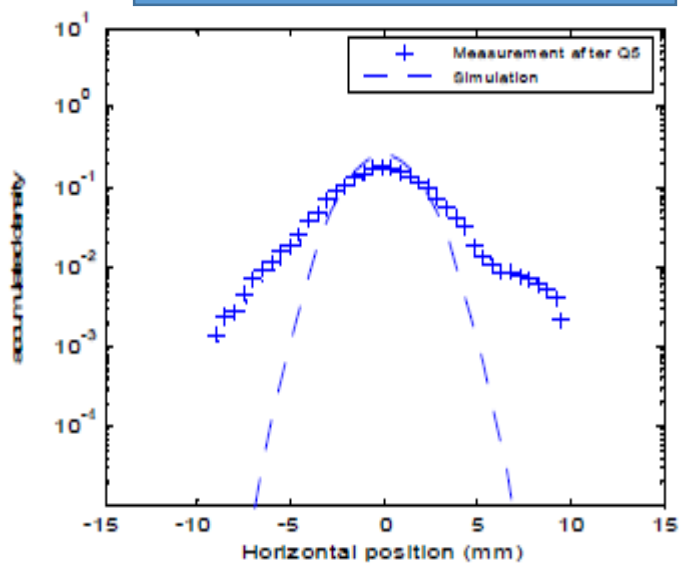

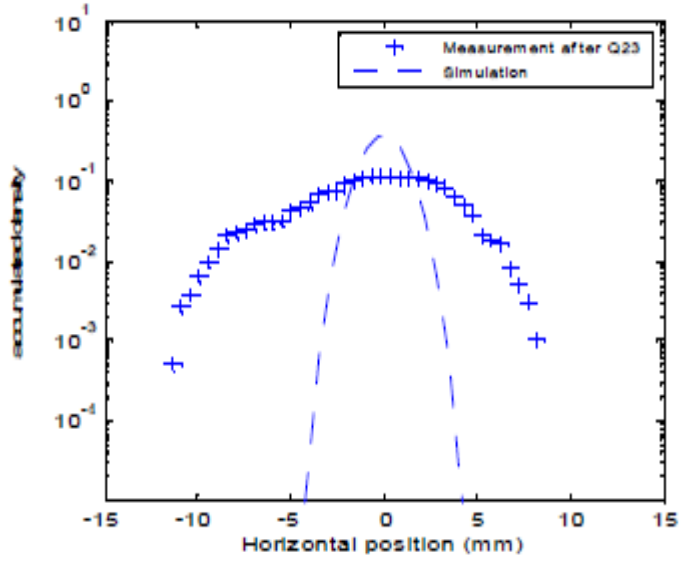

Dynamic parameters

- Emittance growth for mismatched beams
- Instabilities
- Electron cloud effects
- Beam losses

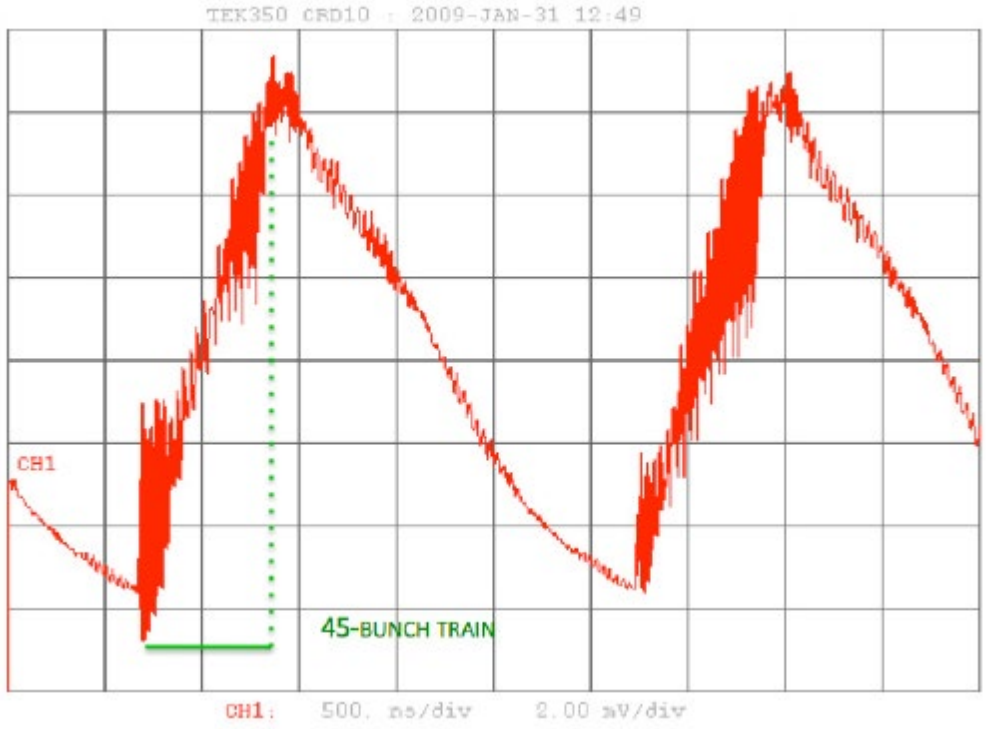

Direct phase measurement in resonant BPM configuration

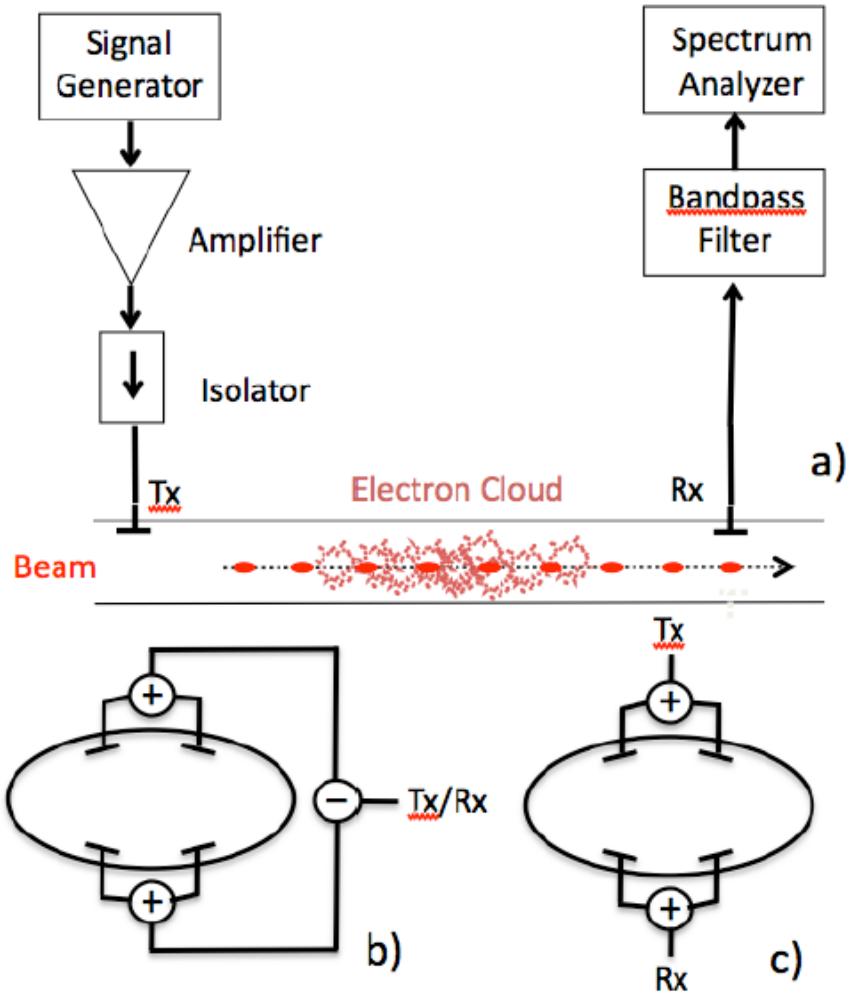

(DeSantis, et al, PAC09 TH5RFP071)

End of Part I

Two Lecture Outline

- Introduction
- Beam Measurement Techniques
  - Beam Generated Signals
  - Beam Properties
  - Lattice Parameters
  - Beam Processes
- **Beam Instrumentation**
  - Beam-Sensor Interactions
  - Diagnostic Architecture
- Exercises and References

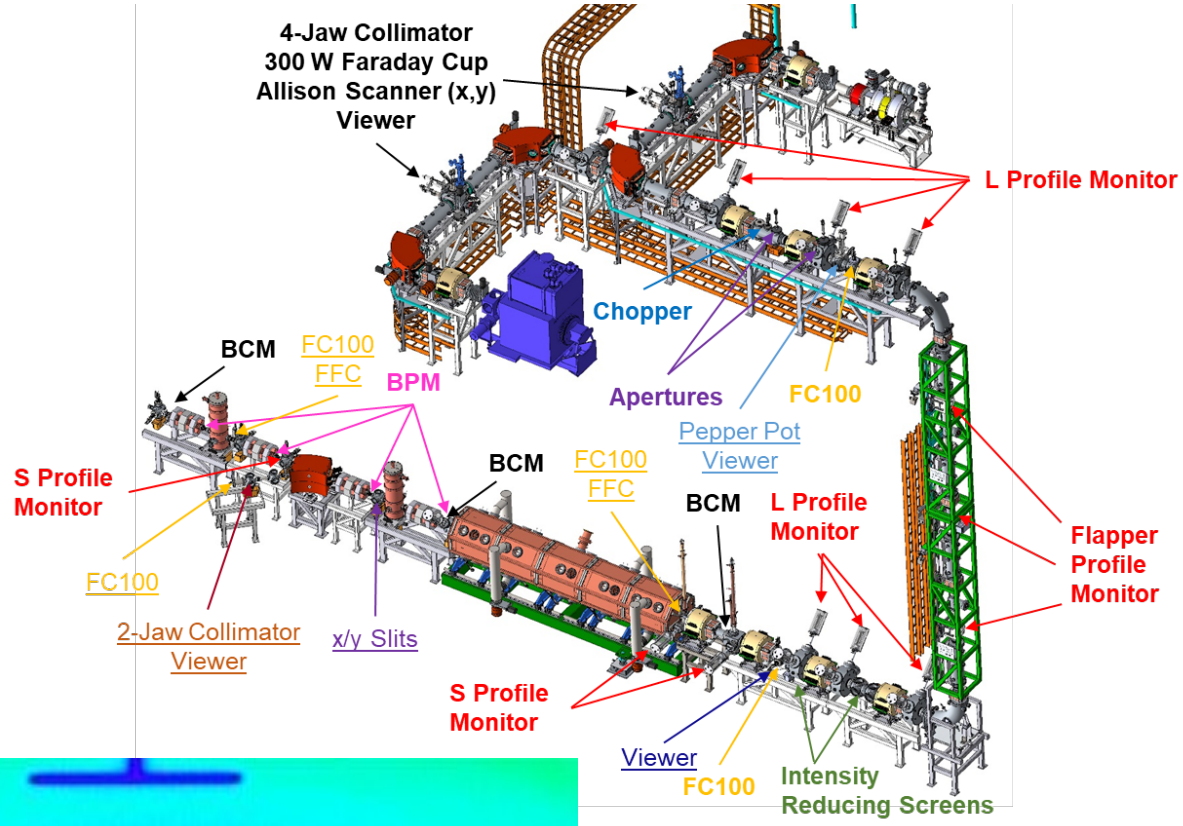

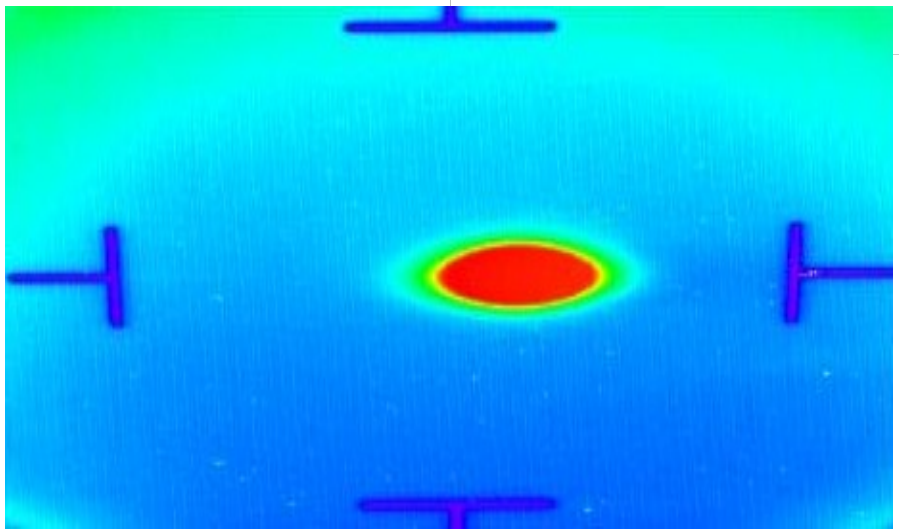

Diagnostic/instrumentation design elements

- **Physics** of beam-sensor interactions
  - EM, Nuclear, AMO, Solid State
  - Charge and mass interception
  - Capacitive, inductive, resonant, thermal field sensing
  - Secondary radiation fields
- **Mechanical** design
  - Thermal, structural, vacuum, actuator
- **Electrical** design
  - Grounding/shielding
  - HV bias and insulation
- **Electronics**
  - Signal acquisition, conditioning, processing
  - Noise, bandwidth, sensitivity, response time

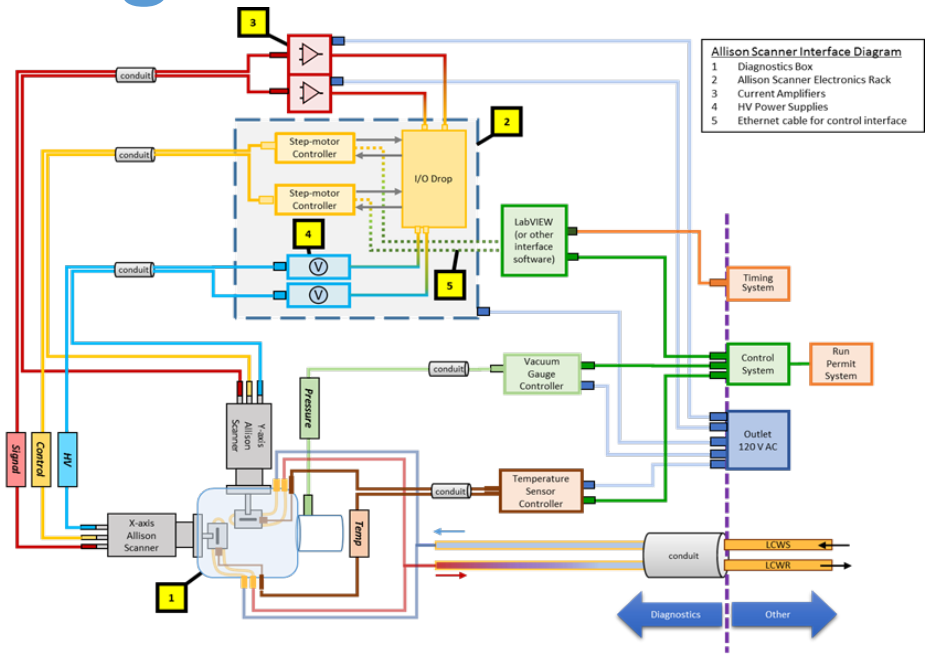

System Interface Diagram

Physics

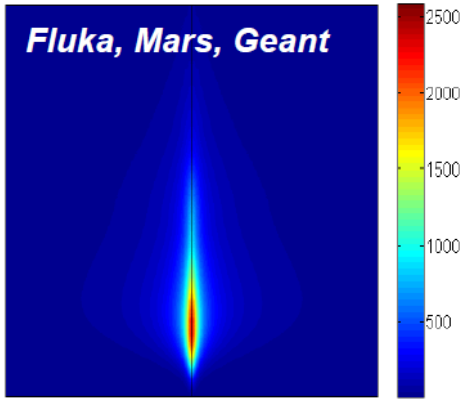

Energy

Thermodynamics

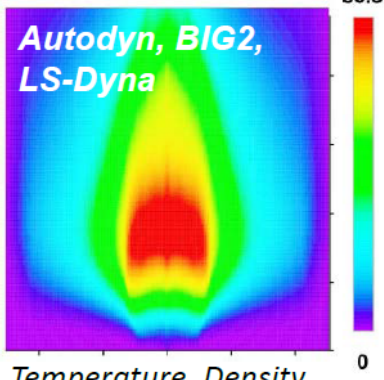

Temperature, Density, Pressure

Structural/mechanical engineering

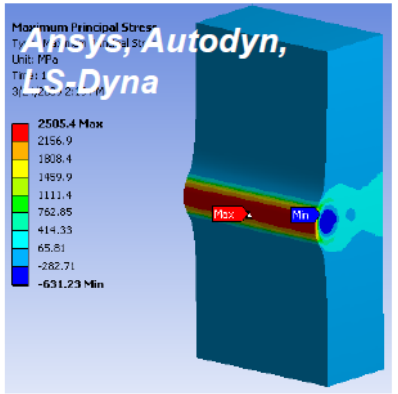

Strains, Stress, Damage

Faraday cups

- Fully intercepting charge measurement
- Sensitivity to 10 pC. ~100 Hz BW ('slow', deep cup)
- Beam charges impinge on Collector, are collected by electronics
- Suppressor negatively biased to repel electrons
- Design is to prevent escape of secondary electrons

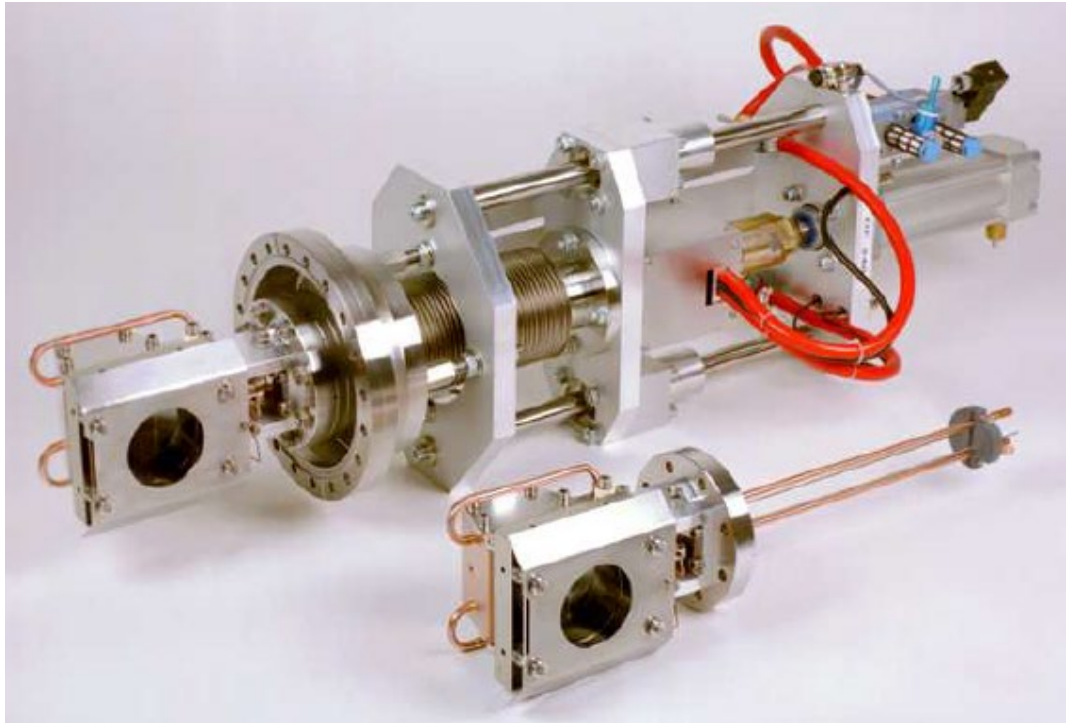

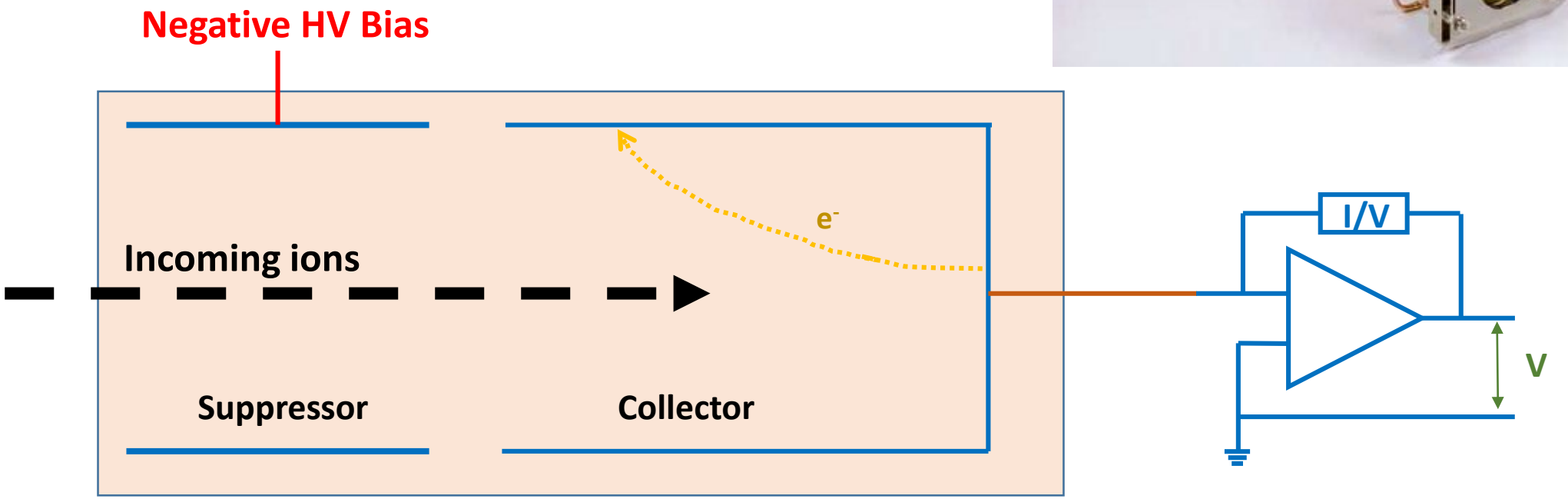

Transimpedance amplifier

Viewers

- Based on scintillator and camera
  - Coated screen (reflection mode)
  - Solid, thick (100 μm) scintillator (transmission mode)
- Scintillator can be single- or multi-crystalline, or sintered powder
- Direct 2D measurement
  - Direct digital output
  - Video out and frame grabber
- Resolution depends on scintillator material (grains), CCD size, optics
- Amplitude response depends on field flatness, scintillator dose and aging effects, temperature

GSI linac, 4 MeV/u, low current, YAG:Ce

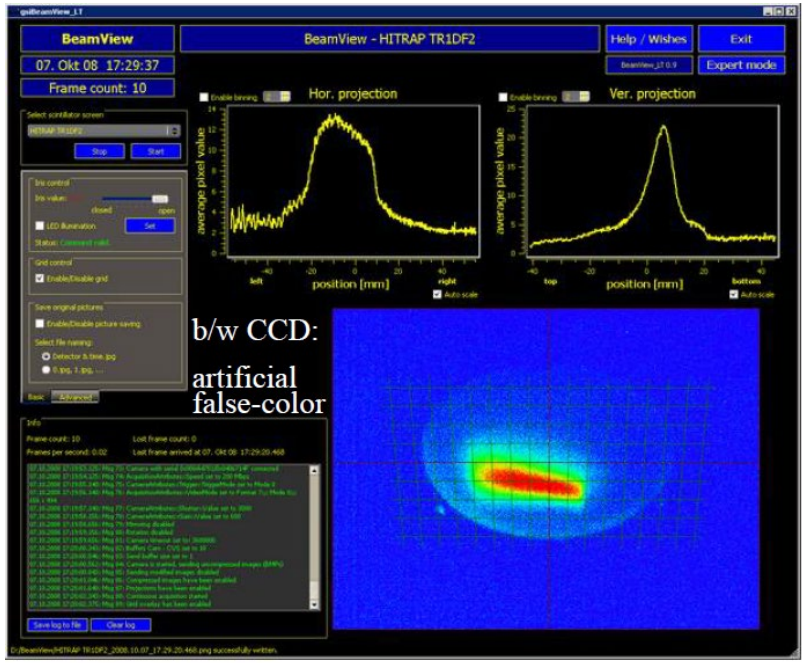

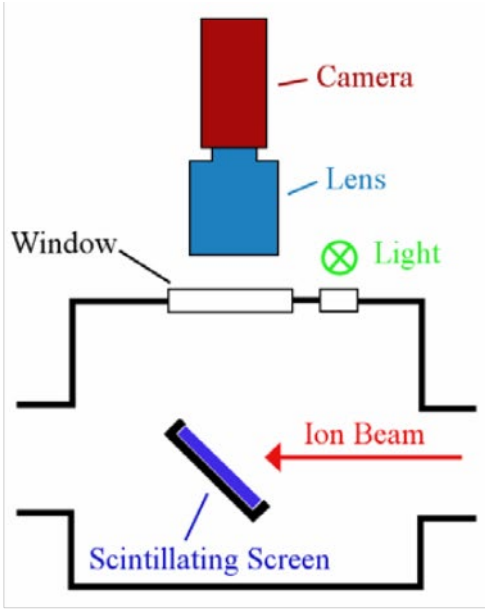

Example: Color CCD camera: Images at different particle intensities determined for U at 300 MeV/u

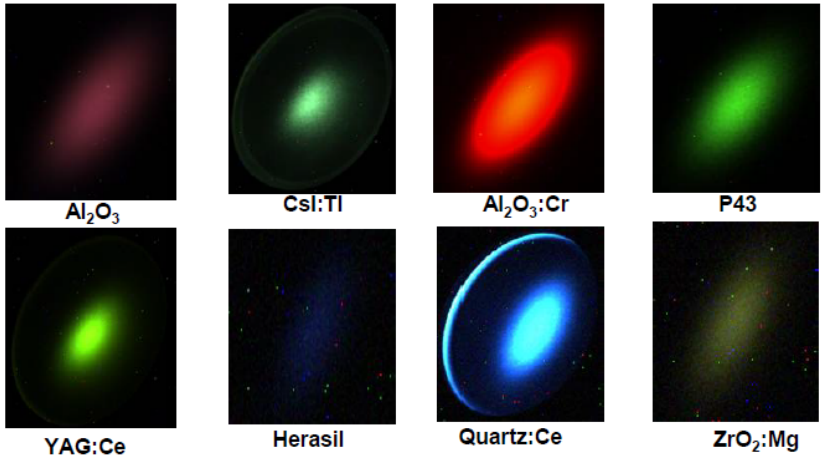

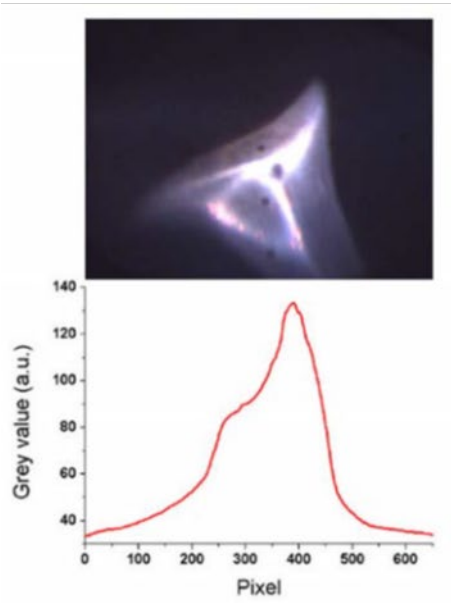

Allison Scanner

- Analyzes intensity J(x or y) at first slit
- Applied voltage across plates + drift + exit slit analyzes momentum
- Reconstructs phase space density

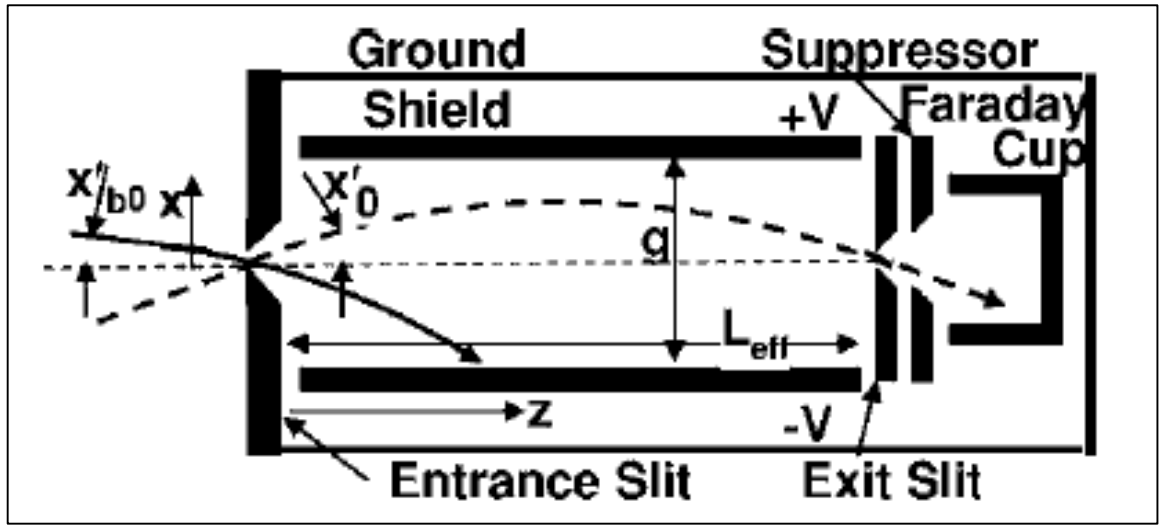

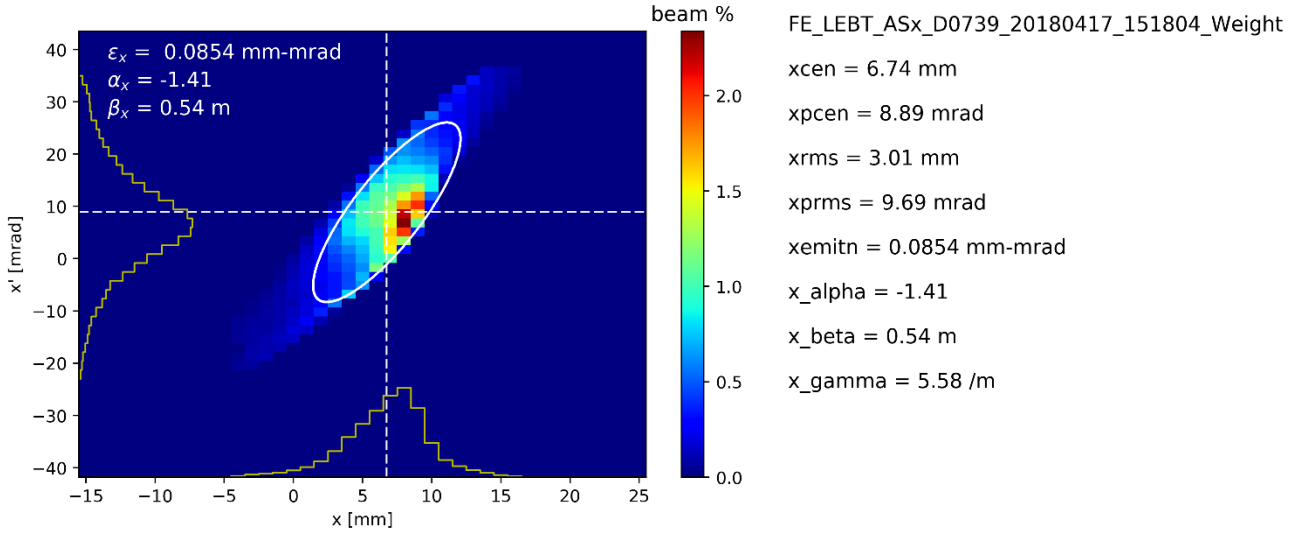

FE_LEBT_ASx_D0739_20180417_151804_Weight

xcen = 6.74 mm

xpcen = 8.89 mrad

xrms = 3.01 mm

xprms = 9.69 mrad

xemitn = 0.0854 mm-mrad

x_alpha = -1.41

x_beta = 0.54 m

x_gamma = 5.58 /m

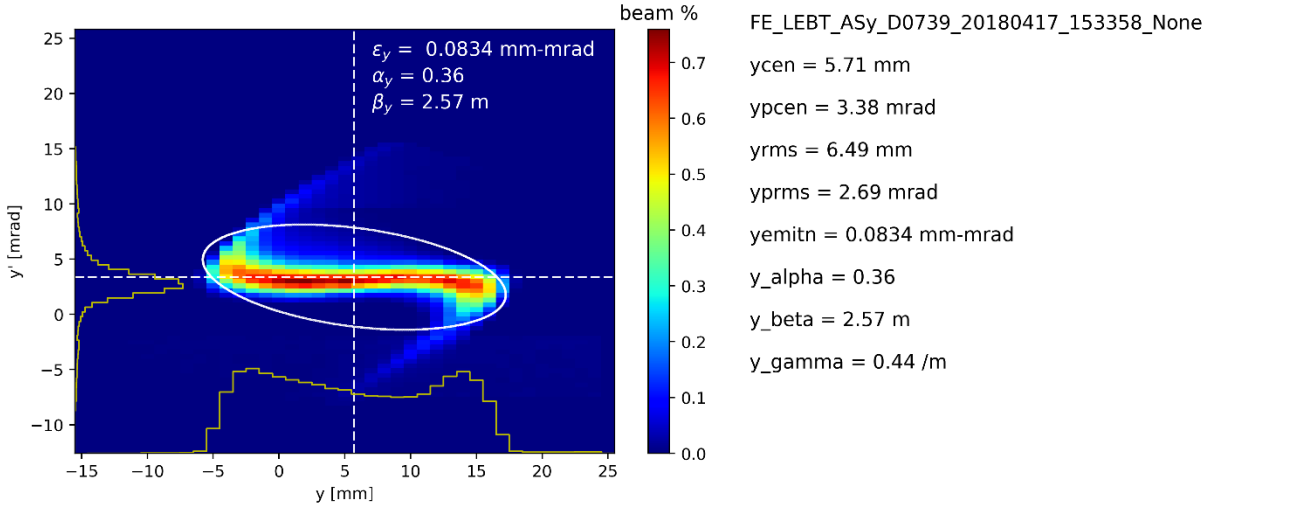

FE_LEBT_ASy_D0739_20180417_153358_None

ycen = 5.71 mm

ypcen = 3.38 mrad

yrms = 6.49 mm

yprms = 2.69 mrad

yemitn = 0.0834 mm-mrad

y_alpha = 0.36

y_beta = 2.57 m

y_gamma = 0.44 /m

Pepperpots, slits, and pinholes

- Devices scan a 1D or 2D beam distribution
- Analyze intensity J(x,y)
- Analyze transverse velocity over drift

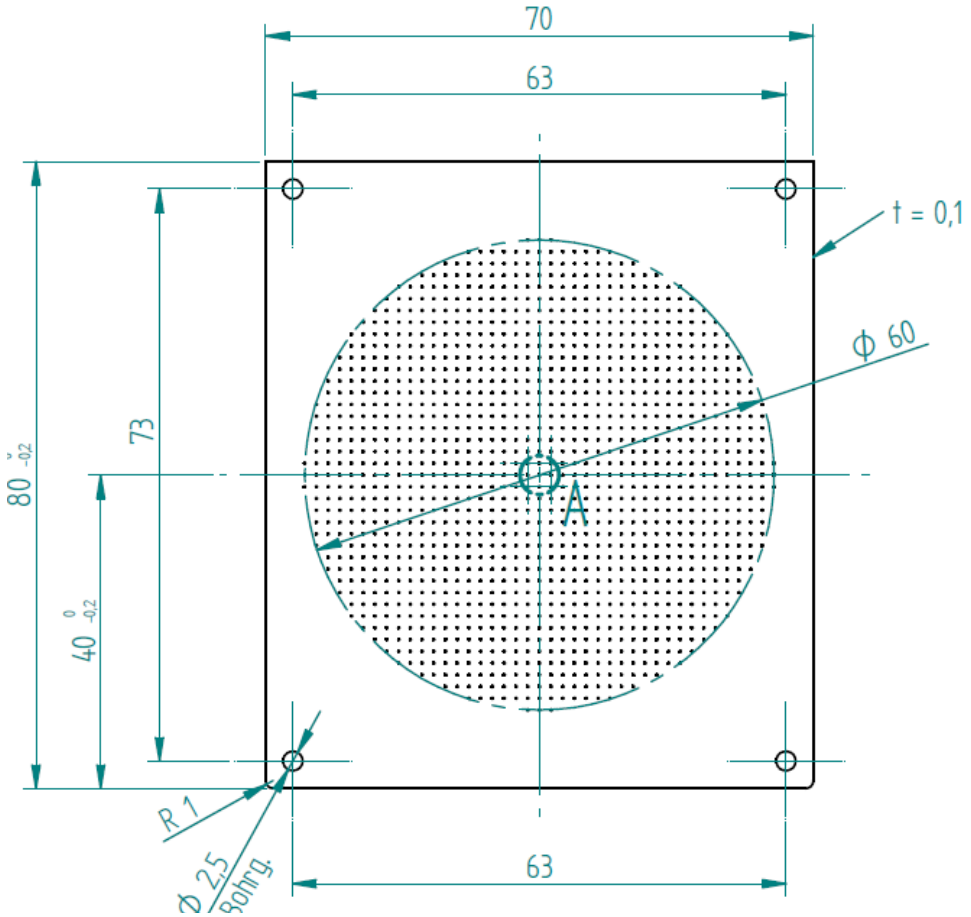

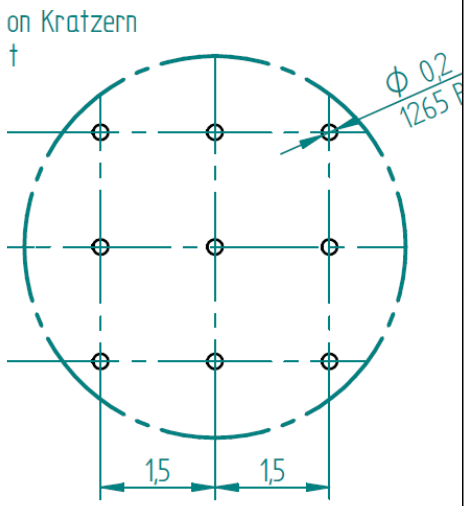

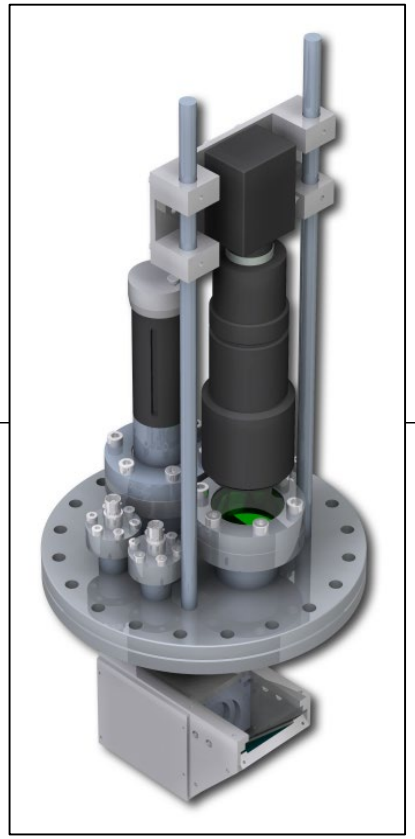

Emittance analysis

$$\Sigma_4 = \begin{pmatrix} \langle xx \rangle & \langle xx' \rangle & \langle xy \rangle & \langle xy' \rangle \\ \langle xx' \rangle & \langle x'x' \rangle & \langle x'y \rangle & \langle x'y' \rangle \\ \langle xy \rangle & \langle x'y \rangle & \langle yy \rangle & \langle yy' \rangle \\ \langle xy' \rangle & \langle x'y' \rangle & \langle yy' \rangle & \langle y'y' \rangle \end{pmatrix} = \begin{pmatrix} \Sigma_x & C \\ C^T & \Sigma_y \end{pmatrix}$$

$$\langle f\,g \rangle = \frac{\sum_i \rho_i f_i g_i}{\sum_i \rho_i} \qquad \det \Sigma_x = |\Sigma_x| = \langle xx \rangle \langle x'x' \rangle - \langle xx' \rangle^2 = \tilde{\varepsilon}_x^2$$

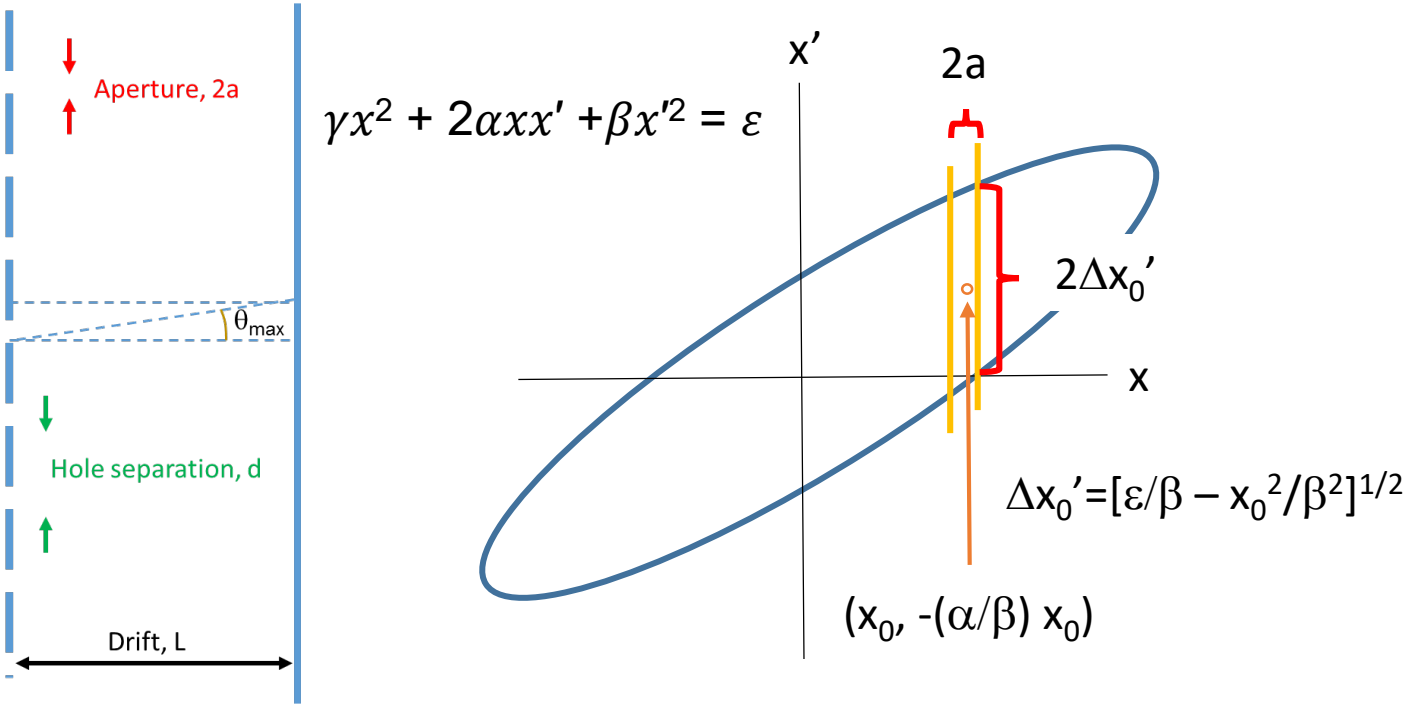

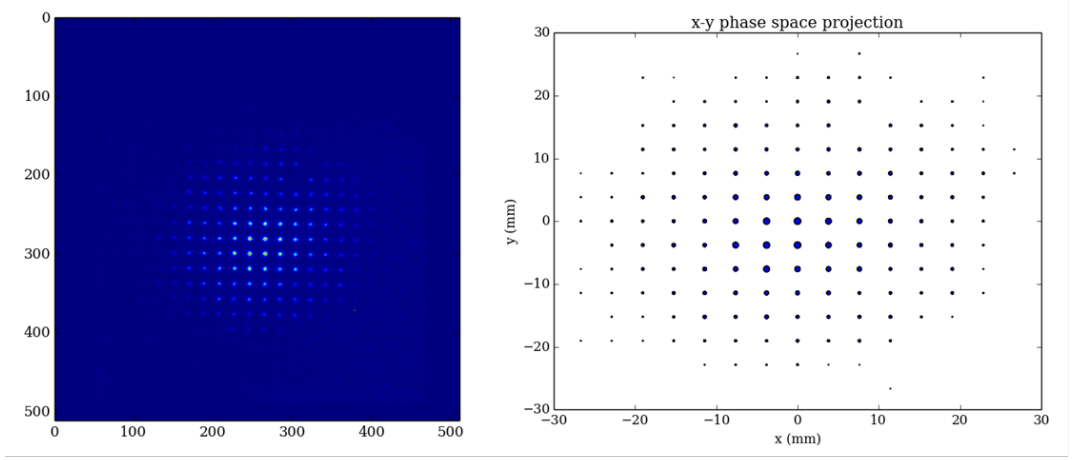

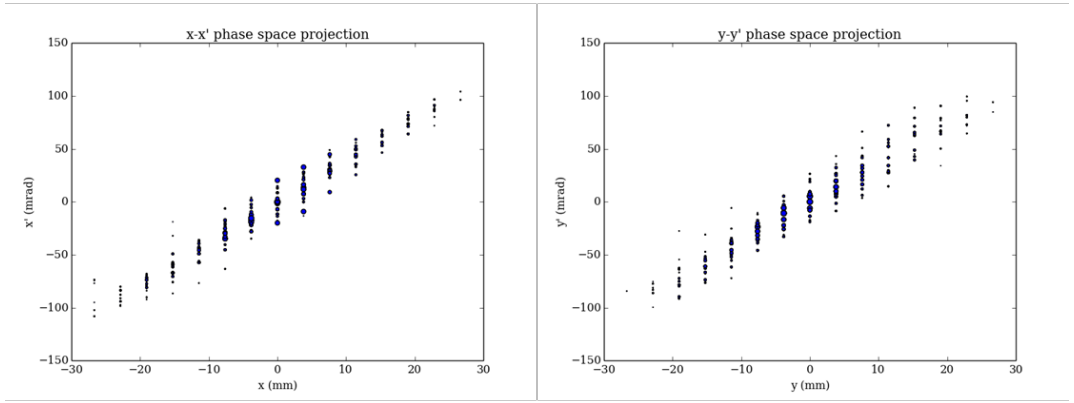

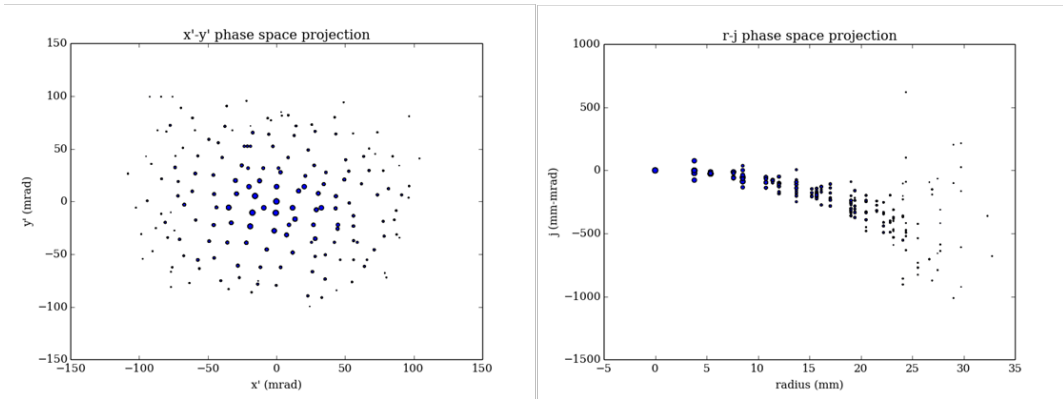

Slice envelope properties from slit/slit-cup diagnostic

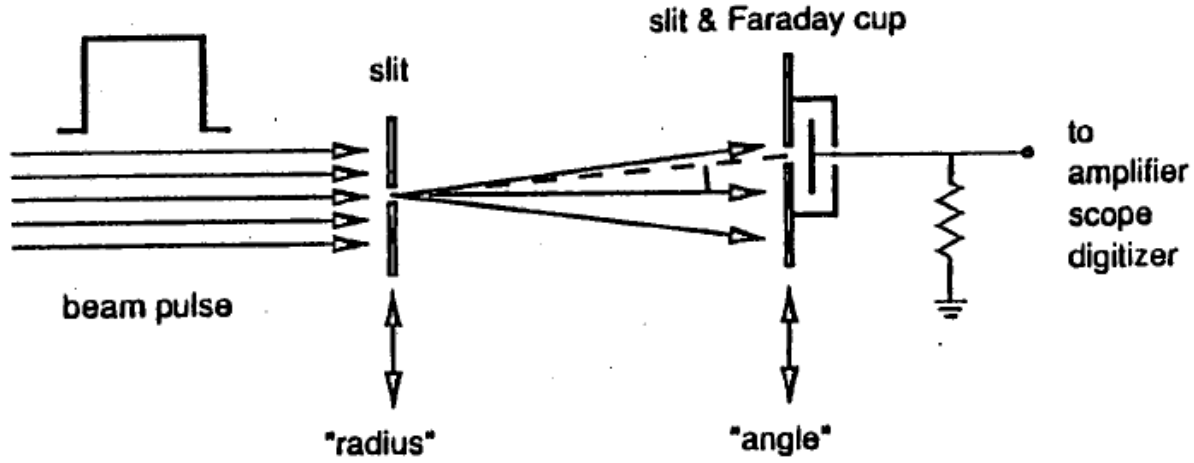

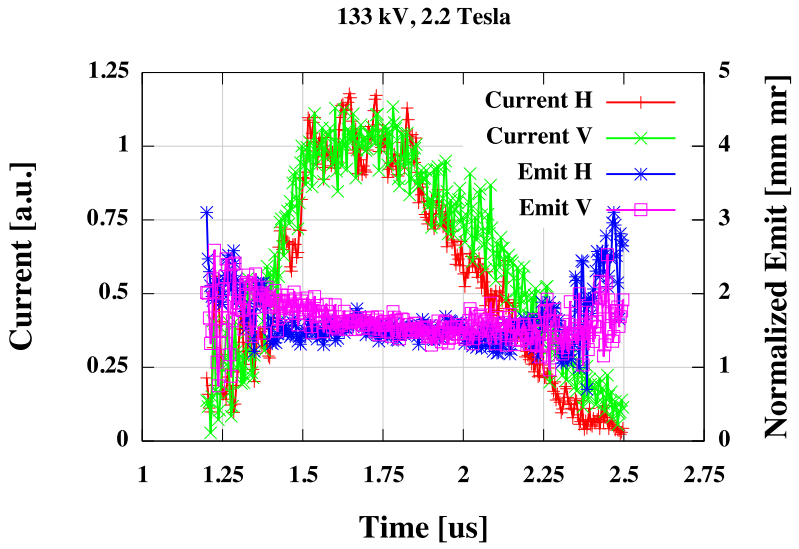

50 mA Li+

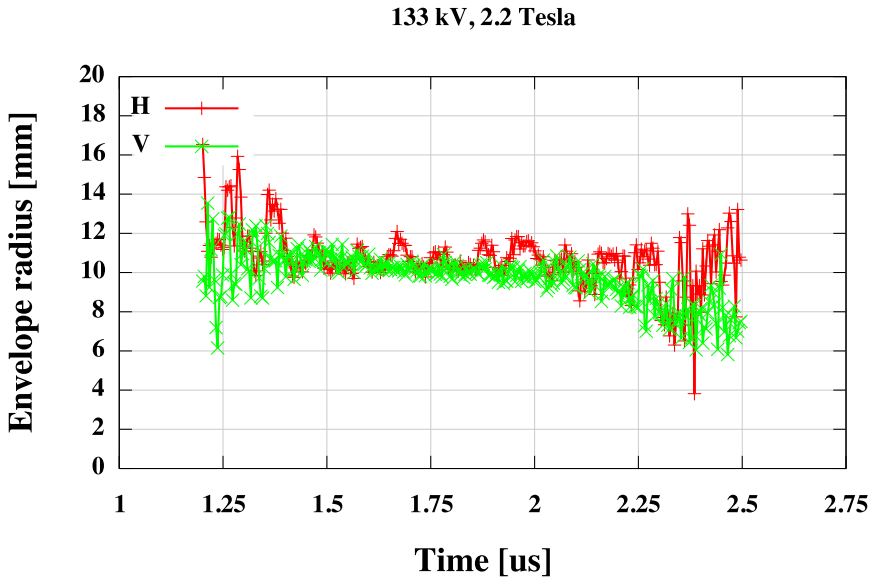

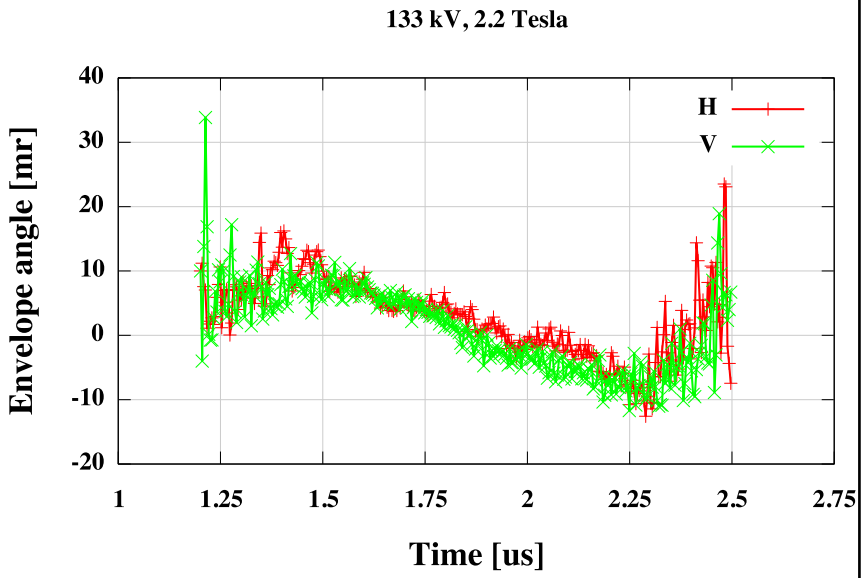

Profile monitors

- Interceptive diagnostic onto W, C, Cu-Be wires
- Wide range of wire based geometries
- Biased wire to discourage (or encourage) secondary e⁻'s
- Slit + Faraday cup

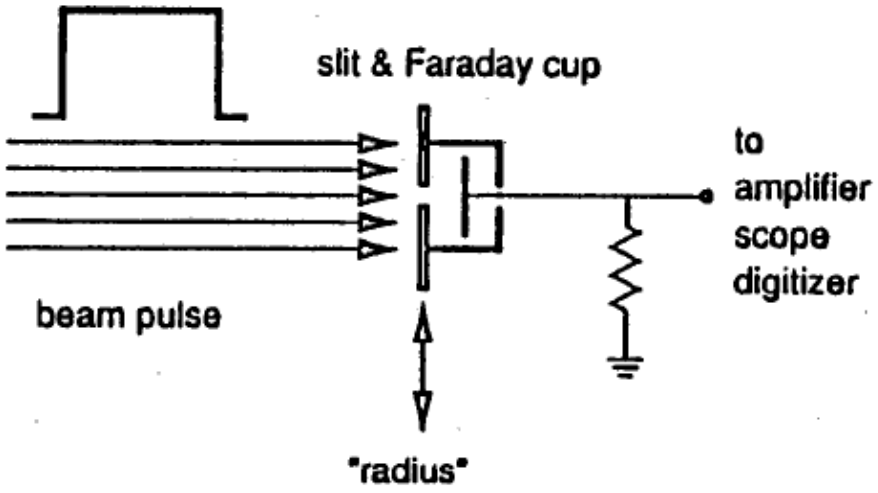

Linear actuated
(3 wires)

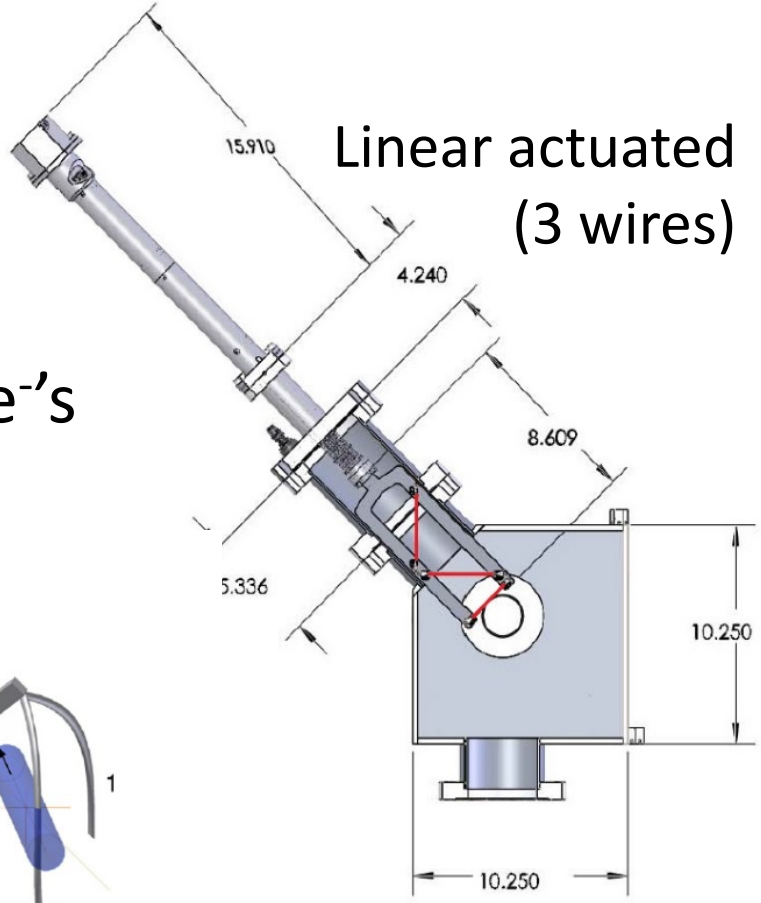

Rotating wire

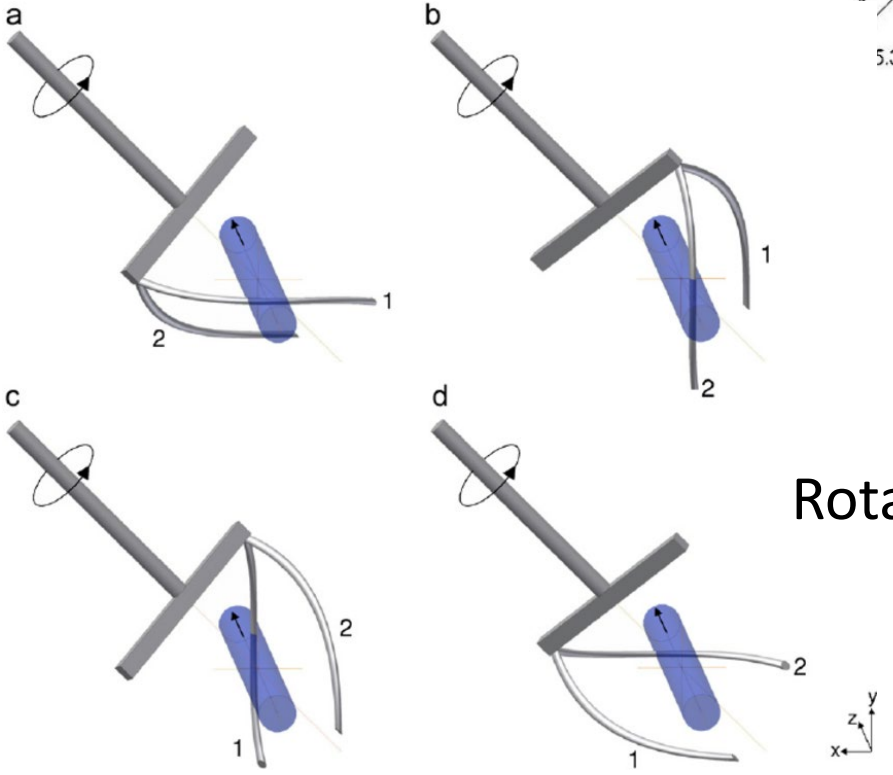

Reconstruct beam parameters from profile data

- We observe day-to-day variation of transverse beam parameters
  - Two most significant factors are: ECR setting and beam center matching to the RFQ

Typical

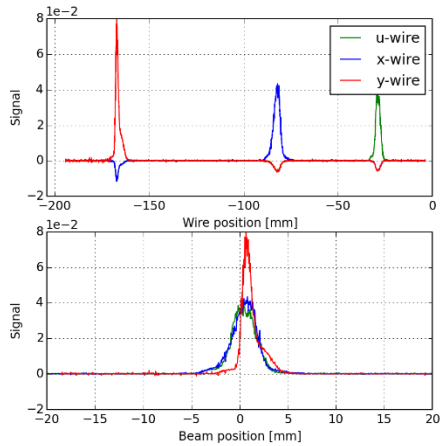

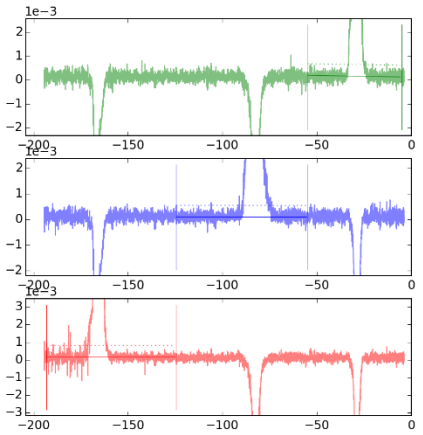

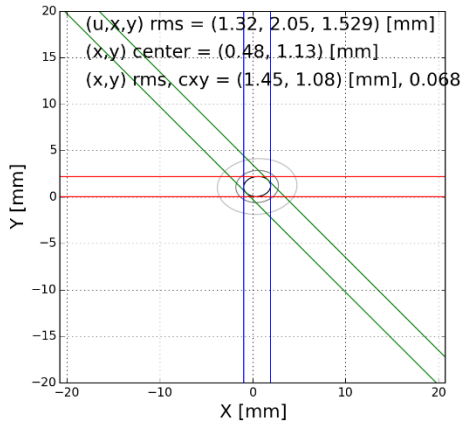

FE_MEBT_PM_D1092_20180808_155920.dat

	u-wire	x-wire	y-wire
Time	15:58:38	15:58:38	
Sum	0.117	0.18	0.17
Center	0.413	0.685	1.6
RMS	1.32	2.05	1.529

	x	y	u	v
Pos	0.485	1.131	0.413	-0.272
RMS	1.449	1.082	1.32	1.236
cxy	0.068			
R90%	2.296	1.734	2.084	1.984
cxy90%	0.051			
R99%	4.282	3.002	3.778	3.616
cxy99%	0.047			

Large emittance

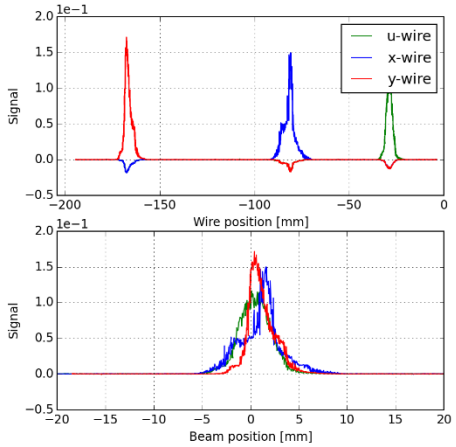

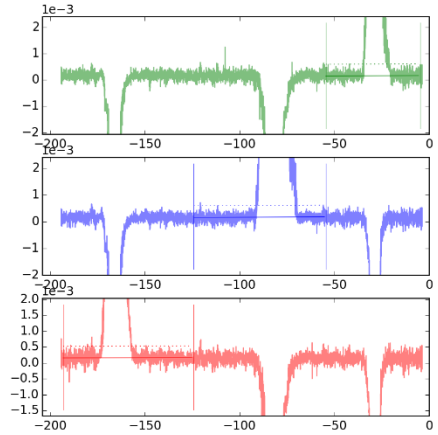

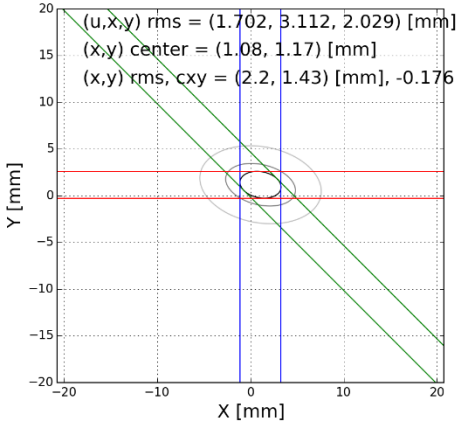

FE_MEBT_PM_D1092_20180810_103606.dat

	u-wire	x-wire	y-wire
Time	10:30:22	10:30:22	
Sum	0.436	0.638	0.601
Center	0.514	1.533	1.656
RMS	1.702	3.112	2.029

	x	y	u	v
Pos	1.084	1.171	0.514	-1.02
RMS	2.201	1.434	1.702	2.001
cxy	-0.176			
R90%	3.742	2.28	2.706	3.447
cxy90%	-0.267			
R99%	6.512	4.176	5.024	5.882
cxy99%	-0.172			

(FRIB data courtesy T. Maruta)

Bunch Shape Monitor

- Used for hadron beamlines
- Scanning wire produces secondary electrons
- Electrons are accelerated in DC field, sorted in RF field
- Time-correlation converted to position on detector

A.V.Feschenko, et. al, Proc. of the XIX Int. Linear Acc. Conf., 1998, p.905-907.

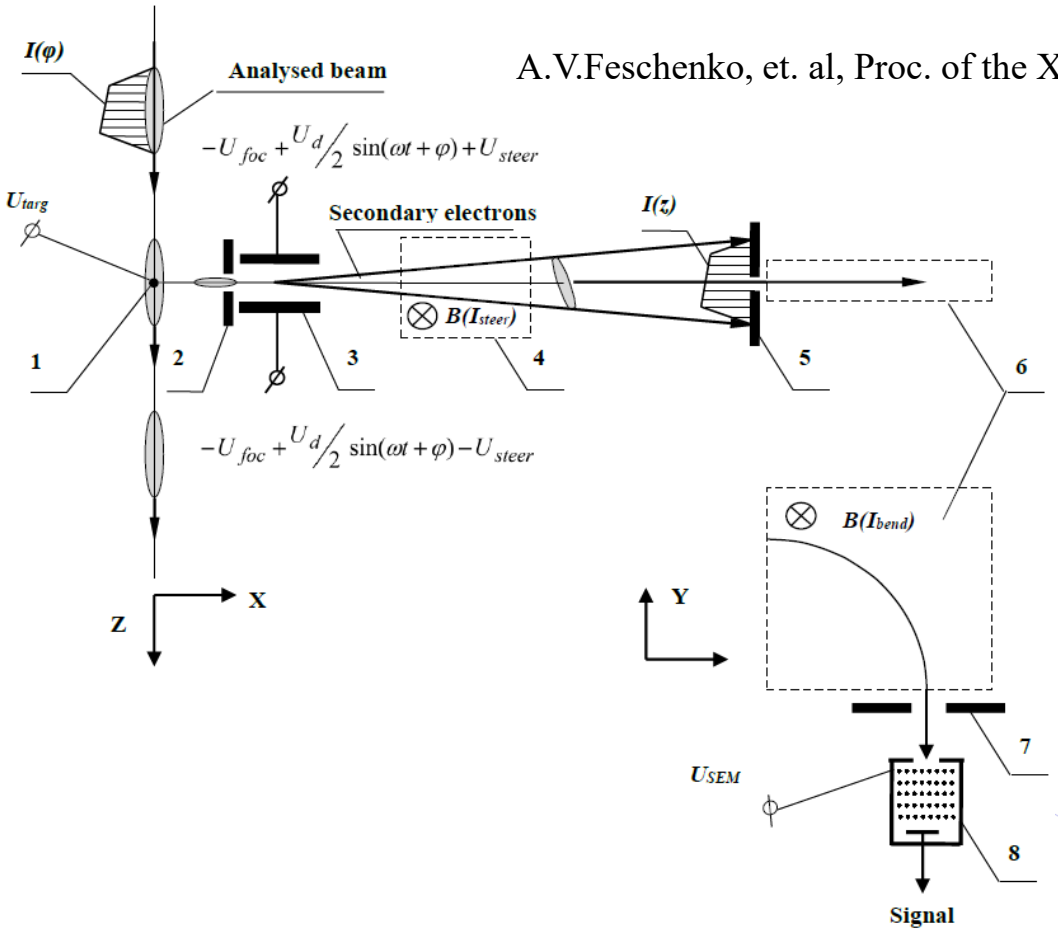

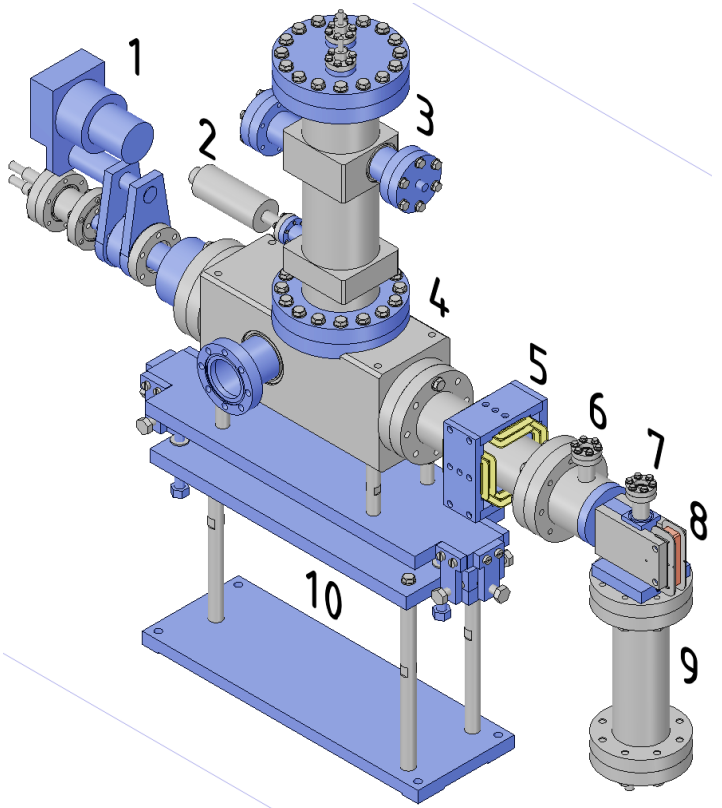

Fig. 2. Operation design of Bunch Shape Monitor
(1 – target, 2 – inlet collimator, 3 – RF-deflector, 4 – correcting magnet,
5 – outlet collimator, 6 – bending magnet,
7 – registration collimator, 8 – secondary electron multiplier).

Stop here

Frequency dependence of wall currents, skin depth

$$\nabla \bullet \mathbf{D} = \rho$$

$$\nabla \times \mathbf{E} = -\frac{\partial \mathbf{B}}{\partial t}$$

$$\nabla \bullet \mathbf{B} = 0$$

$$\nabla \times \mathbf{H} = \mathbf{J} + \frac{\partial \mathbf{D}}{\partial t}$$

In metals:

$$\boldsymbol{\nabla} \times \boldsymbol{E} = j\omega \boldsymbol{B} = j\omega\mu \boldsymbol{H}$$
$$\boldsymbol{\nabla} \times \boldsymbol{H} = \boldsymbol{J} - j\omega \boldsymbol{D}$$

Good conductor: $|\omega \boldsymbol{D}| \ll |\boldsymbol{J}|$

Ohm's Law: $\boldsymbol{J} = \boldsymbol{E}/\sigma$

$$\boldsymbol{\nabla} \times \boldsymbol{J} = j\omega\sigma \boldsymbol{B}$$
$$\boldsymbol{\nabla} \times \boldsymbol{B} = \mu \boldsymbol{J}$$

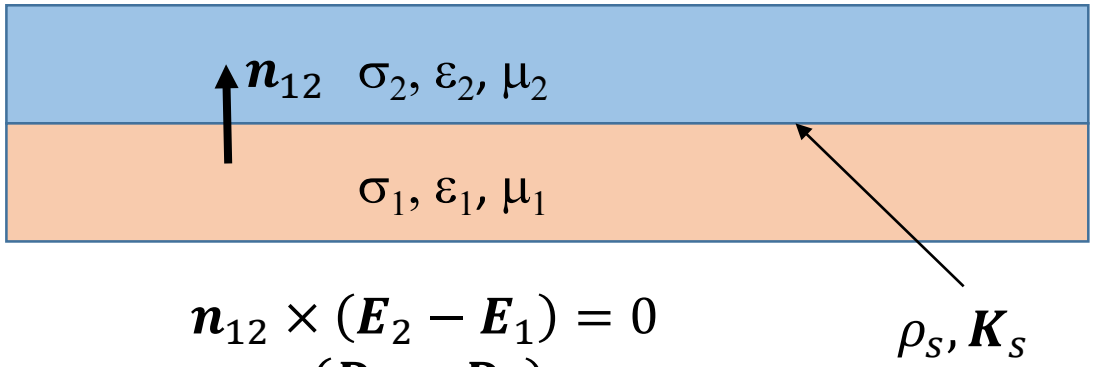

$$\boldsymbol{n}_{12} \times (\boldsymbol{E}_2 - \boldsymbol{E}_1) = 0$$
$$\boldsymbol{n}_{12} \cdot (\boldsymbol{D}_2 - \boldsymbol{D}_1) = \rho_s$$
$$\boldsymbol{n}_{12} \times (\boldsymbol{H}_2 - \boldsymbol{H}_1) = \boldsymbol{K}_s$$
$$\boldsymbol{n}_{12} \cdot (\boldsymbol{B}_2 - \boldsymbol{B}_1) = 0$$

Assuming Cartesian geometry and variation only along n_{12} we can show that

$$\boldsymbol{B}_\perp(z) = \boldsymbol{B}_\perp(z=0)e^{-(1+j)\kappa z} \quad J_\parallel(z) = J_\parallel(z=0)e^{-(1+j)\kappa z} \quad \text{where } \kappa = {}^1/_{\delta_c} = \sqrt{\frac{\mu\omega\sigma}{2}}$$

Material	$f = 60$ Hz	$f = 10^3$ Hz	$f = 10^6$ Hz	$f = 10^9$ Hz
Copper	8.61 mm	2.1 mm	0.067 mm	2.11 μm
Iron	0.65 mm	0.16 mm	5.03 μm	0.016 μm
Seawater	32.5 m	7.96 m	0.25 m	7.96 mm
Wet soil	650 m	159 m	5.03 m	0.16 m

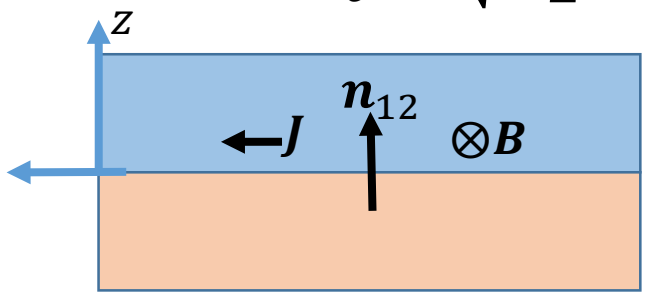

Surface resistance and Joule losses

- The tangential electric field in the conductor derives from Ohm's Law (not present in perfect conductor)

$$\boldsymbol{E} = \frac{1}{\sigma}\nabla \times \boldsymbol{H} \cong \frac{1}{\sigma}\boldsymbol{n} \times \frac{\partial \boldsymbol{H}}{\partial z} = -Z_s \boldsymbol{n} \times \boldsymbol{H}_\perp$$

- The transverse electric field satisfies an *impedance boundary condition*, with surface impedance, Z_S

$$Z_s = \frac{1 + jsgn(\omega)}{\sigma \delta_c} = R_s\big(1 + jsgn(\omega)\big)$$

- A *surface resistance* (Ohms) is defined as

$$R_s = \frac{1}{\sigma \delta_c} = \sqrt{\frac{\mu\omega}{2\sigma}}$$

- Power deposition (W/area) to the surface follows from

$$\frac{dP_{surf}}{dA} = \boldsymbol{S} \cdot \boldsymbol{n} = \frac{1}{2}\Re(\boldsymbol{E} \times \boldsymbol{H}^*) \cdot \boldsymbol{n}$$
$$= \frac{1}{2}R_s|K_s|^2$$

Resistive wall impedance

The beam senses the wall through resistive loading

- The *longitudinal resistive wall impedance* can be defined as

$$\frac{Z_0^{\parallel}}{length} = \frac{Z_s}{2\pi b} = \frac{1}{2\pi b}\sqrt{\frac{\mu\omega}{2\sigma}}\left(1 + jsgn(\omega)\right)$$

- The beam will experience a voltage change

$$V(\omega) = -I(\omega)Z_0^{\parallel}(\omega)$$

- Impedance: $Z_0^{\parallel} = ReZ_0^{\parallel} + j\ ImZ_0^{\parallel}$ (longitudinal, monopole)

What is the significance of the of the resistive and reactive components?

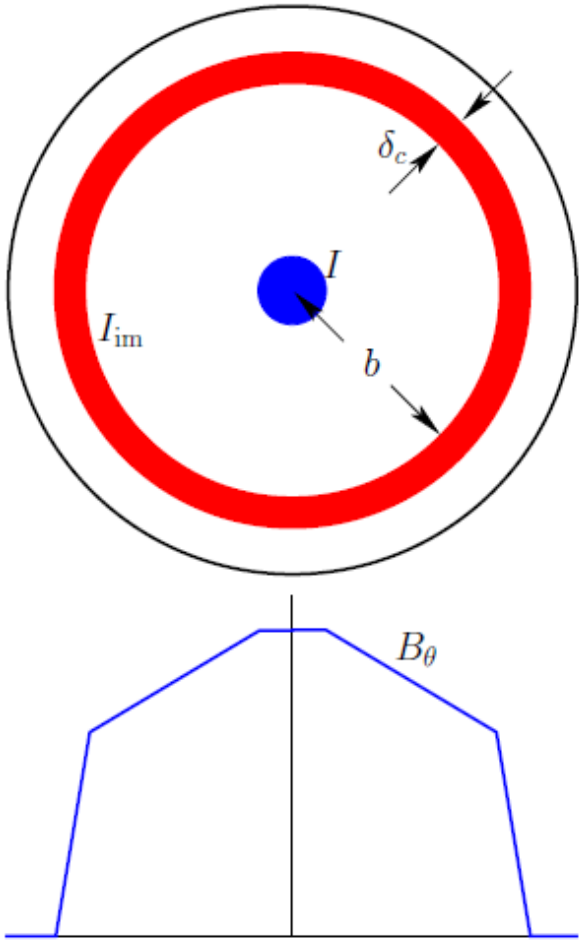

Building a detector

- A non-intercepting monitor can be based on monitoring the wall return currents.
- A ceramic break in the beampipe will force the wall current to seek other paths.
- If nothing else is done, the wall currents will find alternative paths.
- The gap impedance is a combination of the gap capacitance and all external parallel elements
  - At low frequencies the lowest impedance return path can be distant from the gap itself
- The gap voltage $V_{gap} = I_{wall} Z_{gap} = I_{beam} Z_{gap}$ can be generated up to the beam voltage

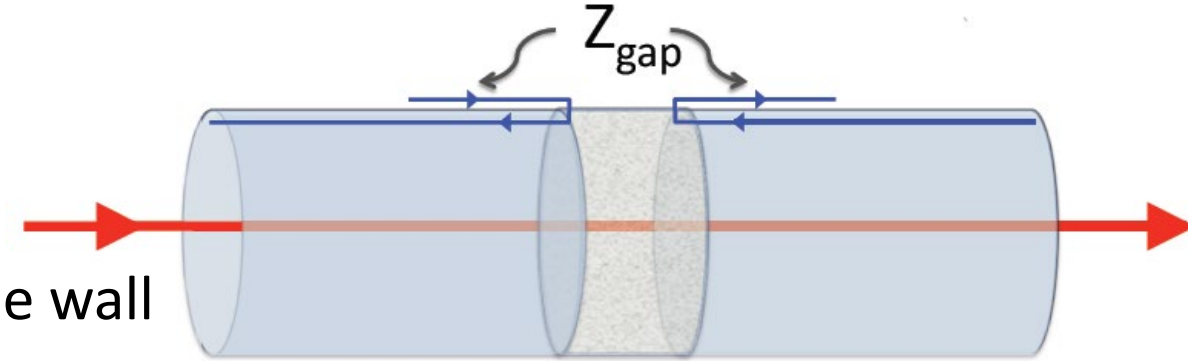

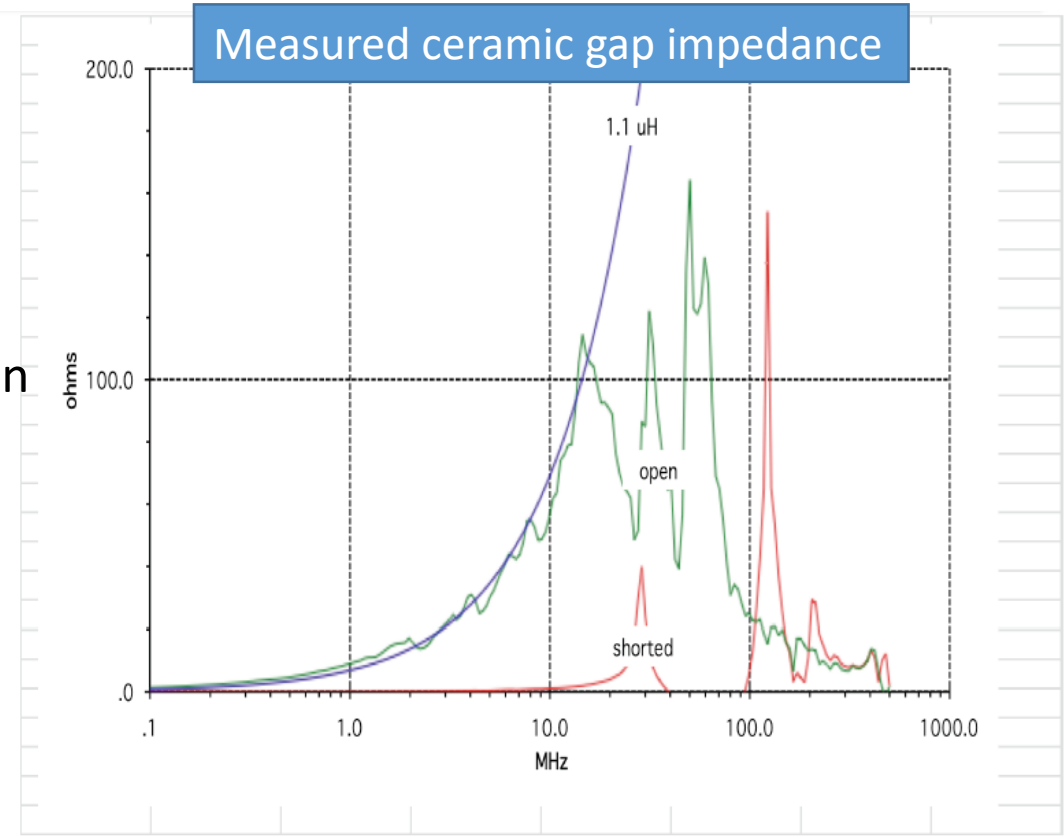

Courtesy of Jim Crisp & Mike Reid @FNAL

Impedance models and behavior

- We model the beam-monitor interaction with an equivalent circuit
- Beam drive is modeled as a pure current source (infinite input impedance)
- A gap impedance C_{gap} is inevitably present
  - Electrodes pierce the beam wall with isolated feedthroughs
  - Typically few – 100s pF
- The specific signal pickup as well as the signal transmission line and passive analog components are represented by $\boldsymbol{Z_{mon}}$.

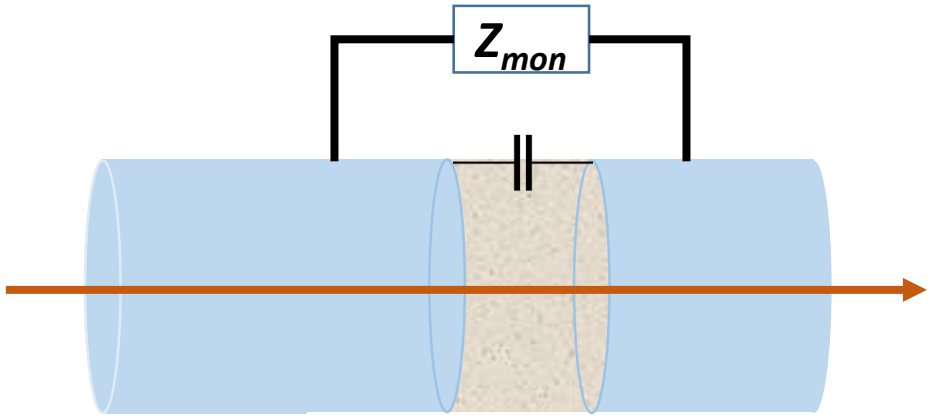

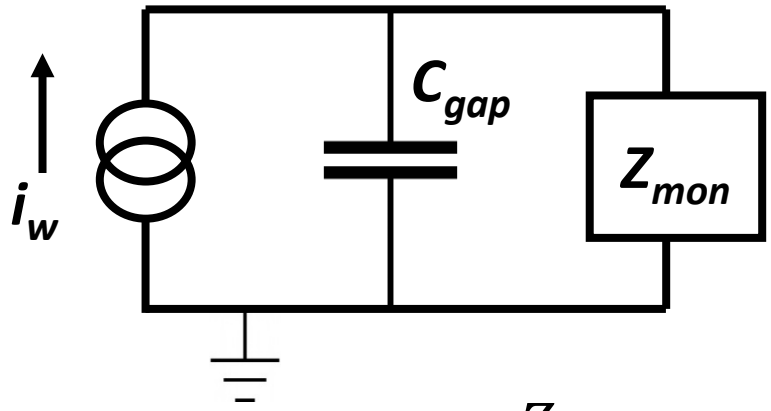

$$V_{mon}(\omega) = i_w(\omega)\frac{Z_{mon}}{1 - j\omega C_{gap} Z_{mon}}$$
$$= i_b(\omega) Z_t(\omega)$$

Wall current monitor

- We add a network of *n* resistors across the gap. $R_{tot} = R_{single}/n$
- $Z_{mon} = R_{tot} \,||\, C_{gap}$
- Broadband pickup
  - $V_{mon}(\omega) = i_b(\omega) \frac{R_{tot}}{1 - j\omega C_{gap} R_{tot}}$
  - Within passband $V_{mon}(\omega) = \left(R_{single}/n\right) i_b(\omega)$
- Practical implementations (eg. SPS WCM)
  - Ceramic gap
  - Many resistors (30 – 100) to reduce sensitivity to beam position
  - Ferrite rings to tailor low frequency response ~10 kHz
  - High frequency response to several GHz
  - Shield for ground currents and noise isolation

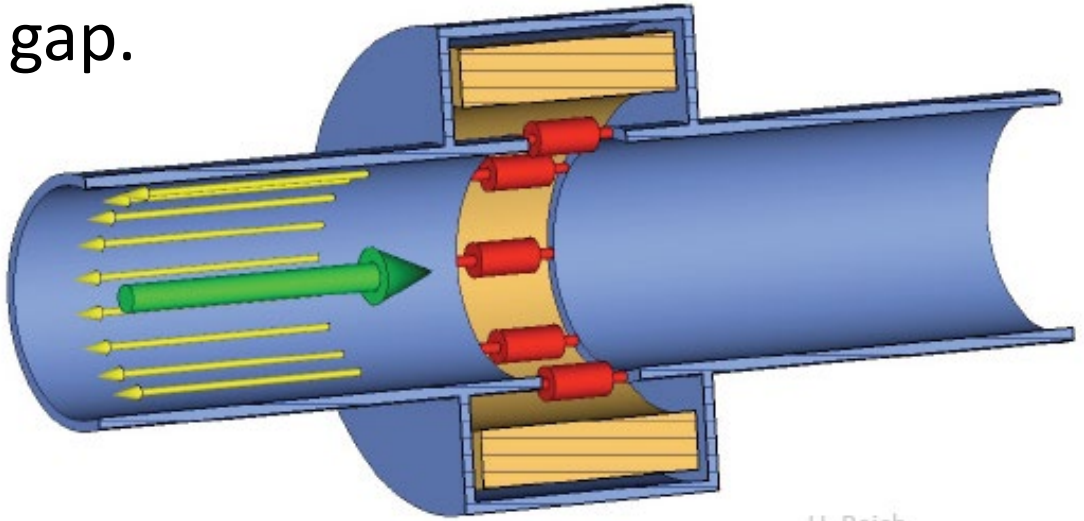

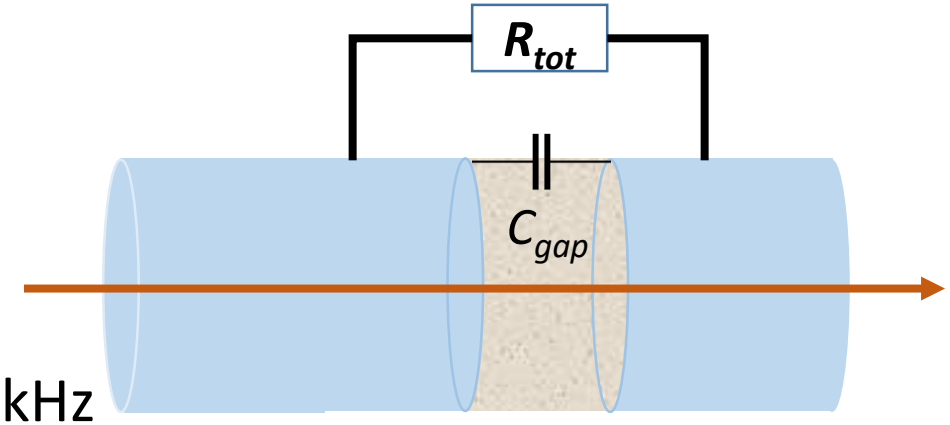

Wall Current Monitor equivalent circuit and response

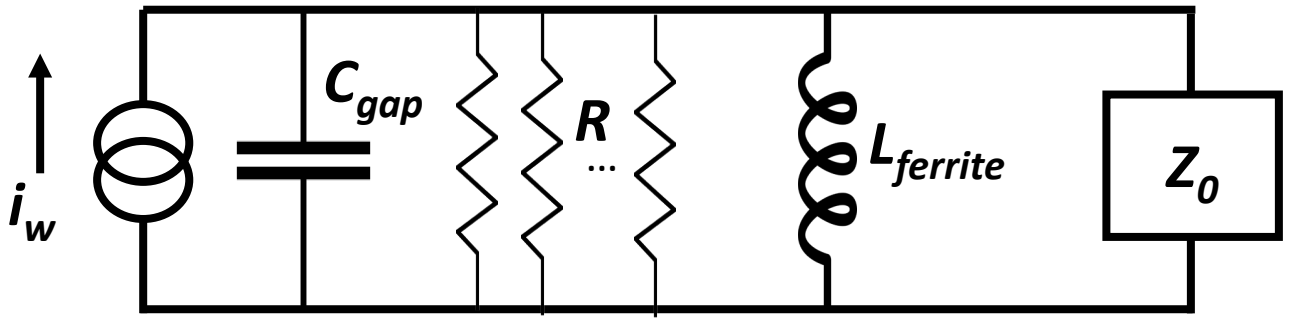

- Very high frequency response dominated by gap capacitance
- Very low frequency response dominated by ferrite and shield induction

ω_{cutoff}
$\omega_{high} = 1/RC$
$\omega_{low} = R/L$

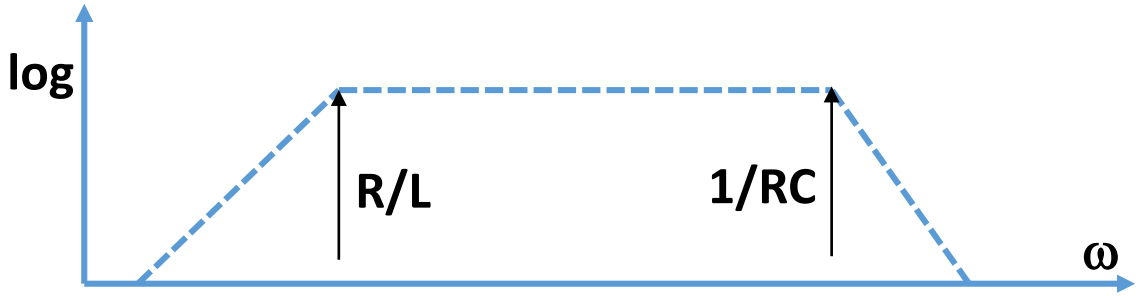

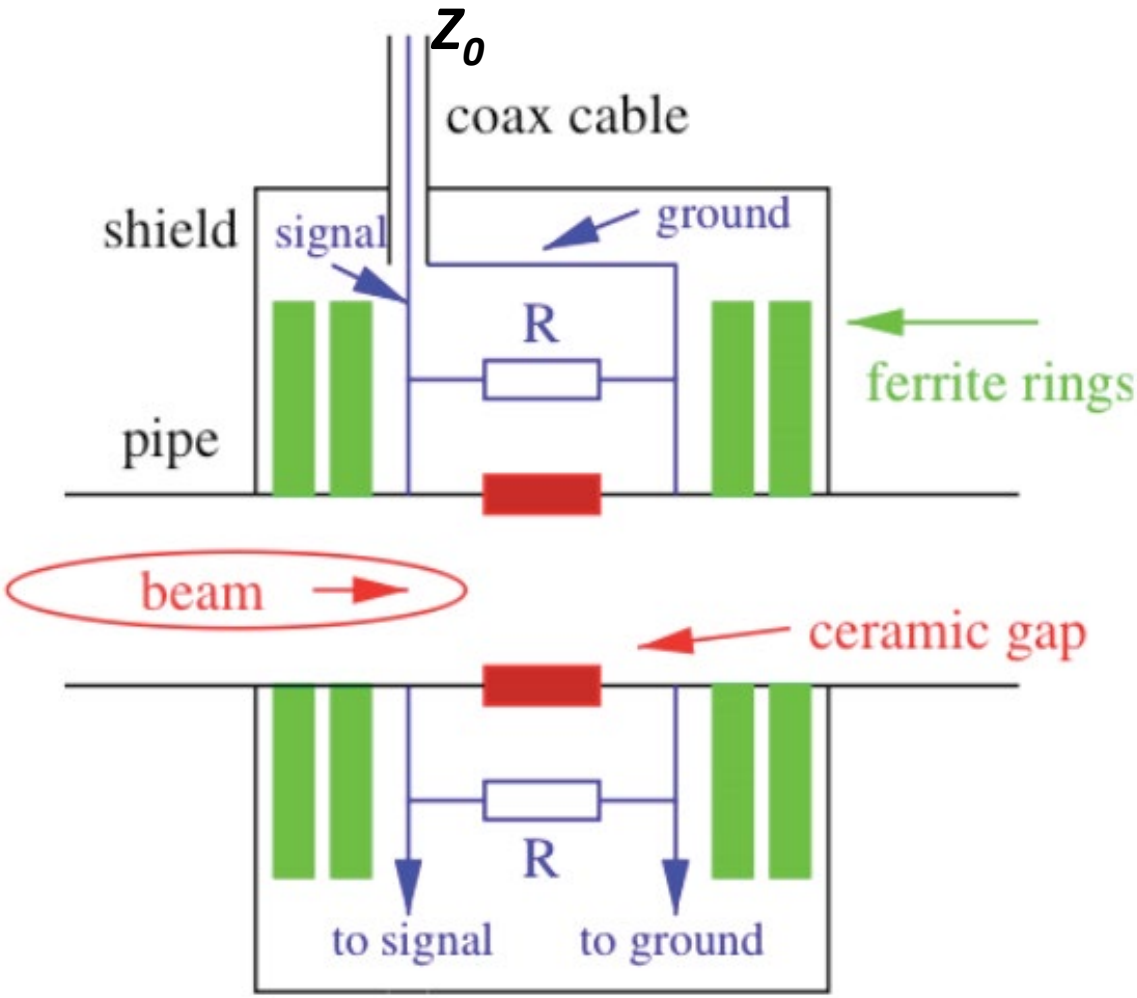

Induced charge densities from capacitive coupling

- Induced charge densities on the beam pipe walls can be approximated or numerically calculated.
- Total induced charges on the electrodes (assuming 2D Laplace solution) for electrodes of length L

$$Q_{plate} = Lb \int_{sector} \sigma(\theta) d\theta$$

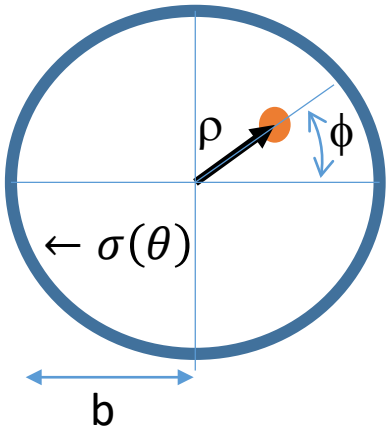

$$\sigma(\theta) = \frac{-\lambda_b}{2\pi b}\left[\frac{b^2 - \rho^2}{b^2 + \rho^2 - 2b\rho\cos(\theta - \phi)}\right]$$

$$\sigma(\theta) = \frac{-\lambda_b}{2\pi b}\left[1 + 2\sum_{n=1}^{\infty}\left(\frac{\rho}{b}\right)^n \cos(n\{\theta - \phi\})\right]$$

Signals from capacitive coupling

- The pickup plate presents a capacitance *C* to ground.
- The finite length of the pickup drives a differential current into the monitor.
- $V_{mon}(\omega) = i_B(\omega) Z_{\parallel}(\omega)$
- The image current on the pickup is related to the beam current

$$i_{im}(t) = -\frac{A}{2\pi a l}\frac{dQ_{beam}}{dt} = -\frac{A}{2\pi a l}\frac{l}{\beta c}\frac{di_B}{dt}$$

- $i_{im}(\omega) = j\omega \frac{A}{2\pi a l}\frac{l}{\beta c} i_B(\omega)$
- $V_{mon}(\omega) = \frac{R}{1-j\omega CR} i_{im}(\omega) = \frac{R}{1-j\omega CR} j\omega \frac{A}{2\pi a l}\frac{l}{\beta c} i_B(\omega)$
- $Z_{\parallel}(\omega) = \frac{1}{\beta c}\frac{1}{C}\frac{A}{2\pi a}\frac{jRC}{1-j\omega RC}$

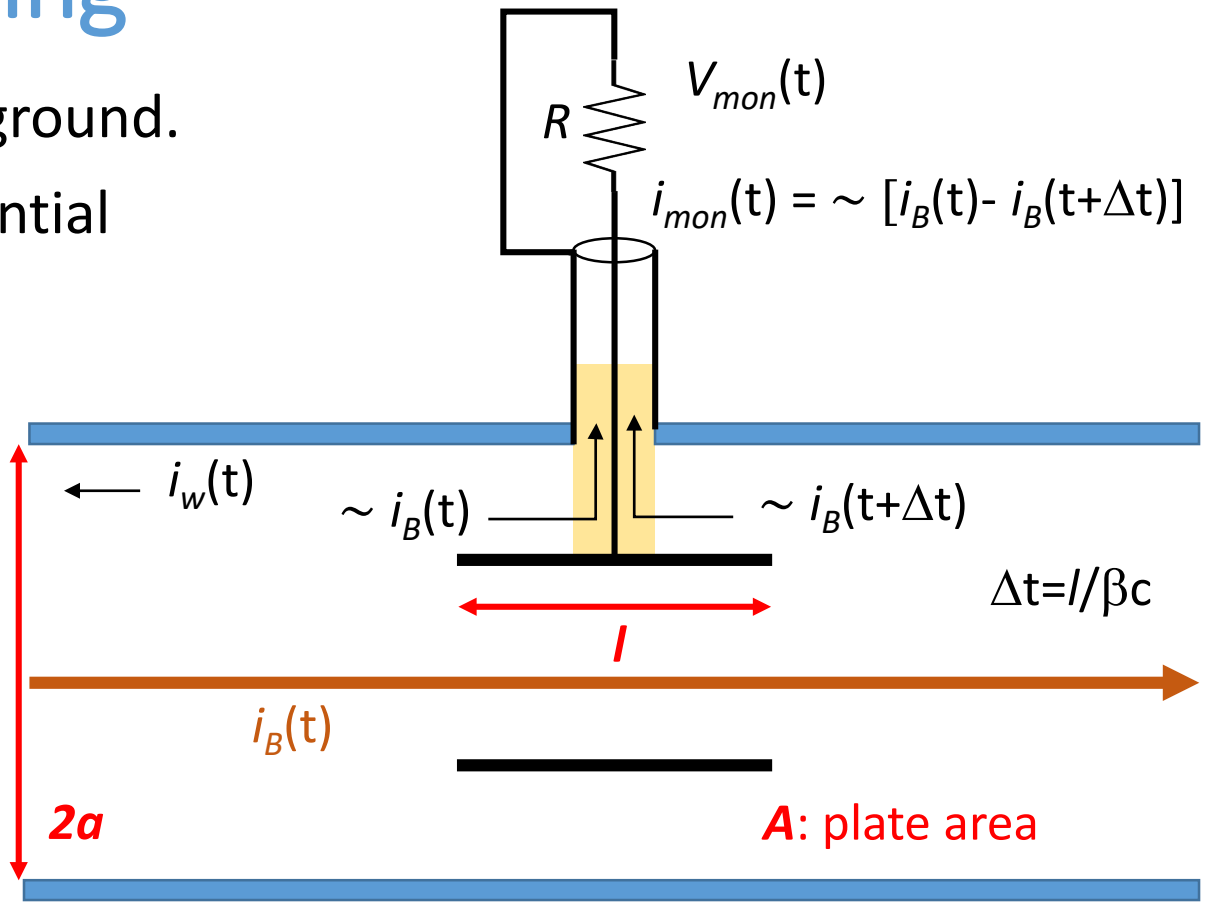

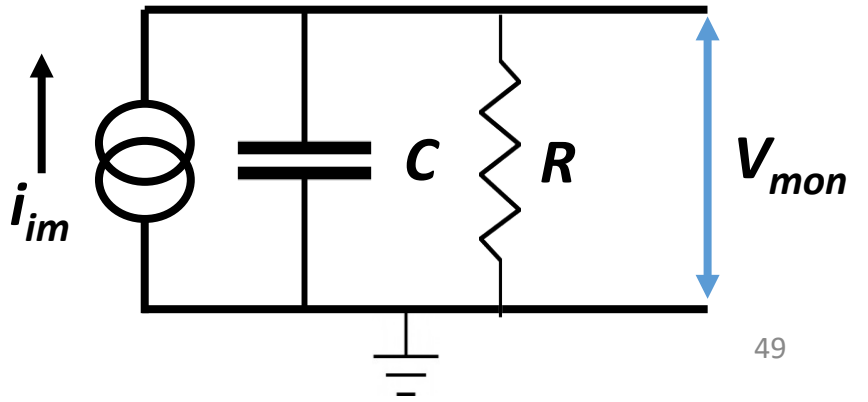

Beam Position Monitors

- Beam positions can be monitored using a 4-electrode array of capacitive pickups on the beampipe circumference.
- Various geometries are employed for sensitivity, compactness, protection from intense radiation

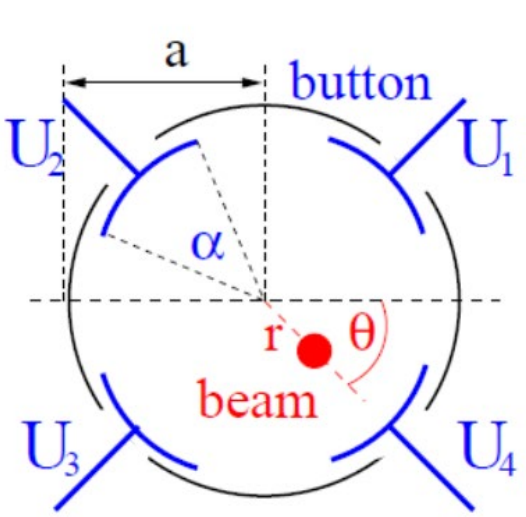

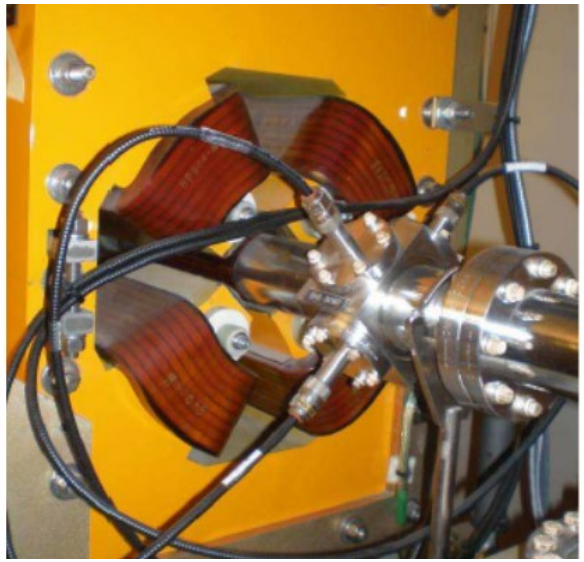

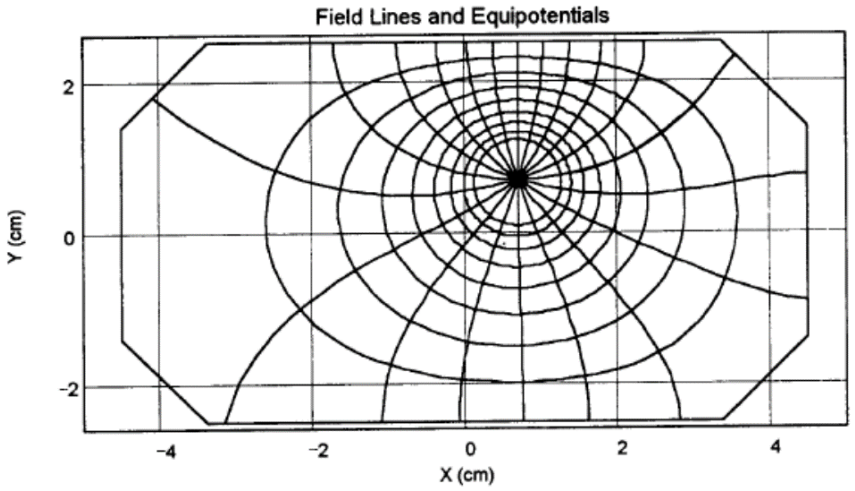

Figure 8. Field lines and equipotential contours found by conformal mapping.

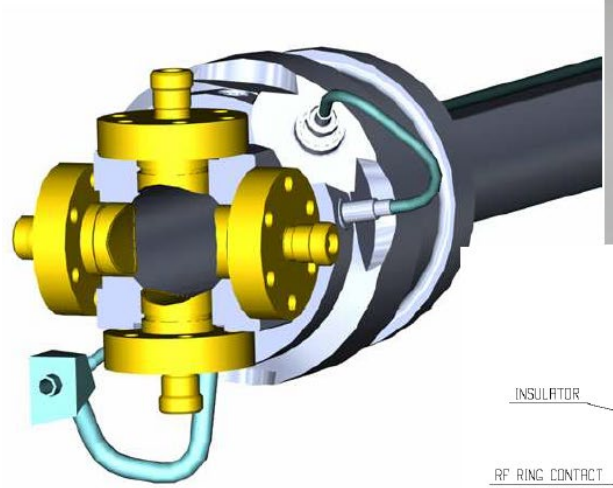

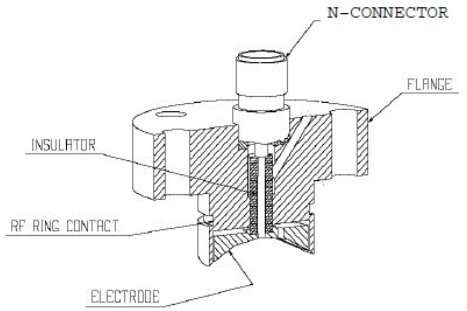

BPM Position Algorithm

- Positions are estimated from the normalized intensities using the *difference over sum* algorithm

$$\Delta x = \frac{1}{S_x}\frac{V_2 - V_4}{V_2 + V_4}\ , \Delta y = \frac{1}{S_y}\frac{V_1 - V_3}{V_1 + V_3}$$

- Position sensitivities are proportionality constants between beam displacement and signal strength.

$$S_x = \frac{d}{dx}\left(\frac{\Delta_x}{\Sigma_x}\right)\left[\frac{\%}{mm}\right] \text{ or } S_x = \frac{d}{dx}\left(\frac{V_2}{V_4}\right)\left[\frac{dB}{mm}\right] \text{ where } \left(\frac{V_2}{V_4}\right)[dB] = 10\log\left(\frac{V_2}{V_4}\right)$$

- Offset displacements also occur and must be measured and calibrated.
- Button-button capacitive coupling introduces frequency dependent offset and sensitivity variation.
- Intensities at each button can be calculated from the transfer impedance, using the electrode surface area.

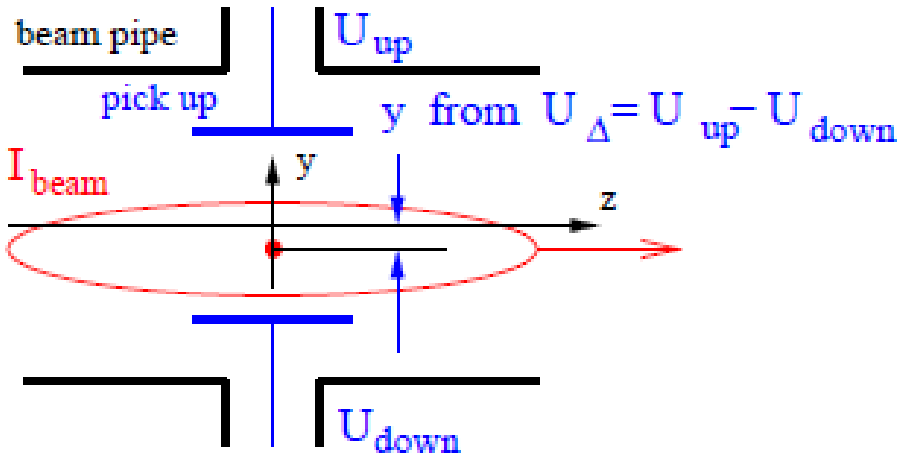

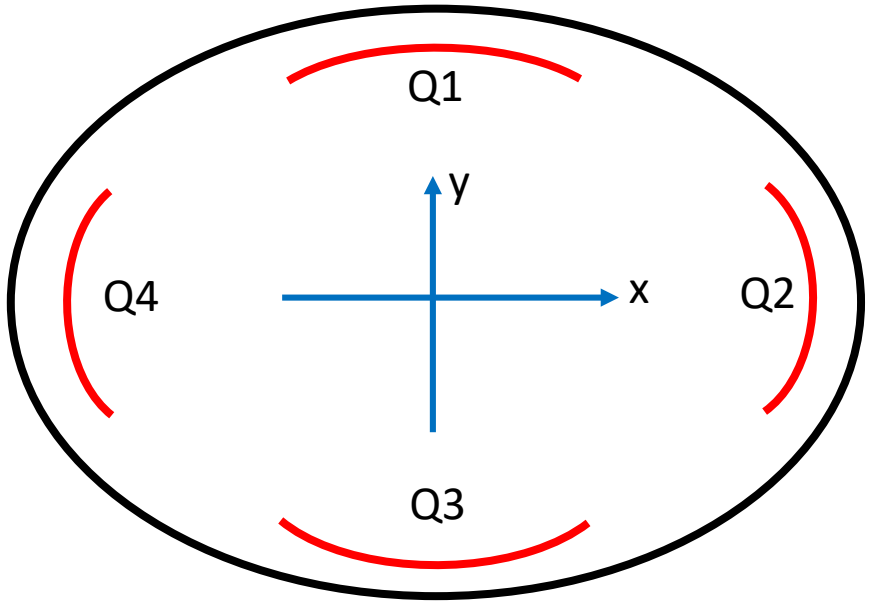

Coupling to the beam's magnetic field

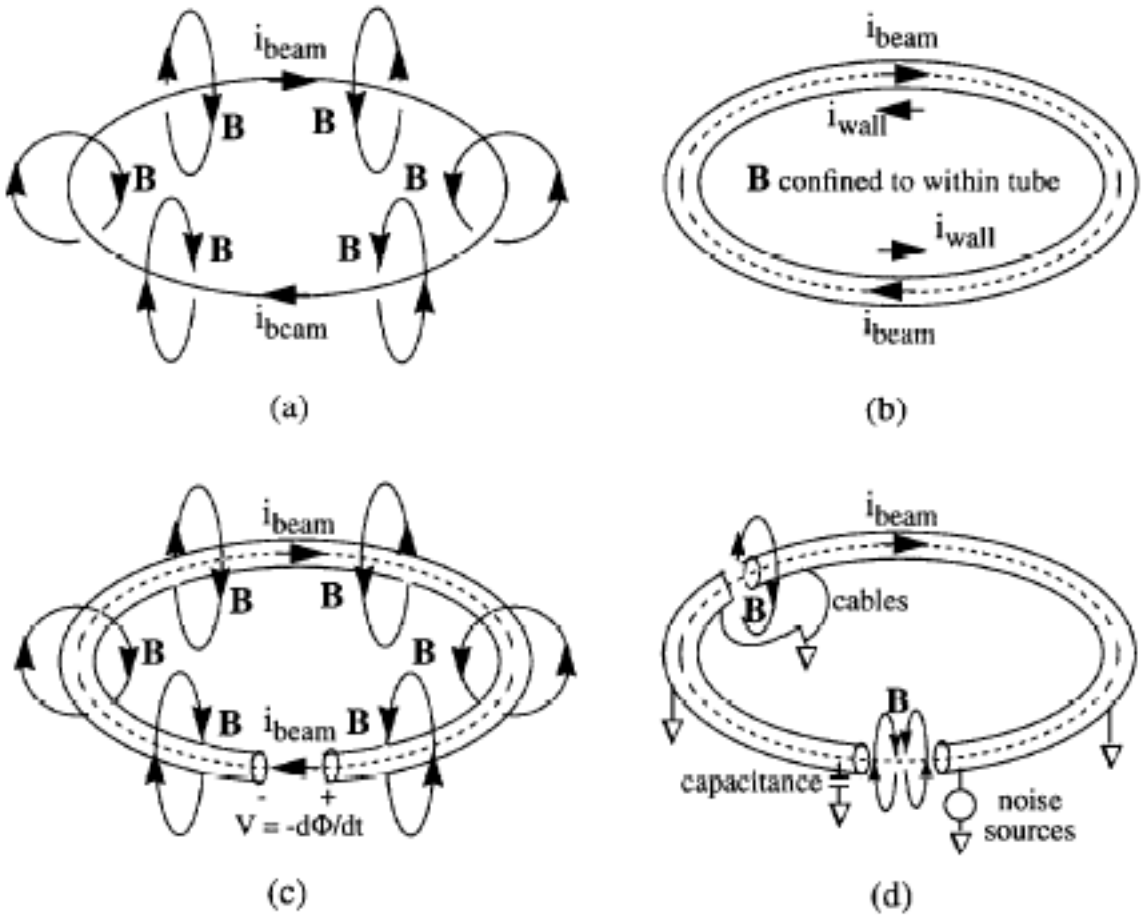

Figure 1. (a) Lines of magnetic induction around circulating beam. (b) Wall currents induced in beam tube attenuate external **B**. (c) Break in tube impedes wall currents permitting external **B** and appearance of induced voltage. (d) Layout of typical accelerator shows complex and distributed paths available to induced currents.

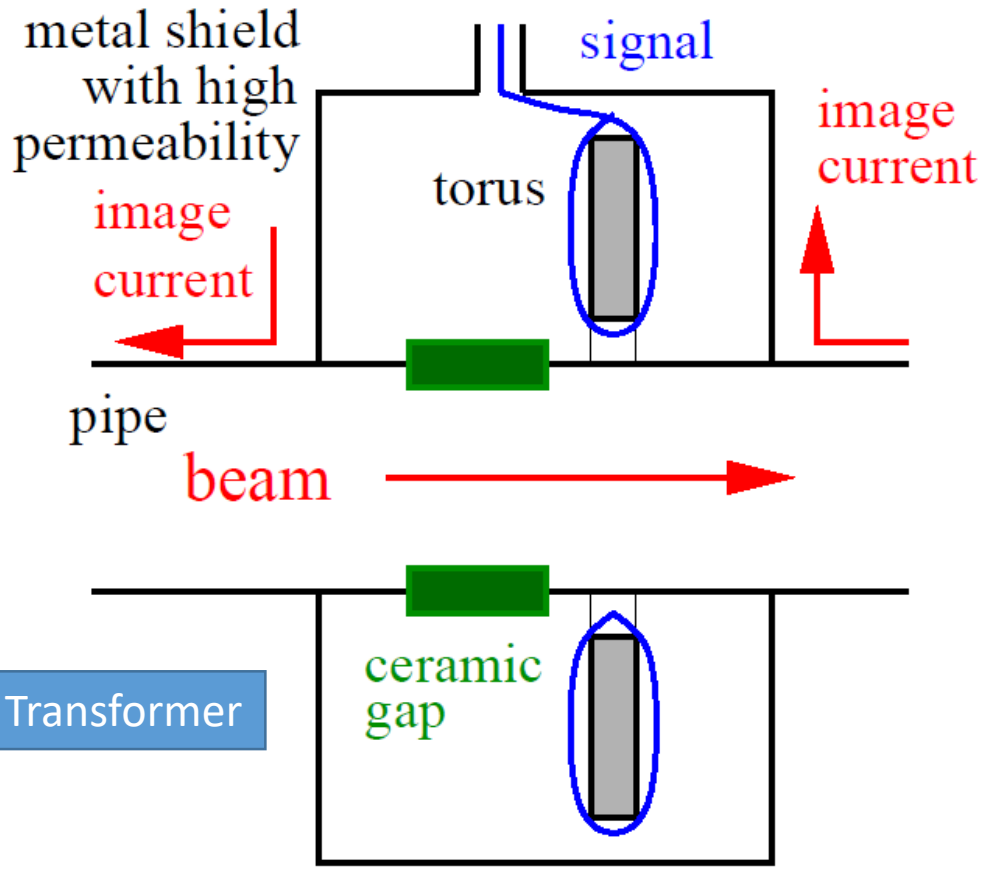

Current Transformer

Inductive coupling

The magnetic field of the beam is used to measure the beam current or intensity.

$$\vec{B} = \mu \frac{I_B}{2\pi r} \vec{\varphi}$$

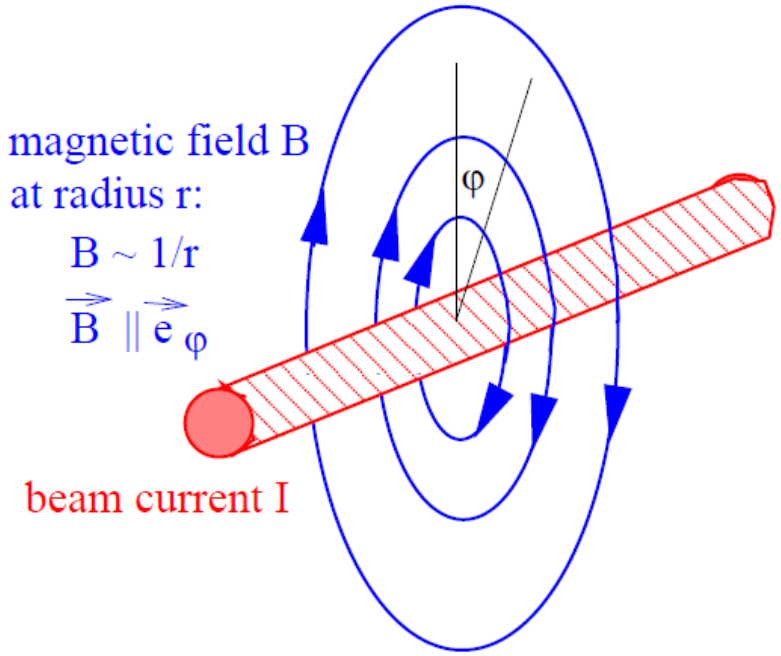

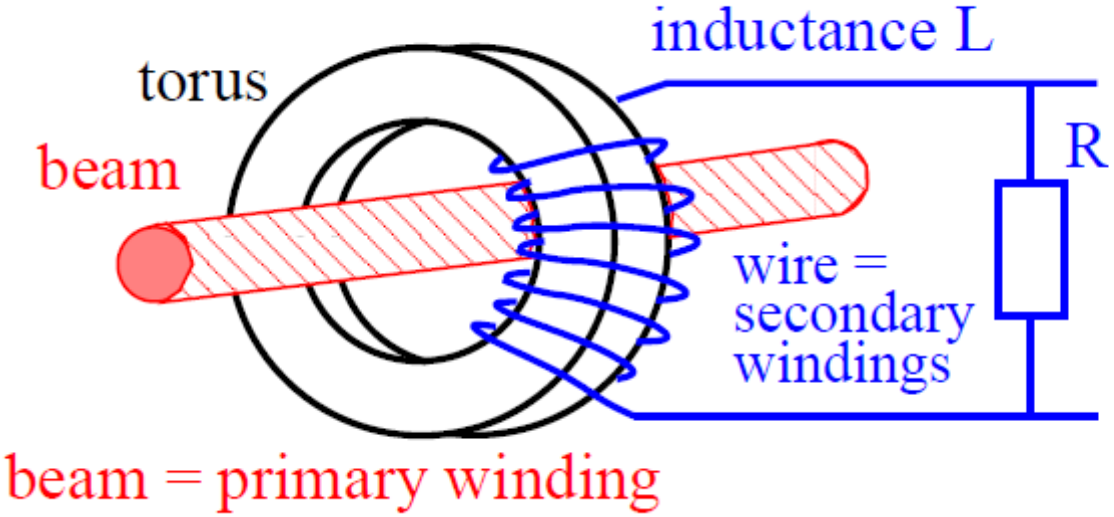

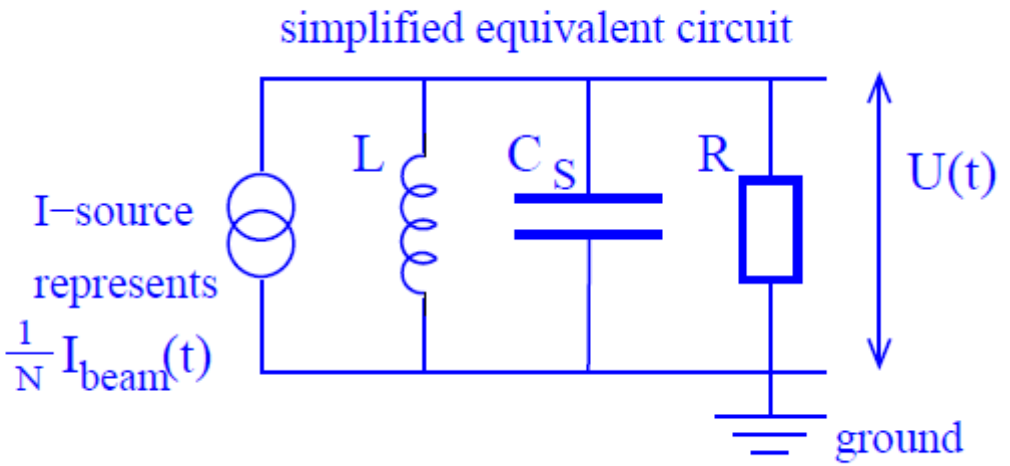

Current Transformers

Ampere's Law:

$$\oint H \cdot dl = N_p I_p + N_s I_s = I_p + N_s I_s \quad \text{with } N_p = 1 \quad \Rightarrow$$

$$H = (I_p + N_s I_s)/2\pi r \qquad (1)$$

Flux: (thin toroid approximation)

$$\Phi = \int_S B\, dS = \mu H A = \mu A (I_p + N_s I_s)/2\pi r \quad \text{with } A \text{ as area} \qquad (2)$$

Faraday's Law:

$$V_s = -N_s \cdot \frac{d\Phi}{dt} = I_s \cdot R_s \qquad (3)$$

Combine (2) and (3):

$$I_s \cdot R_s = -N_s \cdot \frac{\mu A}{2\pi r} \cdot \frac{d(I_p + N_s I_s)}{dt} \quad \text{with} \quad L_s = \frac{N_s^2 \mu A}{2\pi r} \Rightarrow$$

Differential equation:

$$\frac{dI_s}{dt} + \frac{R_s}{L_s} I_s = -\frac{1}{N_s} \cdot \frac{dI_p}{dt} \qquad (4)$$

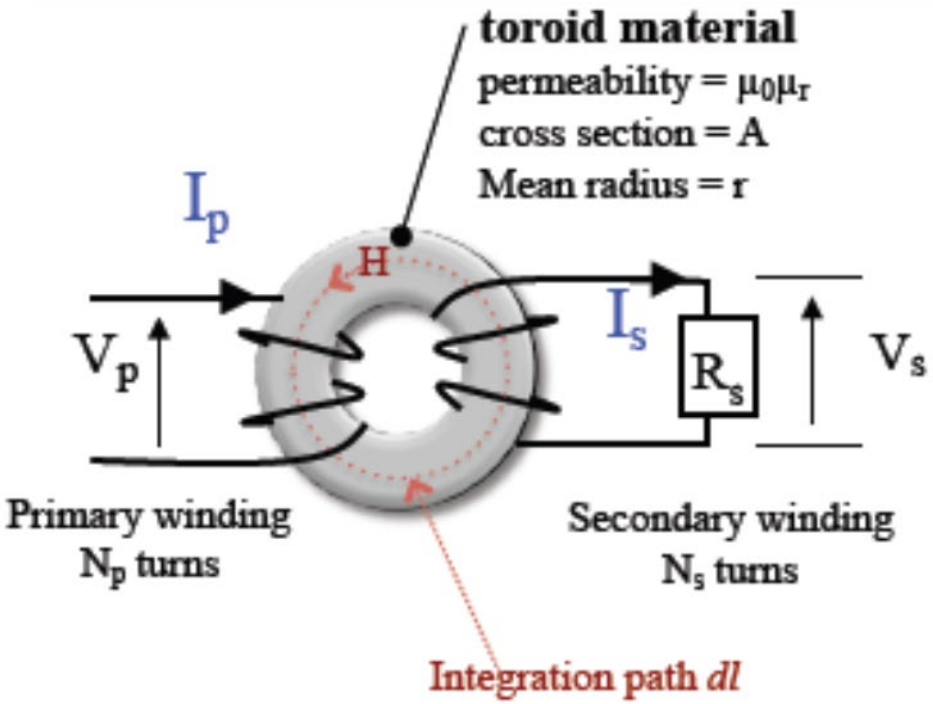

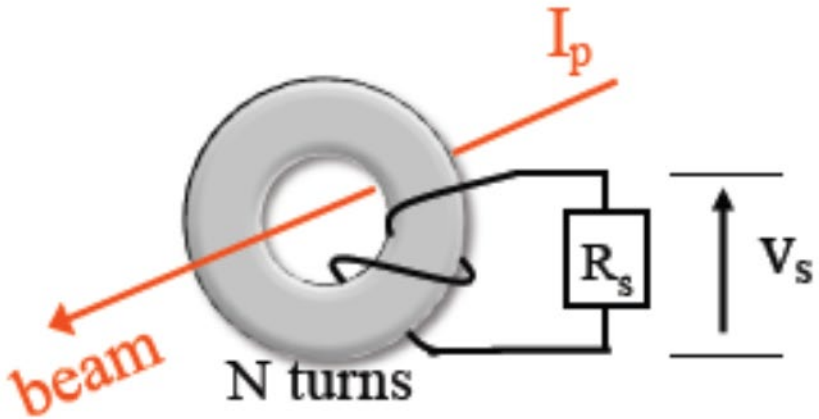

Response from passive transformer

Stray cable capacitance increases risetime.

$$\tau_{rise} = \sqrt{L_s C_s}$$ with cable

$$\tau_{rise} = RC$$ without cable

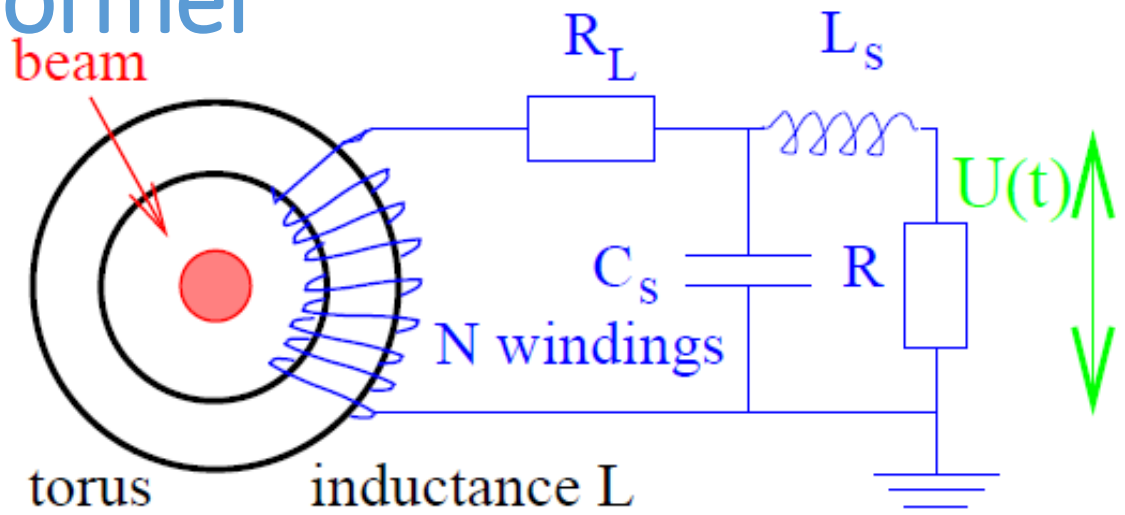

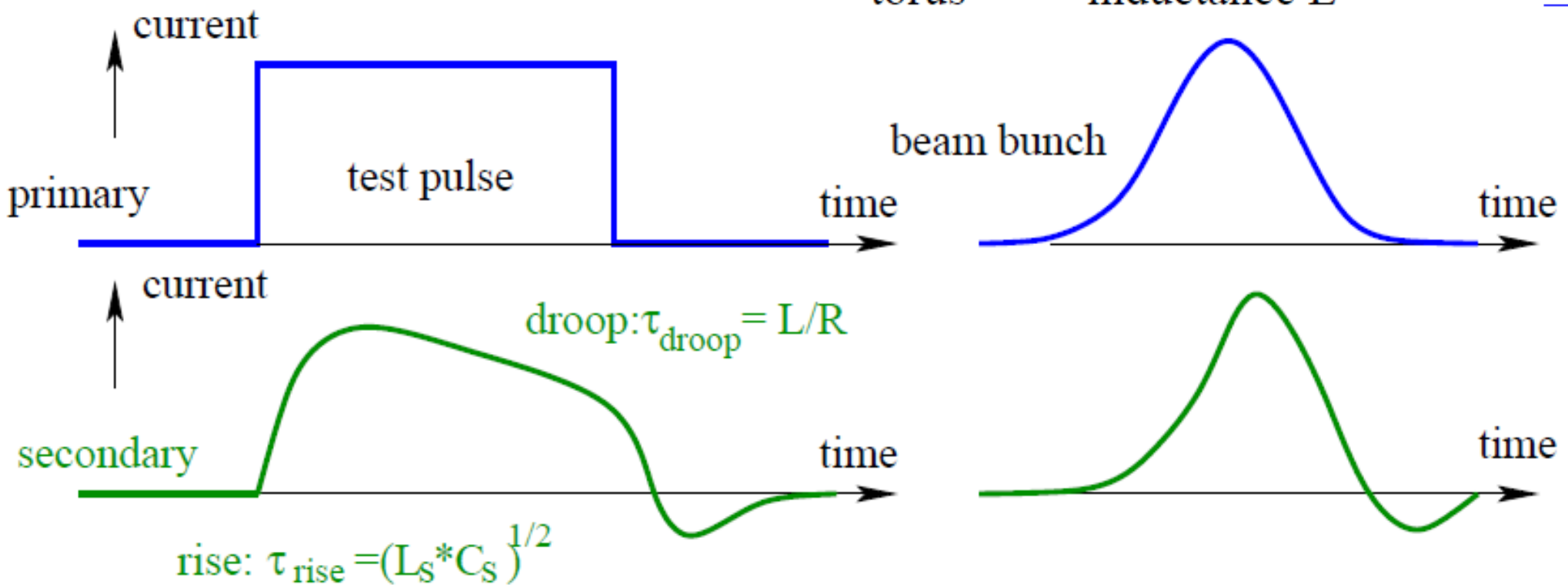

Resonant effects - Modal circuit equation

- We adopt a single mode resonance to calculate the coupling impedance
- The transient cavity-beam-waveguide system can be expressed as an equivalent *circuit equation* (cf. Whittum)

$$\left\{\frac{d^2}{dt^2}+\omega_0^2\right\}V_c=-\frac{\omega_0}{Q_w}\frac{d}{dt}V_c+\frac{\omega_0}{Q_e}\frac{d}{dt}(V_F-V_R)+\omega_0\left[\frac{r}{Q}\right]\frac{d}{dt}I_b$$

Here $V_F=nV^+$, $V_R=nV^-$ are the normalized forward and reverse waveguide voltages, such that $V_C = V_F + V_R$. Here, n is called the *transformer ratio* for the mode coupling.

- We can show that the longitudinal coupling impedance presented by this mode is

$$Z_{\parallel}(\omega)=\frac{j\omega\omega_0[r/Q]}{\omega_0^2-\omega^2+j\omega\omega_0/Q_L}=Q_L[r/Q]\cos\psi\, e^{j\psi}$$

- Impedances can be expressed as $Z = R + jX$ with the reactance $X=\left(\omega L-\frac{1}{\omega C}\right)$

Cavity Dipole-mode BPMs (resonant coupling)

- Used mainly for high energy electron beams
- Resonant dipole modes have higher shunt impedance than buttons or striplines
  - High sensitivity
  - Wakefields act back on beam
- Cavity BPMs have been developed to produce sub-μm position resolution, for ~mm displacements
- Monopole mode excitation is proportional to beam current
- Antennae pick up combined monopole+dipole signals. Technique requires independent calibration of monopole voltage.
  - Pillbox: f_{mono} ~ 1.2-1.5* f_{dipole}
- Q_{load} for both modes ~100 – 1000
  - Mode must decay before arrival of next pulse

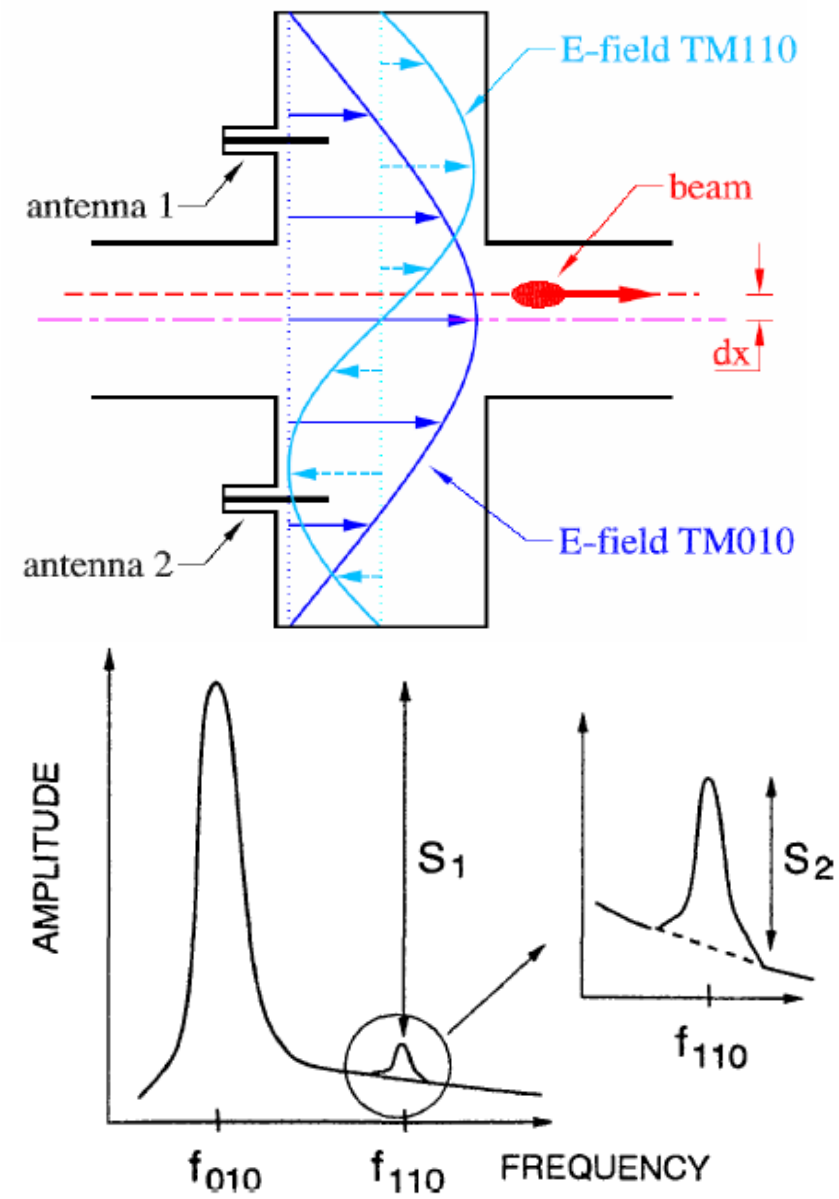

Beam spectrum, impedances and beam loading

- Beam impedance response
  - $V(\omega) = I_b(\omega)\, Z(\omega)$
- Everything that sees the beam can be described in terms of a beam coupling impedance
- Narrowband impedances from resonant structures
- Related to wake functions
- Panofsky-Wenzel relates longitudinal to transverse wake/impedances for ultrarelativistic particles

DAΦNE RF cavity longitudinal impedance

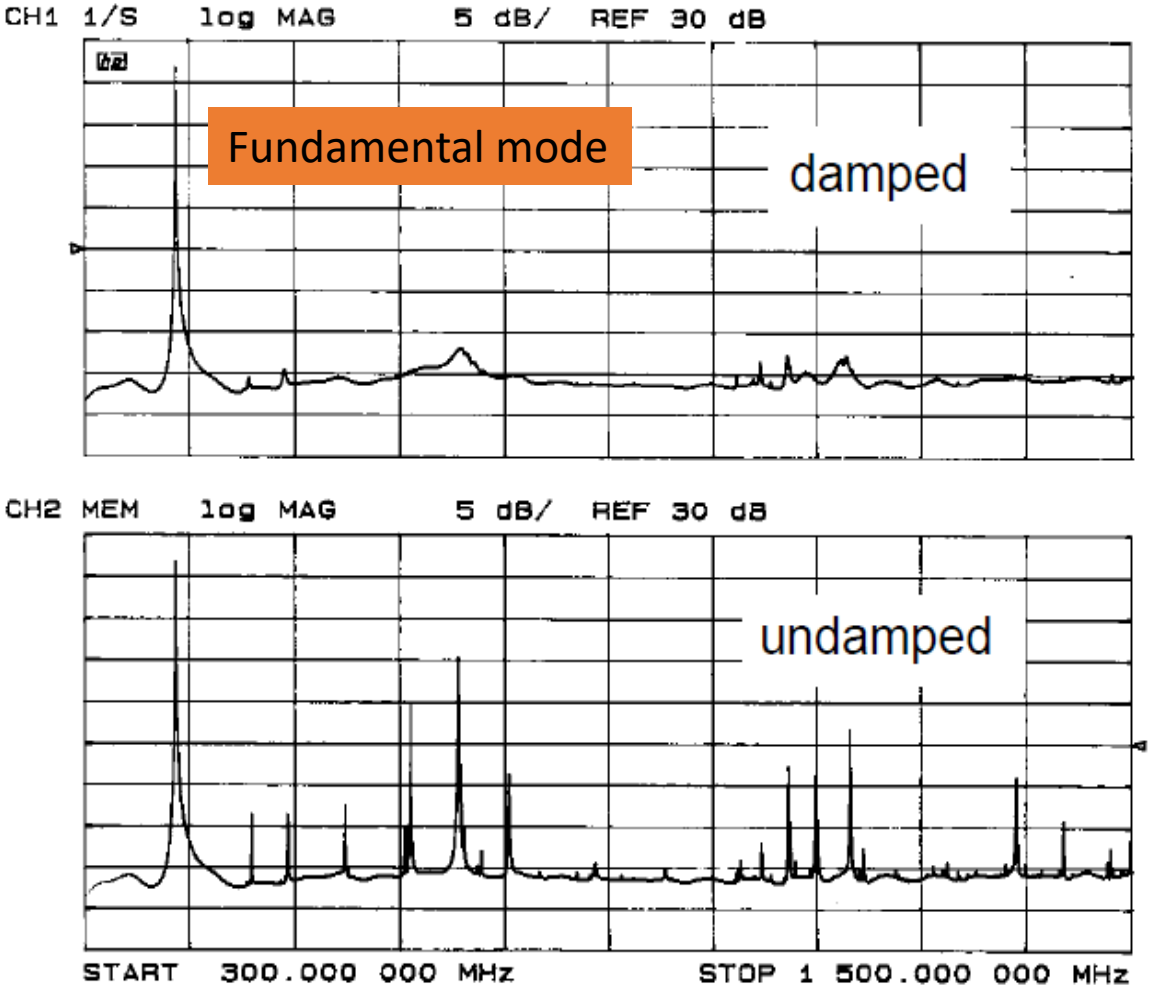

Beam coupling impedance to broadband device

- Devices may posses narrowband as well as broadband impedance characteristics.
- Impedances can be characterized on benchtop measurement stands

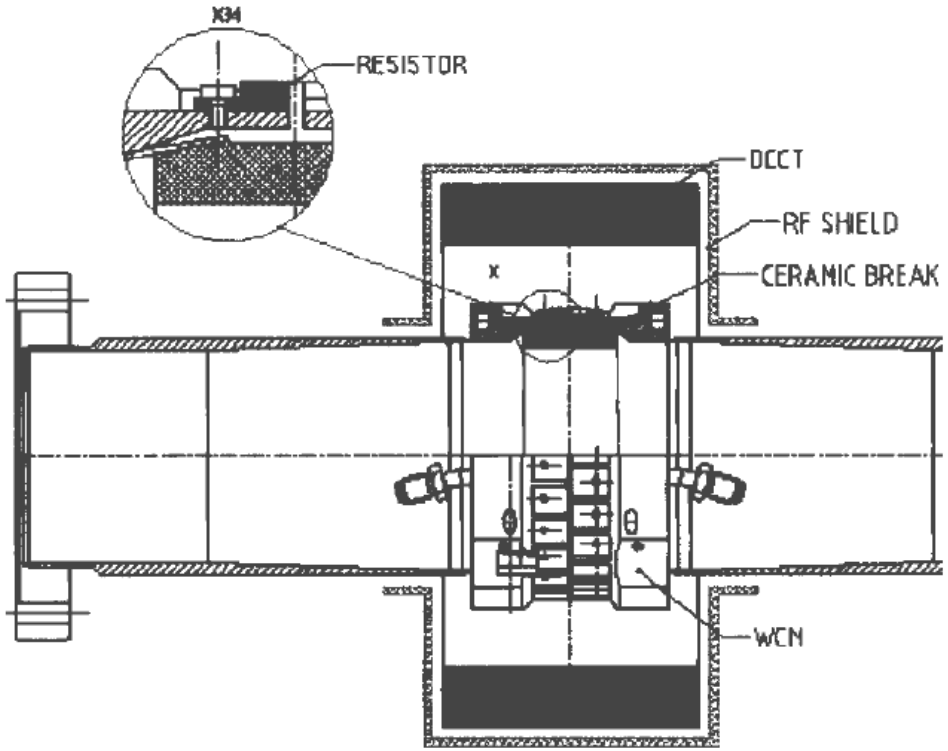

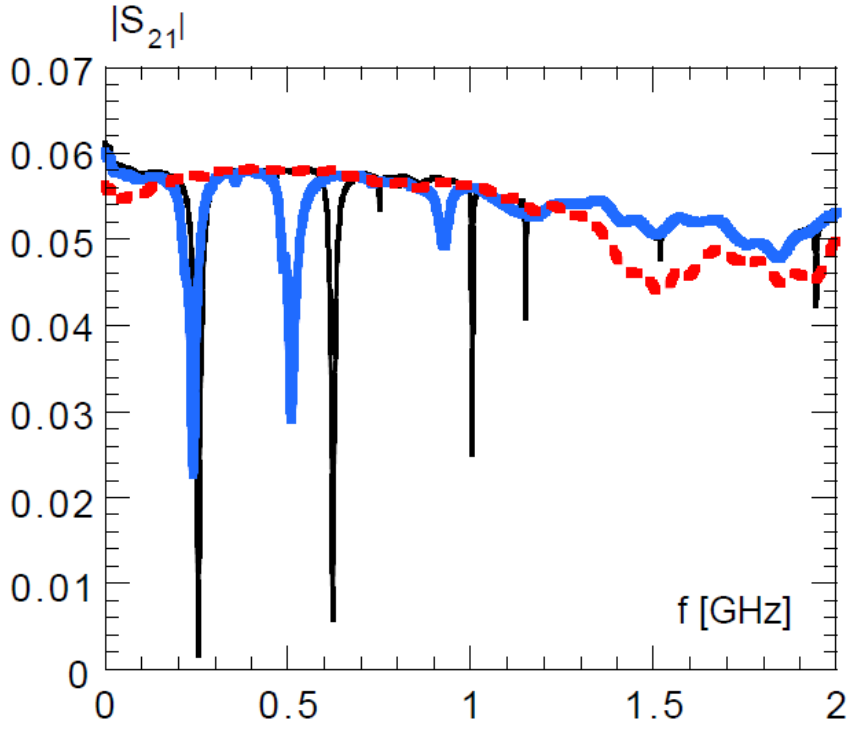

Figure 18: Wire measurement frequency response of the shielded ceramic break (thin line: outer shield without DCCT; thick line: outer shield with DCCT inside; dotted line: gap shielded by shunting resistors).

Far field EM radiation for high energy charged particle beams

- Bremmstrahlung
- Synchrotron

- Other types found in beam diagnostics
  - Cerenkov
  - Transition
  - Diffraction (electrons)

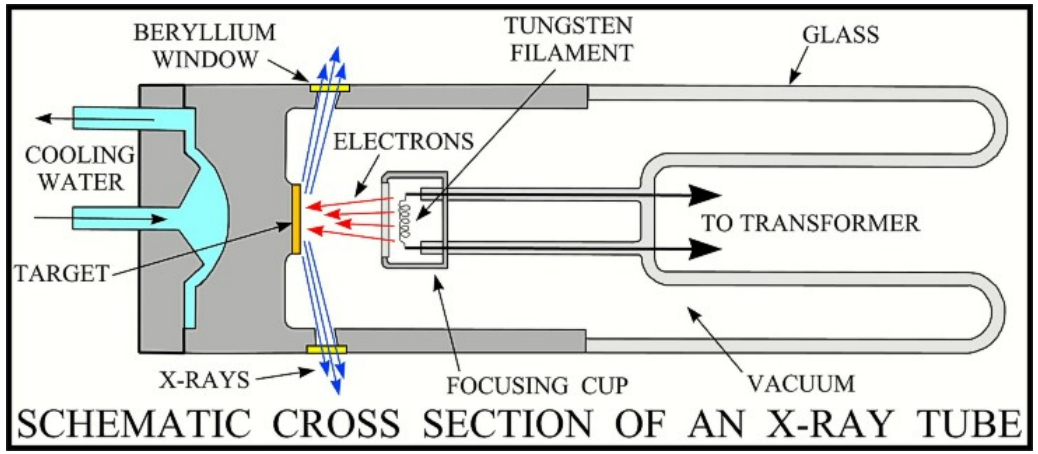

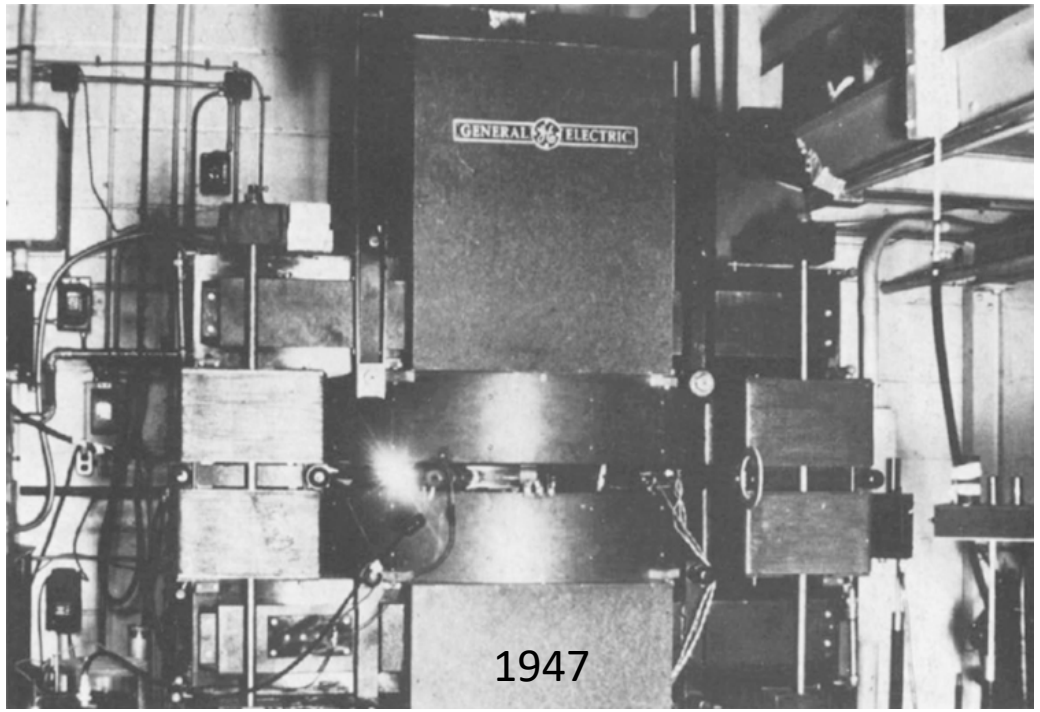

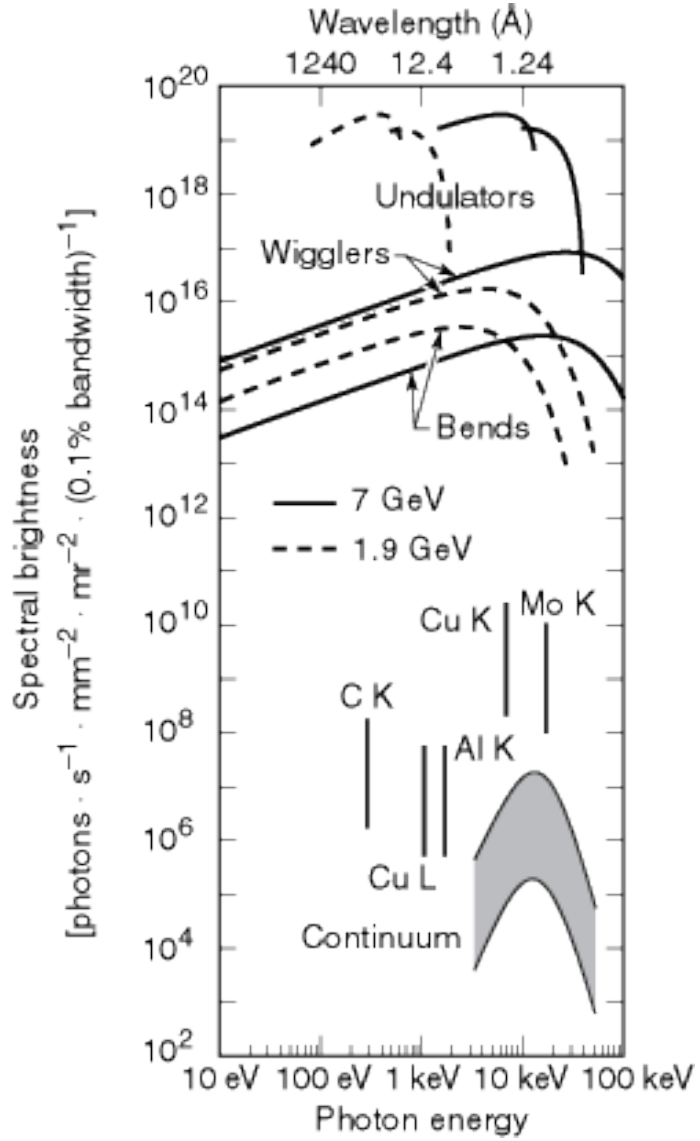

Synchrotron Radiation

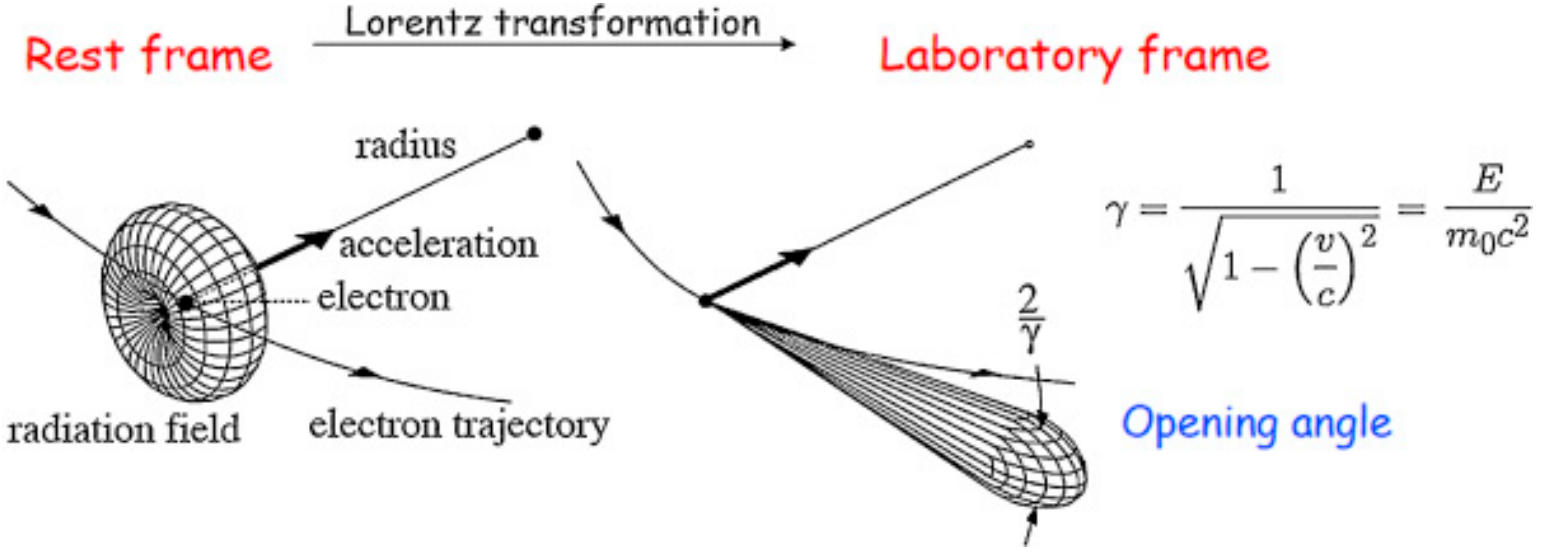

$$\gamma = \frac{1}{\sqrt{1-\left(\frac{v}{c}\right)^2}} = \frac{E}{m_0 c^2}$$

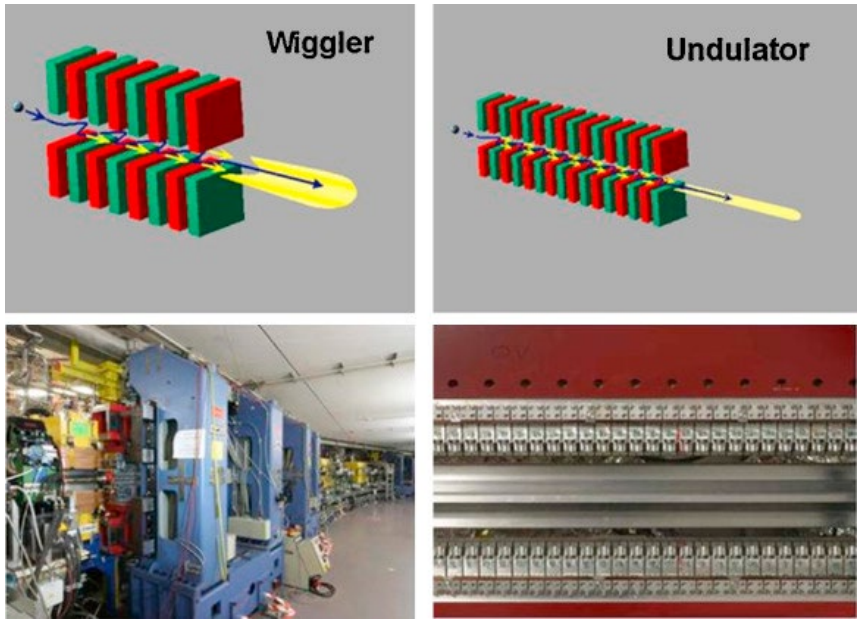

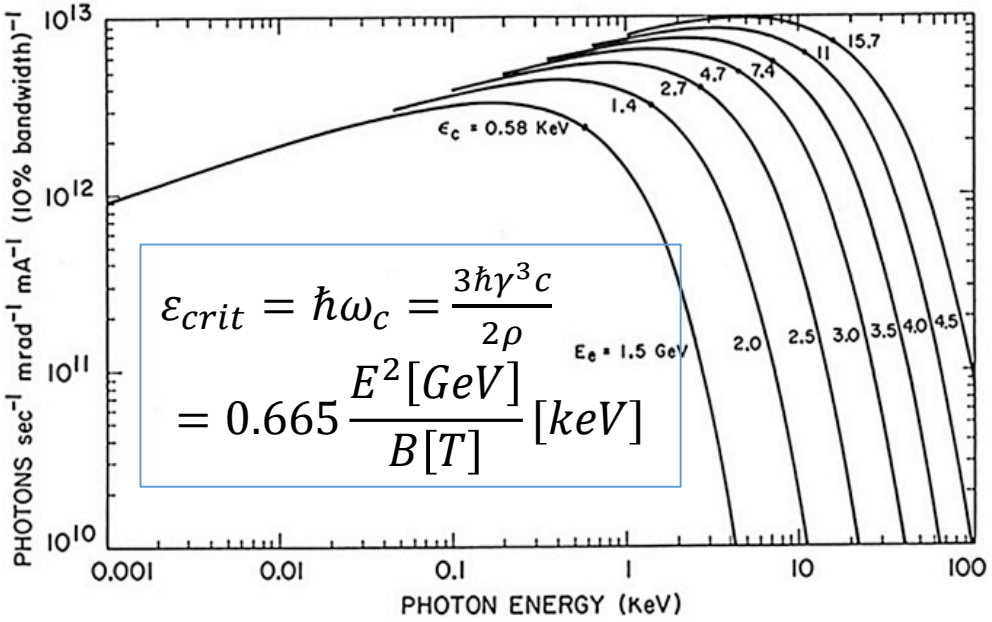

$$\varepsilon_{crit} = \hbar\omega_c = \frac{3\hbar\gamma^3 c}{2\rho} = 0.665\frac{E^2[GeV]}{B[T]}[keV]$$

- Relativistic beams, γ >>1
- Parasitic, nonintercepting
- Photon image reproduces electron beam distribution
- Optics, coupling
- Impedances, instabilities
- IR -> Hard X-rays

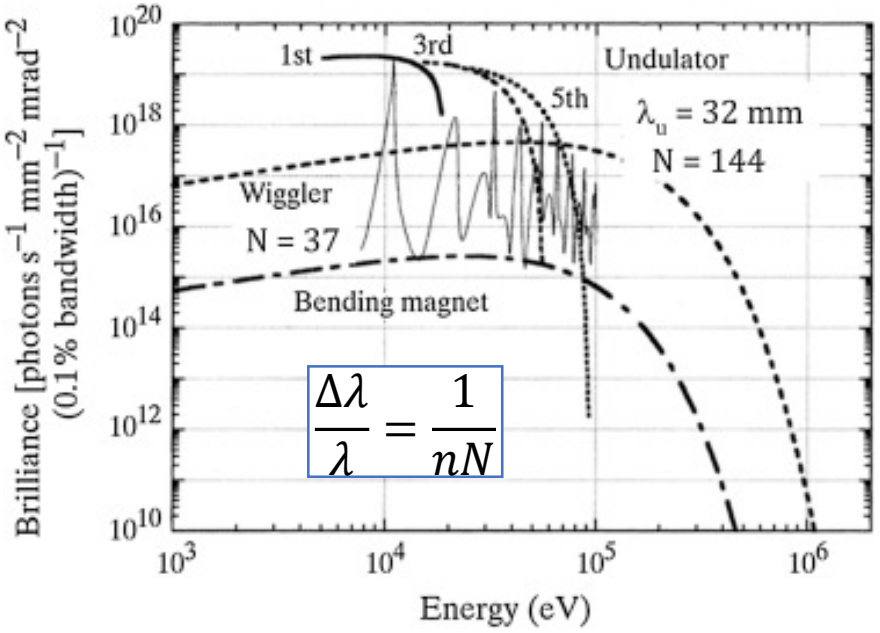

$$\frac{\Delta\lambda}{\lambda} = \frac{1}{nN}$$

Nonlinear Optics for Short Pulse Measurements

- 4th generation light sources produce intense electron bunches in the psec to fsec bunch length regime
- THz to X-ray wavelengths
- Can utilize self-fields or radiation → Single shot!

Electro-Optical Spectral Decoding:

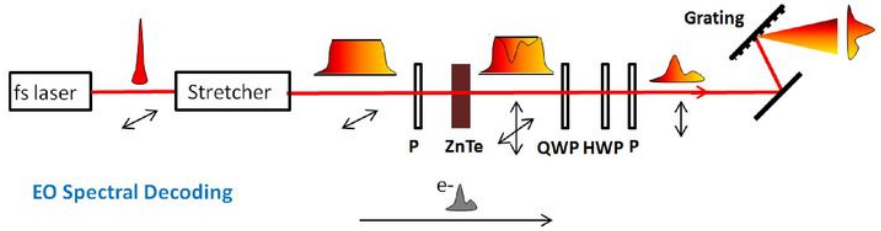

EO bunch profile measurements:
--EO spectral decoding
--EO temporal decoding
--EO spatial encoding
--EO up conversion

- Linear chirped optical pulse
- Polarization variation caused by Coulomb field—laser nonlinear effect
- Polarization → Intensity, by two crossed polarizers
- I(λ) ←→ I(t)

$$E_{out} = (0 \quad 1)R(\varphi)M_{hw}R(-\varphi)\,R(\alpha)M_{qw}R(-\alpha)\,R(\theta)M_{EO}R(-\theta)\begin{pmatrix}E_{opt}^{chirp}(f)\\0\end{pmatrix}$$

$R(\theta)$,---- rotation matrix

M_{qw},----Jones matrix for quarter waveplate

M_{hw} ----Jones matrix for half waveplate

Coulomb field temporal profile

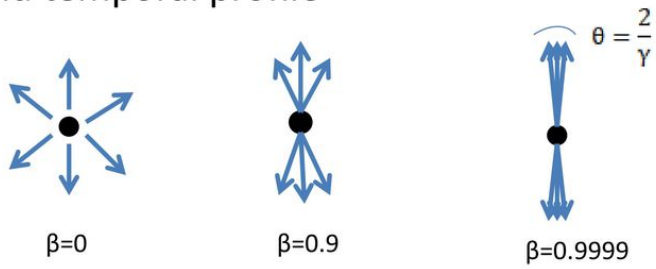

$$E_{e0}(r_0,t) = \frac{e_0\gamma}{4\pi\varepsilon_0}\cdot\frac{r_0}{(r_0^2+\gamma^2v_e^2(t-t_0)^2)^{3/2}}$$

Coulomb field of one electron

- High energy , Coulomb field temporal profile is approximately the bunch temporal profile
- Broadening of profile: $\Delta t \sim \frac{2r}{\gamma}$

Expected temporal resolution

1. Distance between crystal and e-beam

   $\Delta t \sim \frac{2r}{\gamma}$ ~10 fs at r=5 mm

2. The frequency response of crystal (material and thickness)

   for 1 mm ZnTe: ~333 fs ~1/(3THz)

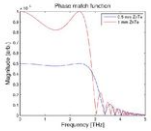

3. EOSD limitation (Laser pulse duration and chirped duration)

   $\tau_{lim} = \sqrt{\tau_0^{FWHM}\tau_c^{FWHM}}$ ~550 fs (100 fs→3 ps)

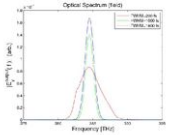

4. Resolution of spectrometer and CCD ~40 fs (512 pixels)

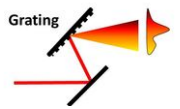

Synchrotron radiation diagnostic beamline

- Multiple/simultaneous ways to measure relativistic beams

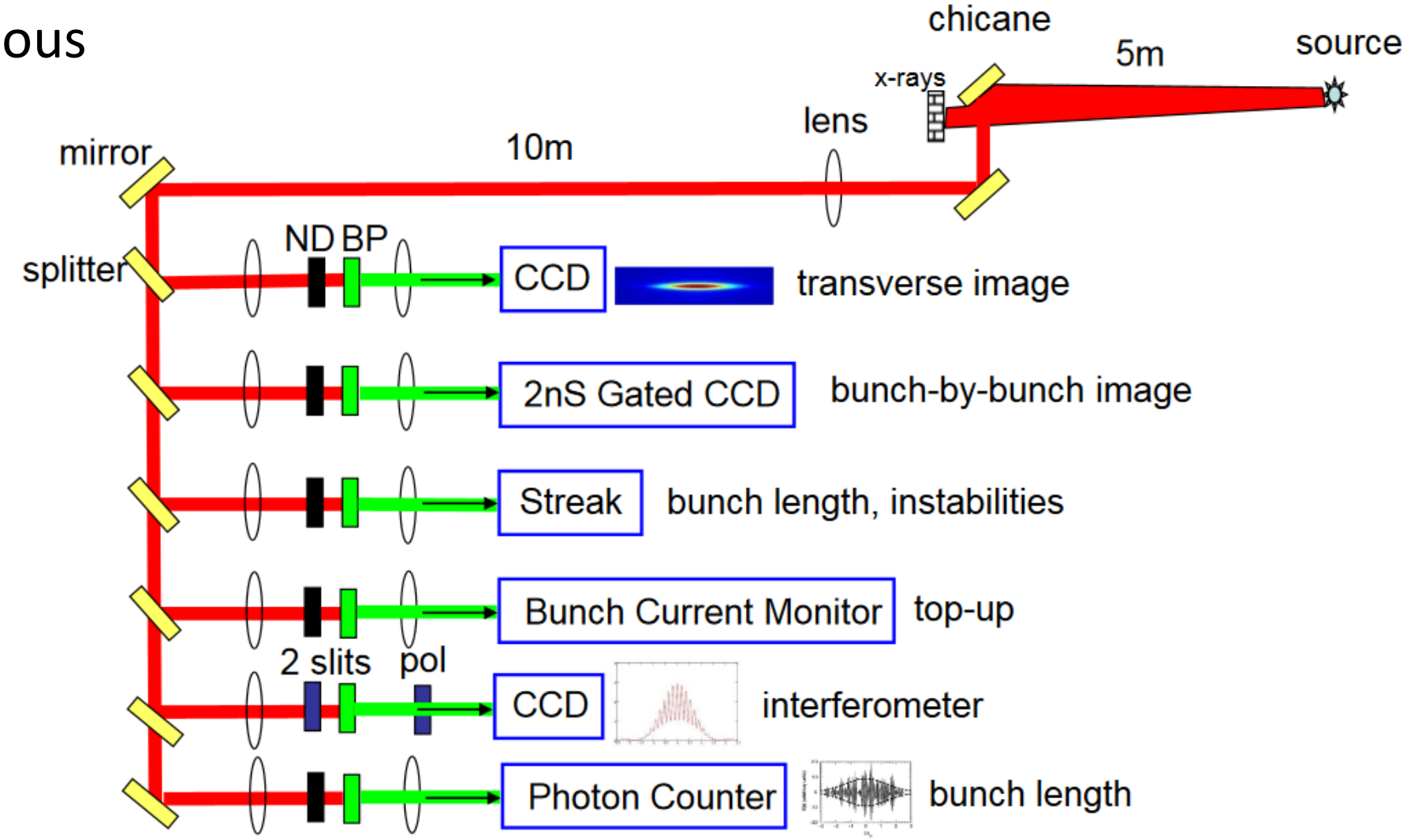

(Figure courtesy J. Corbett, W. Cheng, A. Fisher, W. Mok)

Transition vs. Cerenkov Radiation

Transition radiation occurs when a charge crosses a boundary of two dielectric media. No acceleration is required, nor is it necessary for charge to move faster than the speed of light as in Cherenkov radiation. In this respect, transition radiation is a least demanding radiation mechanism. Radiation emitted from a charge approaching a conductor is an extreme case of transition radiation with an infinite permittivity, and may be regarded as the inverse process of radiation accompanying β decay. Disappearance, rather than creation, of charge is responsible for transition radiation.

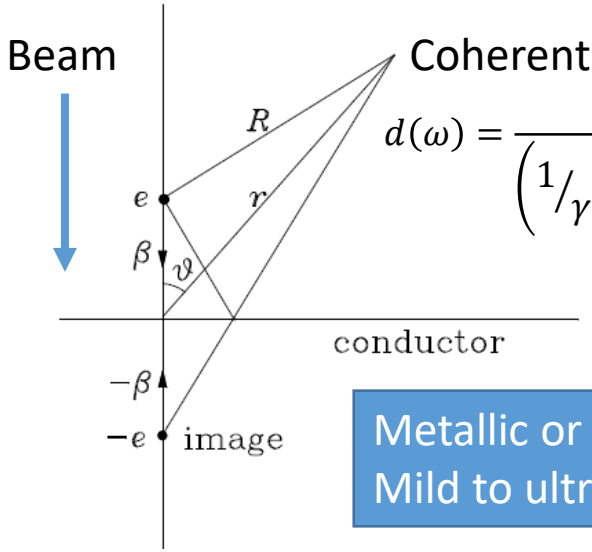

Coherent formation length

$$d(\omega) = \frac{2\,c/\omega}{\left(1/\gamma^2 + \vartheta^2 + \omega_p^2/\omega^2\right)}$$

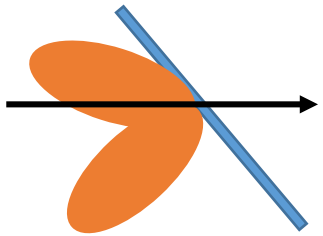

Metallic or metallized foils, plates
Mild to ultrarelativistic particles

$$\frac{dI(\omega)}{d\Omega} = \frac{1}{2\pi} r^2 c\mu_0 \left|H_\phi(\mathbf{r},\omega)\right|^2$$
$$= \frac{e^2\beta^2 c\mu_0}{32\pi^3}\left(\frac{1}{1+\beta\cos\theta} + \frac{1}{1-\beta\cos\theta}\right)^2 \sin^2\theta$$
$$= \frac{1}{4\pi\varepsilon_0}\frac{e^2 v^2}{2\pi^2 c^3}\frac{\sin^2\theta}{(1-\beta^2\cos^2\theta)^2}, \quad -\infty < \omega < \infty.$$

Cherenkov radiation occurs when a charged particle travels faster than electromagnetic waves in a material medium. It does not require acceleration of charges and the basic mechanism is very similar to that of sound shock waves in gases. As in the case of β decay, we assume a charge travelling along a straight line at a velocity $\beta = v/c(\omega)$, where

$$c(\omega) = \frac{1}{\sqrt{\varepsilon(\omega)\mu_0}},$$

Dielectric constant, ε

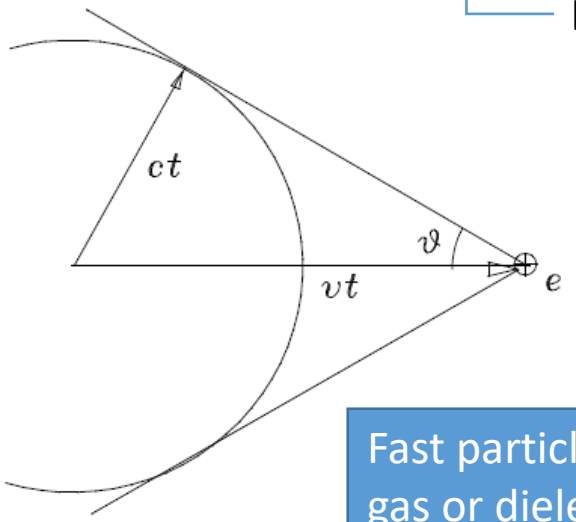

Beam

Fast particles in background gas or dielectric windows

$$\frac{dI(\omega)}{d\Omega} = \frac{\mu_0}{4\pi}\frac{e^2\omega^2}{4\pi^2 c(\omega)}\sin^2\theta\left(\frac{\sin\alpha}{\alpha}\right)^2 (dz)^2,$$

$$\alpha = \frac{1}{2}(1-\beta\cos\theta)\omega\Delta T. \qquad \Delta T = dz/v$$

Beam Loss Measurements

- Beam losses provide useful information on
  - Beam orbit deviations
  - Mismatches between beam distributions and lattice design; beam halo
  - Energy and energy spread mismatches to lattice through chromaticity
- Uncontrolled beam losses are potentially harmful to the machine
  - Damage to sensitive components (cryomodules!)
  - Radioactiviation of high loss areas of the beamline – affects maintenance and access
- Diagnostics employed to detect losses
  - Beam current/intensity, often in a differential mode to detect changes
  - Secondary radiation production – gammas, neutrons, electrons
  - Others – halo monitors, beamline thermometry, changes to cryo loading

Ionization chambers

Gas-type ionization chambers are in wide use as x-ray and gamma detectors

133 cm^3 Ar gas
Typical bias 1 kV
Sensitivity 70 nC/rad
Response time ~1-2 μs

SNS type

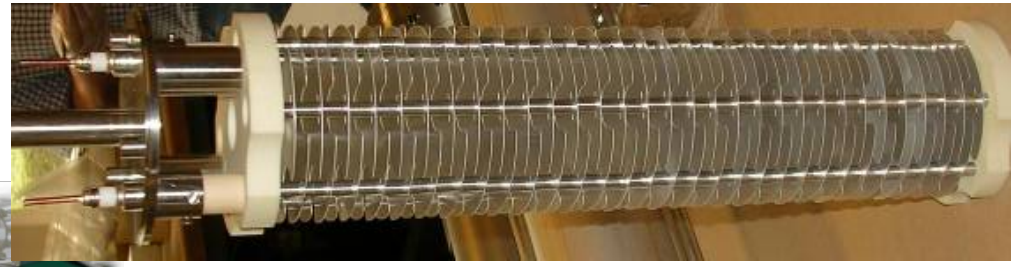

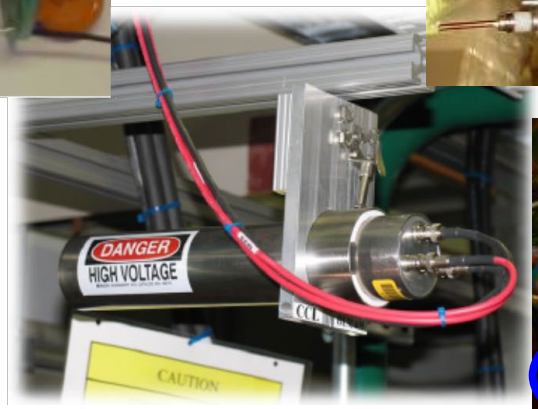

1.5 L volume
100 mbar overpressure N_2
0.5-mm separated Al plates
Bias 1500 V
Sensitivity ~ 54 μC/Gy
Response time ~300 ns e^-,
80 μs ions

Table 34.5: Properties of noble and molecular gases at normal temperature and pressure (NTP: 20° C, one atm). E_X, E_I: first excitation, ionization energy; W_I: average energy per ion pair; $dE/dx|_{\rm min}$, N_P, N_T: differential energy loss, primary and total number of electron-ion pairs per cm, for unit charge minimum ionizing particles.

Gas	Density, mg cm^{-3}	E_x eV	E_I eV	W_I eV	$dE/dx\|_{\rm min}$ keV cm^{-1}	N_P cm^{-1}	N_T cm^{-1}
He	0.179	19.8	24.6	41.3	0.32	3.5	8
Ne	0.839	16.7	21.6	37	1.45	13	40
Ar	1.66	11.6	15.7	26	2.53	25	97
Xe	5.495	8.4	12.1	22	6.87	41	312
CH_4	0.667	8.8	12.6	30	1.61	28	54
C_2H_6	1.26	8.2	11.5	26	2.91	48	112
iC_4H_{10}	2.49	6.5	10.6	26	5.67	90	220
CO_2	1.84	7.0	13.8	34	3.35	35	100
CF_4	3.78	10.0	16.0	54	6.38	63	120

Ionization chamber schematic

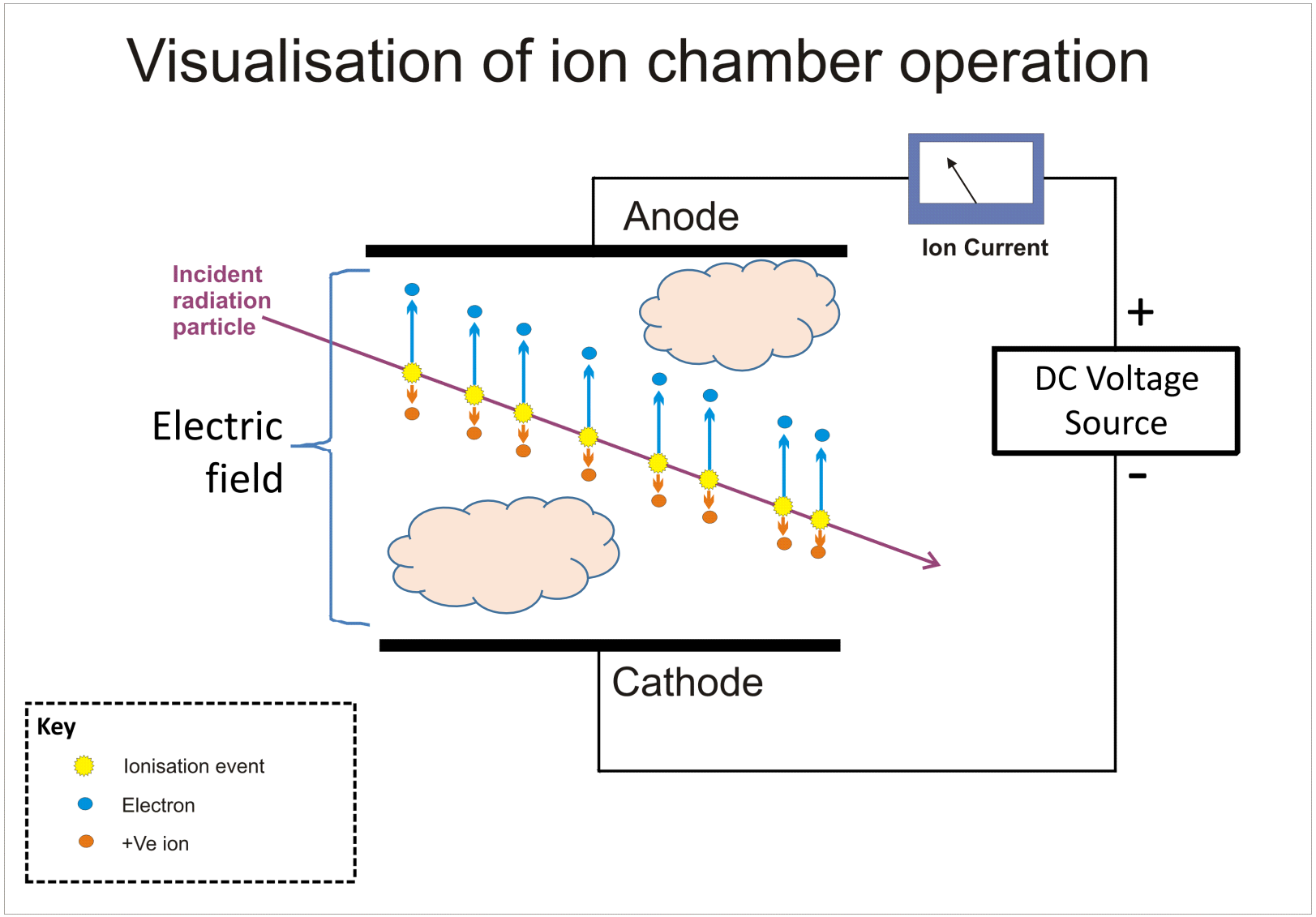

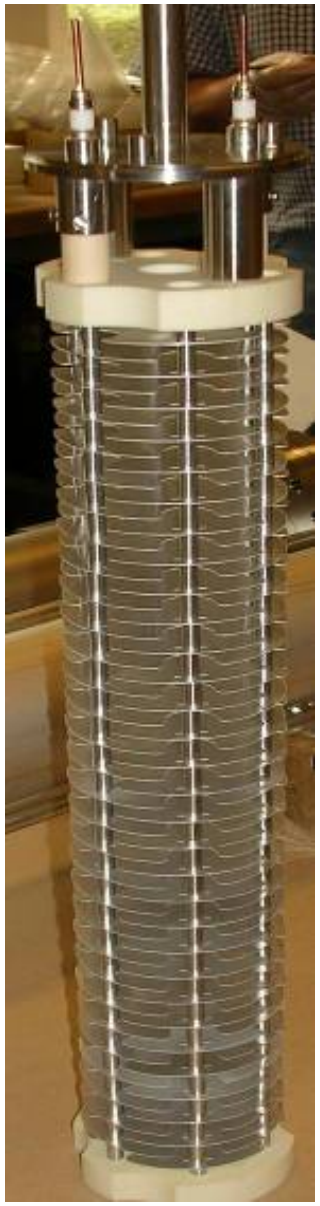

Scintillation based detectors (gammas, neutrons)

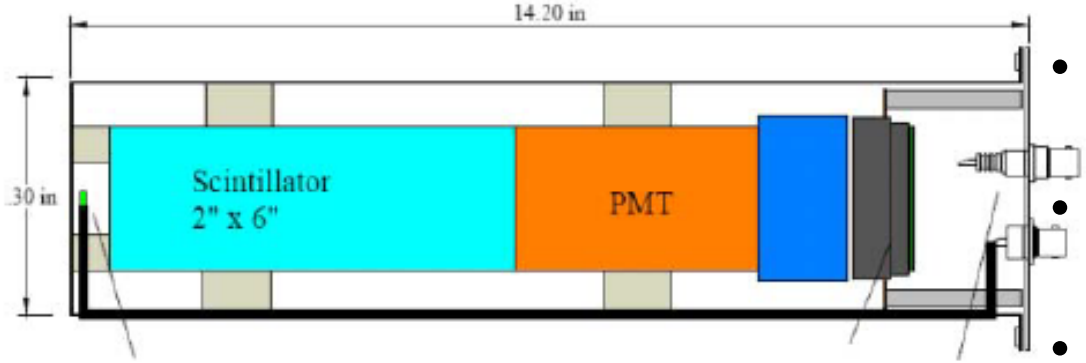

SNS Fast Detector

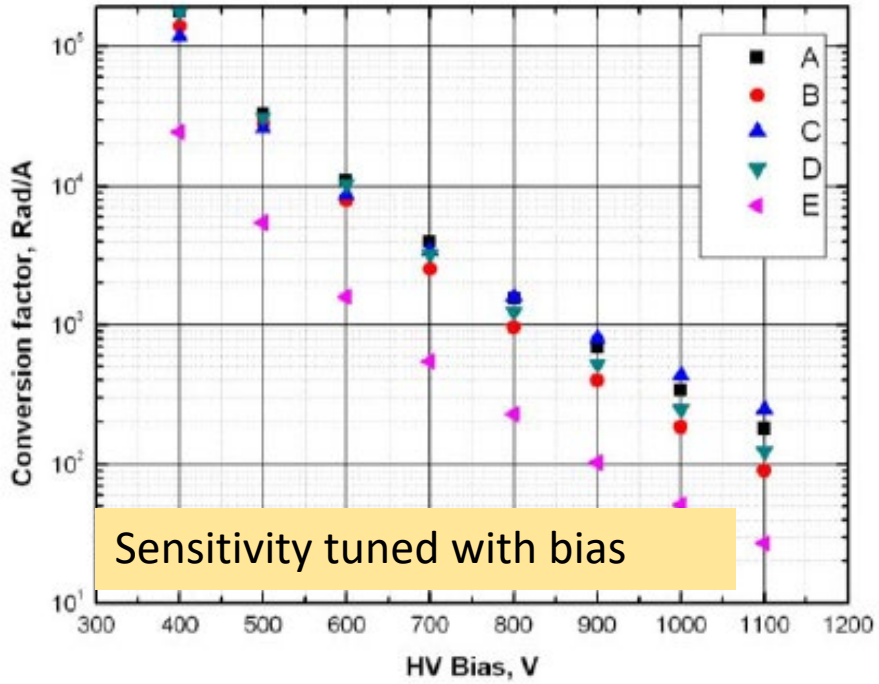

- Typically employ photomultiplier tubes for high gain (10^5-10^8) with applied HV
- Many types of scintillators fluoresce under gamma bombardment
- Li- or B- doped plastic scintillators respond to neutrons
- Additional moderation increases sensitivity at the expense of time response.
- Outside Cd layer provides discrimination against gammas

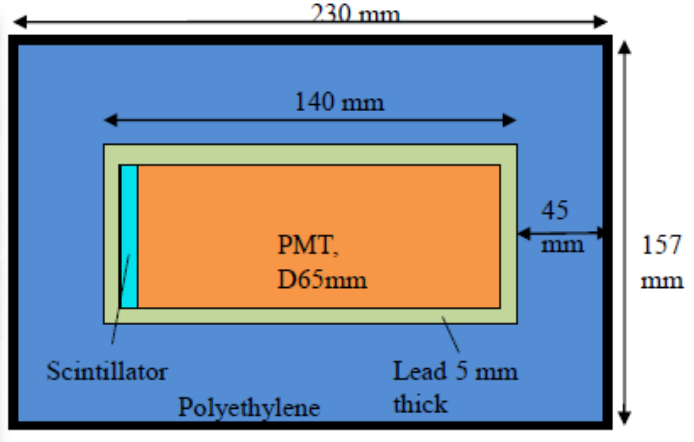

SNS Neutron chamber (SBLM)

FRIB Beam Loss Monitoring Network

LS1 monitors

- Halo monitoring rings (fast/slow loss)
- Fast beam pipe thermometry (slow loss)
- Differential current monitoring network (fast loss)

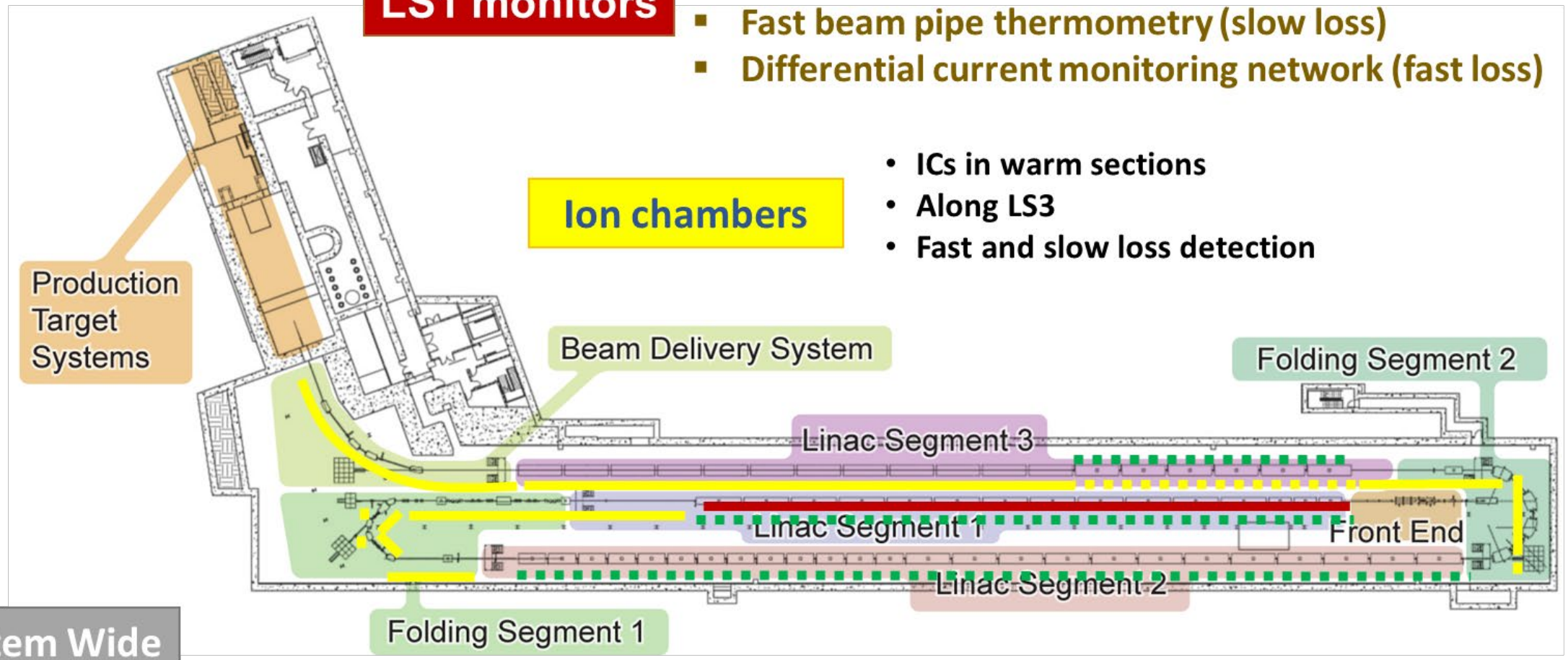

System Wide

- DBCM
- HMR

Neutron detectors

- LS2/3, LS1 (tuning only)
- Mix of fast/slow detection

Architecture of a diagnostic measurement

- The complete diagnostic system starts with beamline (or nearby) sensor
- Cabling to transport signals to data acquisition (DAQ) systems
- Processing electronics, and controls/operator interfaces

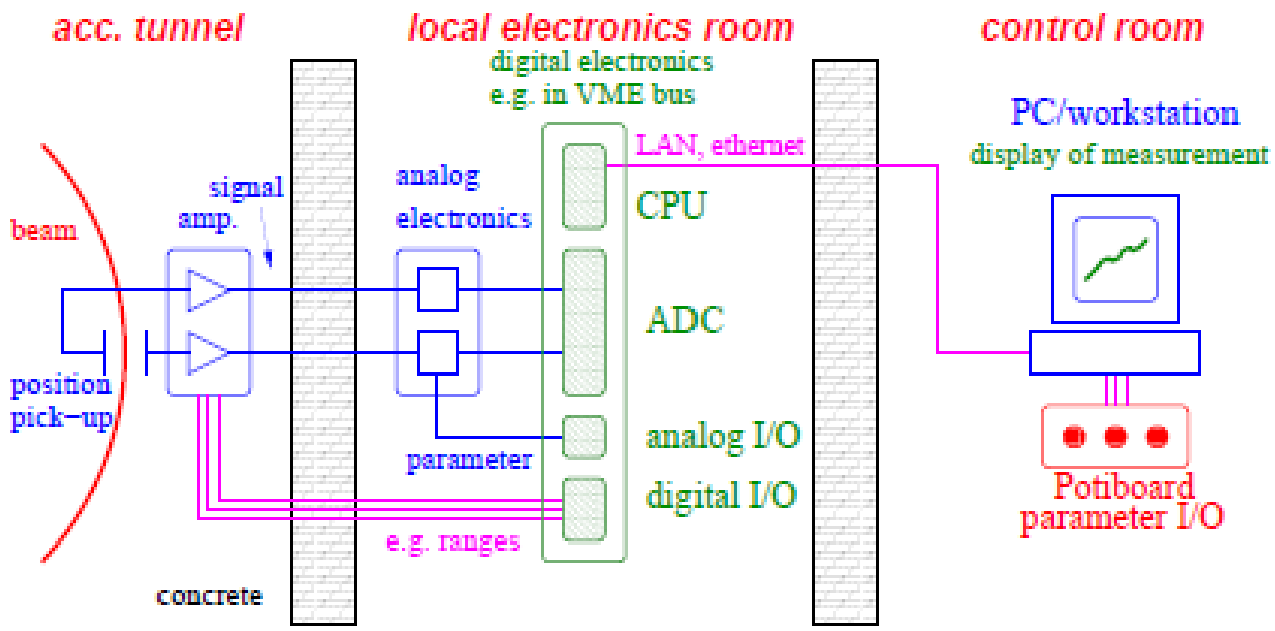

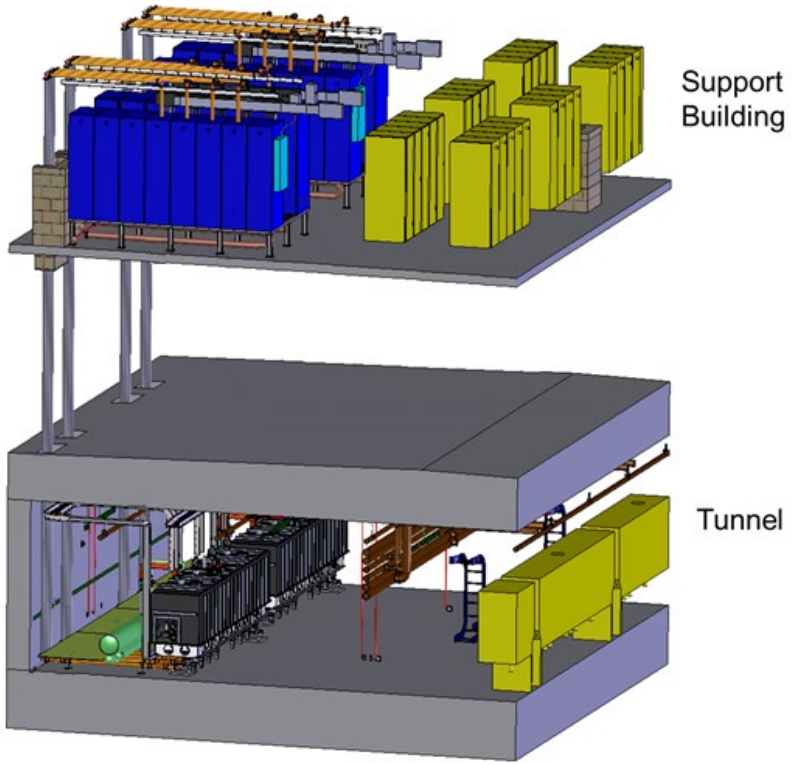

- Penetrations and racks are laid out for instrumentation
  - Cable runs about **100 ft**
  - Diagnostics will use ¼" superflex (Heliax)
    - » solid copper jacket provides >120 dB shielding effectiveness
- **No electronics in the tunnel!**

Many interfaces are needed to deploy diagnostics

- Controls and actuation for interceptive devices
- Global timing and triggering
- Interlocks for machine, device, and personnel protection
- High level controls for data acquisition, analysis, visualization

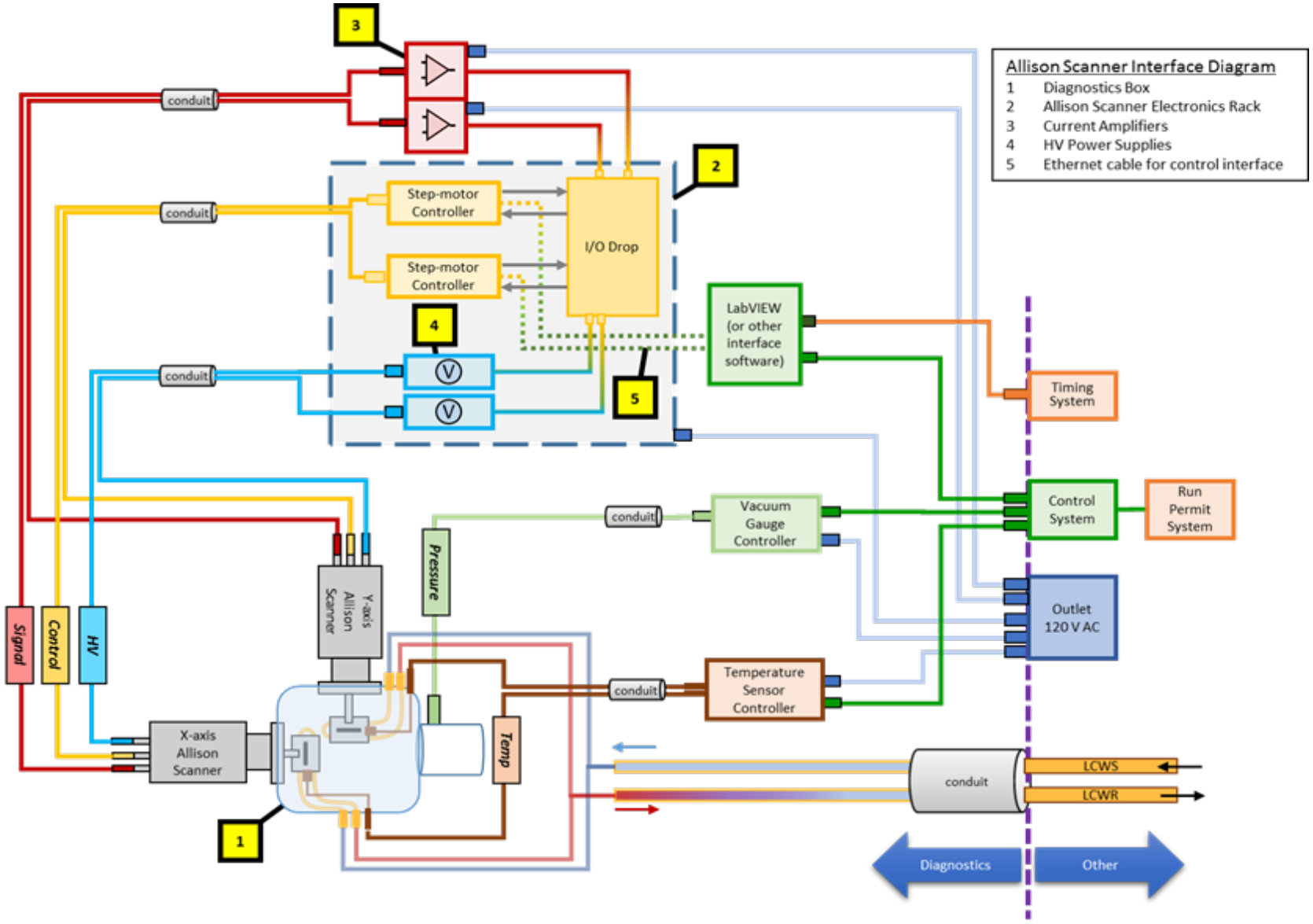

Beam Current Monitor System Design

- AC current transformer (baseline sensor) (Bergoz)
- ACCT high-resolution electronics (AFE) (Bergoz)
- Analog-to-digital converter (ADC)
- Transformer digital signal processing algorithms (FPGA, LabView, etc.)
- Connection to accelerator control system, operator interface, etc.

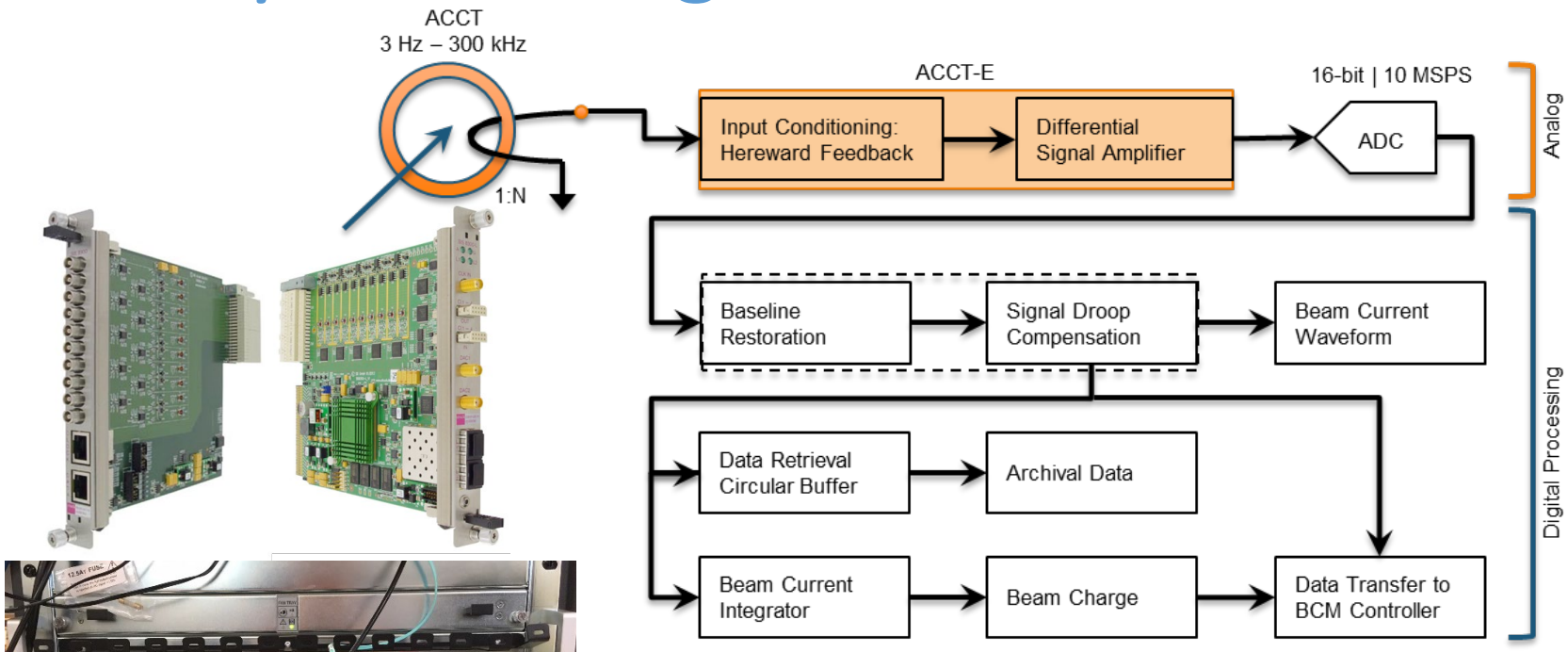

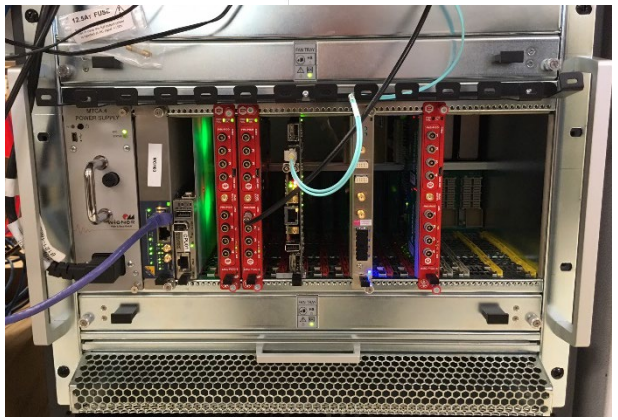

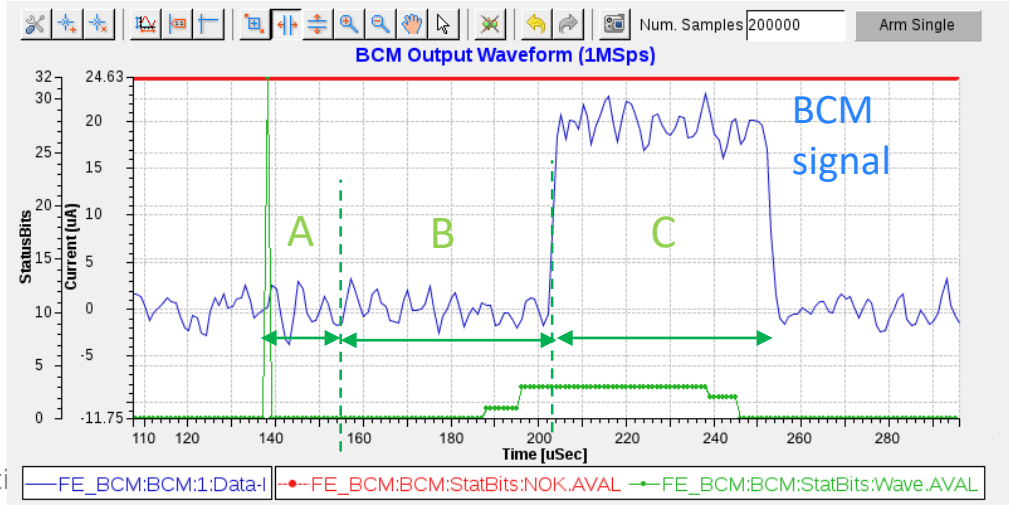

A. ToF delay (Chopper to BCM), ~15 usec
B. Beam "gap", 50 usec
C. Beam active, 50 usec

Thank you!

References

- Review of Particle Physics, http://pdg.lbl.gov
- P. Strehl, Beam Instrumentation and Diagnostics (Springer, 2006).
- M.G. Minty and F. Zimmerman, Measurement and Control of Charged Particle Beam (Springer, 2003).
- R. Shafer, "Beam Position Monitoring", in AIP Conf. Proc. **212** (1990) 26-58.
- R. Shafer, "Beam position monitor sensitivity for low-β beams", Proc. Beam Instr. Workshop (1994) 303.
- J.H. Cuperas, "Monitoring of particle beams at high frequencies", *Nucl. Instrum. Methods Phys. Res.* **145** (1977) 219-231.
- D. Whittum, "Introduction to Electrodynamics for Microwave Linear Accelerators", http://uspas.fnal.gov/materials/14Knoxville/slac-pub-7802(1).pdf
- J. Byrd, et. al., http://uspas.fnal.gov/materials/13CSU/USPASMWLecture.pdf
- G. Dome, CERN PAS
- M. Plum, "Interceptive Beam Diagnostics - Signal Creation and Materials Interactions", *BIW 2004*.
- J. Bosser, ed., "Beam Instrumentation", *CERN-PE-ED 001-92* (rev. 1994).
- D. Brandt, ed., "Beam Diagnostics", *CERN-2009-005*.
- J. Belleman, "From analog to digital", in Digital Signal Processing (D. Brandt, ed.), *CERN-2008-003*, 131-166.
- P. Forck, "Lecture Notes on Beam Instrumentation and Diagnostics", *JUAS* (2011).
- R.H. Siemann, "Spectral Analysis of Relativistic Bunched Beams", *SLAC-PUB-7159* (1996).
- K. Wittenburg, "Specific instrumentation and diagnostics for high-intensity hadron beams"

References, contd.

- J. Bechhoefer, "Feedback for physicists: A tutorial essay on control", *Rev. Mod. Phys.* **77** (2005) 783-836.
- http://labs.physics.berkeley.edu/mediawiki/index.php/Introduction_to_Noise
- Knoll, Radiation Detection and Measurement
- Leo, Techniques for Nuclear and Particle Physics Experiments
- ICFA Advanced Beam Dynamics Workshop on Beam-Halo (Halo '03)
- Workshop on Halo Monitoring, SLAC, September 2014, https://portal.slac.stanford.edu/sites/conf_public/bhm_2014/Presentations/Forms/AllItems.aspx
- K. Wittenburg, "Beam halo and bunch purity monitoring" in Brandt (2009).
- S.W. Smith, Digital Signal Processing. A practical guide for Engineers and Scientists, (Newnes, 2003).
- J.A. Hernandes and A.K.T. Assis, "Electric potential due to an infinite conducting cylinder with internal or external point charge", J. Electrostatics **63** (2005), 1115-1131.
- G. Lambertson, "Dynamic Devices - Pickups and Kickers", AIP Conference Proceedings **153**, 1413 (2016); doi: http://dx.doi.org/10.1063/1.36380
- W. Barry, "Broad-band characteristics of circular button pickups", AIP Conference Proceedings **281**, 175 (2016); doi: http://dx.doi.org/10.1063/1.44335
- S. van der Meer, "An Introduction to Stochastic Cooling", AIP Conference Proceedings **153**, 1628 (2016); doi: http://dx.doi.org/10.1063/1.36351.
- J.D. Jackson, Classical Electrodynamics (Wiley, 1975).
- A. Hirose, "Electromagnetic Theory", http://physics.usask.ca/~hirose/p812/notes.htm, Chapter 8.
- H. Bichsel, "A method to improve tracking and particle identification in TPCs and silicon detectors", *Nucl. Instrum. Methods Phys. Res.* **A 562** (2006) 154-197.